Investigation of Transfection Using Silica-coated Cupric Oxide Nanowires

Åsmund Flobak

Abstract

One-dimensional high aspect ratio nanostructures grown from a copper foil are considered for intracellular delivery of bioactive molecules, such as drugs and genetic material. The cupric oxide (CuO) nanowires are coated with silicon oxides (SiO_x), and embedded in a transparent polymer membrane consisting of the photoresist SU-8 and polydimethylsiloxane (PDMS). Nanowires are envisaged as one way to deliver bioactive molecules to many cells in parallel. It has previously been shown that both HeLa and AR42J cells grow and spread on this nanowire surface. The overarching goal of the current project is to test and optimize delivery of genetic material to cells grown on nanowires.

It is first shown that nanowires are not able to induce knockdown of a constitutively expressed protein by delivering siRNA, when cells are sedimenting on top of an array of nanowires by gravitation. It is then shown that nanowire-mediated transfection of plasmids perform similar to flat surfaces, which are chemically identical apart from the nanowires, when HeLa cells are sedimenting down on a nanowire surface by gravitational pull. Increasing the sedimenting force by centrifugation has no effect on transfection efficiency, with relative centrifugal forces up to $88,500 \times$ g tested. Tapping the nanowire surface face-down on cells deposited at a high concentration, which is a well documented method in published articles, also performs similar to flat surfaces, with transfection efficiencies of ~1% commonly seen, and occasionally higher (~5%).

Fluorescently labeled plasmid is quite efficiently delivered to cells by both flat surfaces and nanowire surfaces, with a trend towards more efficient delivery by nanowires. Delivered cargo is however confined to small sections of cells. Cells are not transfected in experiments with identical setups, indicating that delivered biomolecules are isolated from the internal machinery of a cell.

In conclusion, our transfection efficiency results are on par with most published experiments. In published experiments control experiments with flat surfaces are often lacking, and our results emphasize the importance for proper controls when investigating nanowire-mediated transfection and delivery of biomolecules.

Sammendrag

I dette arbeidet undersøkes transfeksjon av celler ved hjelp av nanostaver dannet fra en kobberfolie. Målet med transfeksjonseksperimentene er intracellulær levering av bioaktive molekyler, som medisiner og genetisk materiale. Nanostavene er en-dimensjonale strukturer av kobberoksid dekket med silisiumoksid og silisiumdioksid, og peker utover fra en gjennomsiktig membran som består av polymerene SU-8 og dimetylpolysiloxan (PDMS). Nanostaver vil kunne brukes til å levere bioaktive molekyler til mange celler parallelt. Formålet med arbeidet som presenteres her er å teste og optimalisere levering av genetisk materiale til celler som vokser på en membran med nanostaver.

Det første forsøket som presenteres viser at nanostaver ikke kan levere siRNA for å redusere genuttrykket av et stabilt uttrykt protein, når cellene sedimenterer ned på en plen av nanostaver ved hjelp av tyngdekraften. Det neste forsøket viser at nanostaver og flate (men ellers kjemisk like) overflater er omtrent like effektive i å levere plasmid til celler som sedimenterer ned på en plen av nanostaver. Sedimenteringshastigheten kan økes ved hjelp av en sentrifuge, men transfeksjonseffektiviten øker ikke, selv ved sentrifugeringshastigheter som tilsvarer en gravitasjon på $88.500 \times$ g. En velbeskrevet metode for å transfektere celler ved hjelp av nanostaver baserer seg på å deponere et høyt antall celler på en overflate, og så legge nanostavoverflaten på toppen, med nanostavene pekende nedover, for så å banke nanostavoverflaten ned på cellene. Denne metoden gir en høyere andel transfeksterte celler sammenlignet med sedimentering- og sentrifugeringsforsøk, vanligvis blir omtrent 1% av cellene transfekterte, og noen ganger en enda høyere andel (5%). Flate overflater viser imidlertid tilsvarende effektivitet i ellers identiske forsøk.

Plasmider som er merket med et fluorescent molekyl leveres forholdsvis effektivt til celler av både flate overflater og nanostavoverflater, med en antydet økt effektivitet for nanostavoverflater. Materialet som leveres er imidlertid avgrenset til små områder av cellene. Celler blir ikke transfektert i tilsvarende eksperimenter med funksjonelt plasmid, noe som tyder på at levert materiale er isolert fra det indre maskineriet til en celle.

Konklusjonen som trekkes er at transfeksjonseffektiviteten vi oppnår er tilsvarende den som oppnås av andre forskningsgrupper. Gode kontrollforsøk, med flate overflater, er imidlertid ofte utelatt i publiserte arbeider innen nanostavdrevet transfeksjon, og våre resultater viser at slike kontrollforsøk er avgjørende for at nanostaver skal kunne tilskrives observert transfeksjonseffektivitet.

Preface

This master thesis was done at the department of physics, NTNU. The experimental work was performed in the biophysics lab at the department of physics and in the cleanroom facilities of the NTNU NanoLab. I would like to express my gratitude for all help, guidance and encouragement provided by my supervisor professor Pawel Sikorski at the Department of Physics, and my co-supervisor professor Astrid Lægreid from the Department of Cancer Research and Molecular Medicine, NTNU. A very special thanks to ph.d-student Kai M.Beckwith, who always has time to discuss new experiments and strategies, and who is always interested in new results, especially when they were not as predicted. I've also enjoyed discussions with master student Jonathan Økland Torstensen, who has done his specialization project on nanowire-induced endocytosis. I would also like to thank ph.d-student Yngve Hofstad Hansen, who spent many hours to help me set up the fluorospectrophotometric experiments.

I would also like to thank the staff at the NTNU NanoLab, and Kristin Sæterbø at the cell lab at the physics department, who are always there to answer technical questions.

Contents

List of Figures

1 Introduction

1.1 Background

We, humans, consist of approximately 10^{13} cells working together to form us; our organs, our body, and our thoughts. Like us, our cells grow, reproduce and die.

Cells continuously regulate their constituents in order to function and prosper in changing surroundings, and to respond to stimuli from the outside. These constituents can be described at the nano-scale, but are not easy to measure. The core of cell functioning stems from the nucleus, where the genes reside. The genes of a cell holds the recipe for creating all the constituents of a cell, either directly (i.e. for proteins) or indirectly (i.e. for metabolites, synthesized by proteins). The central dogma of molecular biology explains how genes can be transcribed to transcripts, which can be translated to proteins [1].

Understanding the internal machinery of cells is a unifying goal in the field of molecular cell biology and complementary areas of research. Numerous techniques exist to probe the state of the cell. To understand the internal machinery of a cell, and how a given stimulus gives a certain response, one could try to interfere with the machinery itself. This can be done by introducing variations of genes that encode individual components of the machinery, and the change in response to known stimuli can elucidate the function of the altered component. The knowledge gained from such experiments can then be used to make idealized models of the internal machinery. Then one must consider how these components of the machinery interact as a whole. With systems biology, utilizing computer modeling of complex intracellular signal transduction networks become more and more important. High throughput (HTP) hypothesis testing is mandatory in this field of research, and being able to interfere with many cells' transcriptional and translational machinery in parallel is a necessity to do HTP hypothesis testing [2, 3, 4].

One technique used in HTP hypothesis testing is reverse transfection, where genetic material is first deposited on an array, whereafter cells are cultured on this array. The term 'reverse' is added to distinguish it from transfection where the genetic material is added to an already growing cell culture [5]. Reverse transfected cell arrays (TCA) are proposed as an important step towards analyzing the intricate signaling networks inside cells [3].

When it comes to introducing foreign genetic material, one challenge is the introduction of the genetic material itself, as cells have many barriers to protect it from

foreign genetic material. These protective mechanisms are located extracellularly and intracellularly. The cellular membrane is an integral part of the protective measures of a cell, and defines the border between the extracellular and the intracellular compartment. The cellular membrane can be overcome by different techniques, i.e. using viral vectors, carrier proteins, or simply by injection of genetic material using micro-needles. Arrays of nanowires can, through impalement of cells, offer a quick way to access the interior of cells, exposing the regulatory machinery governing the state of the cell. Whereas other transfection techniques rely on cellular uptake mechanisms, nanowires are envisaged to bypass all these by simply being pushed through the cellular membrane, and if successful this technique could therefore offer a universal approach for delivery of biomolecules to arrays of cells.

1.2 Project background

CuO nanowires have been studied for several years at NTNU[1]. The synthesis of CuO nanowires has been standardized, and the resulting nanowire array is reproducible from experiment to experiment - albeit with minor variations concerning areal nanowire density and length, partly due to the inherently random process of nanowire growth. The nanowires are embedded in a transparent polymer membrane, allowing for microscopy of live cells using inverted confocal laser scanning microscopy. The nanowires and nanowire-based devices have been well characterized by transmission and scanning electron microscopy (TEM and SEM respectively), also with HeLa cells grown on the nanowires [6, 7]. HeLa cells are cells derived from human cervical cancer, and has been an important cell line for basic medical research since it was isolated in 1951 [8]. AR42J, a cell line derived from rat pancreatic tumor cells, has also been grown on nanowire surfaces [9].

The interaction between cells and nanowires has been characterized using high-resolution TEM imaging. Even though structures as small as the cellular membrane, with a thickness on the order of 4-6 nm [10], are well resolved using TEM imaging, no complete proof has been given that the cell is actually penetrated by a CuO nanowire when the cells are allowed to sediment on a nanowire surface. A TEM image of a HeLa cell impaled by a CuO nanowire can be seen in figure 1.

The fluorescent DNA intercalator YOYO-1 can be used to confirm successful cellular delivery of DNA [11]. YOYO-labeled DNA can be seen taken up by HeLa cells, possibly in vacuoles, as seen in figure 2. However, it is still unknown whether the internalized cargo ever reaches the cytoplasm, or if the cargo is degraded.

To test whether the nanowires can actually deliver molecules to the cell's interior, transfection experiments have been conducted using DNA plasmids encoding green fluorescent proteins (GFP). If the experiment is successful the cell should become fluorescent. This has been shown to happen at a very low transfection efficiency (<1%) when cells are sedimenting onto the nanowires. Figure 3 shows cells successfully transfected with a GFP-encoding plasmid, but as can be seen from figure 4 only very few cells take up and express this plasmid.

After finding low transfection efficiencies it was hypothesized that perhaps only

---

[1]The project was initiated by professor Pawel Sikorski and then ph.d-student Florian Mumm, who continued his work on this project as a post.doc. Kai Müller Beckwith joined the project autumn 2010 for writing his nanotechnology master thesis, and is still working on the project, now as a ph.d-student. Jonathan Torstensen also joined the project autumn 2012 as part of his specialization project in the nanotechnology master program at NTNU.
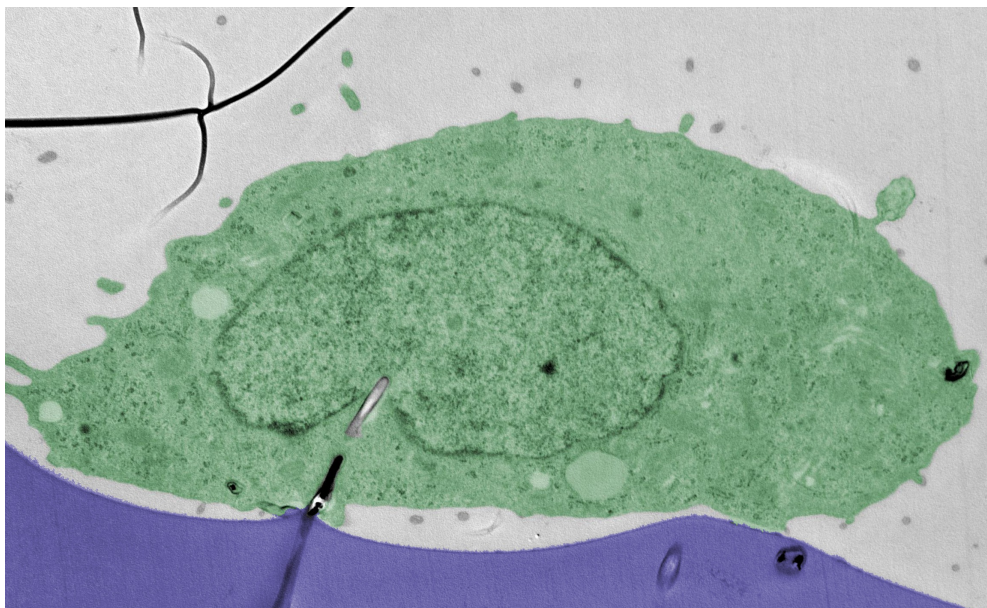
Figure 1: A HeLa cell (green) growing on a polymer surface (blue), impaled by a CuO nanowire (black). Around the portion of the nanowire that is inside the cytoplasm (green) a darker zone can be seen around the nanowire, and this may represent the cellular membrane, but it could also have other origins (i.e. artifacts, adsorbed proteins, cytoskeletal elements etc). Image provided by Kai M. Beckwith.
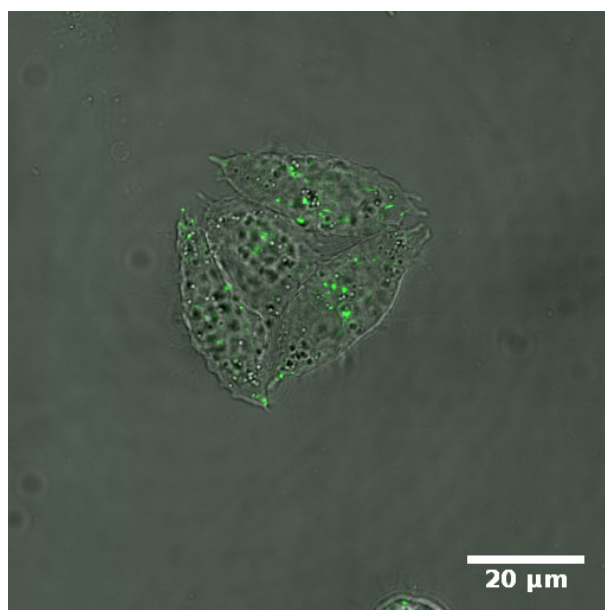
Figure 2: A HeLa cell growing on a CuO nanowire surface has taken up fluorescently YOYO-labeled DNA. Whether this fluorescently labeled DNA is subsequently released from these smaller compartments to the cell interior can not be assessed. Image provided by Kai M. Beckwith.
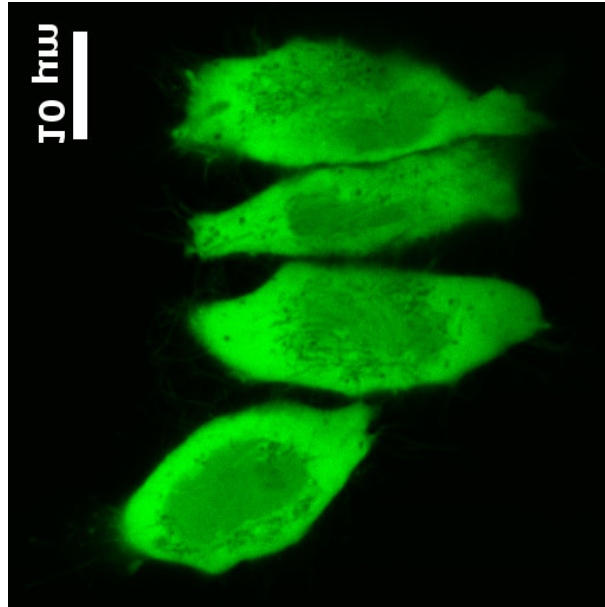
Figure 3: HeLa cells transfected with a GFP-encoding plasmid after adsorbing the plasmid to the CuO nanowire surface, and growing cells on the same surface. Image provided by Kai M. Beckwith.
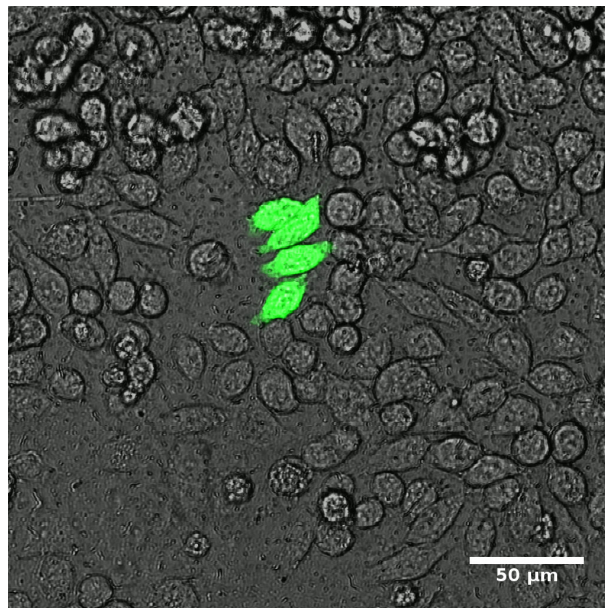
Figure 4: The same area as figure 3, but with lower magnification, reveals that only a few cells are successfully transfected. The four transfected cells in the image probably come from the same mother cell that was initially transfected, which explains why transfection apparently was effective in just a confined area of the sample. Image provided by Kai M. Beckwith.

17

the cellular membrane was penetrated, but that the nuclear membrane remained intact, effectively blocking transfection, since a plasmid must reach the nucleus to be expressed. To test this hypothesis experiments were done with AR42J cells constitutively expressing EGFP. RNA interference, whose integral parts are located in the cytoplasm of cells, was then targeted by the use of siRNAs. The delivery of siEGFP, an siRNA silencing the expression of EGFP, was attempted using silica coated nanowires [9]. Results were somewhat ambiguous, with no clear proof that cellular membranes were indeed penetrated.

1.3 The current project

The goal of this master thesis is to further test and optimize transfection of cells grown on nanowire surfaces. An experiment was first done as a conclusion to the siRNA experiments performed in the specialization project [9]. This final siRNA experiment shows no convincing siRNA transfection, indicating that the cellular membrane is not penetrated by simply allowing cells to sediment on a surface with nanowires protruding out of it.

Optimization techniques were then attempted to increase the efficiency of penetration. It is hypothesized that penetrating the cellular membrane will be sufficient for plasmid transfection, similar to other non-viral transfection techniques (and thus in contrast to the rationale for doing siRNA experiments). The approaches used to achieve a higher probability of membrane penetration can be divided into two categories: Increasing the pressure, and reducing the force barrier, i.e. increasing the force by which the nanowire indents the cellular membrane, and decreasing the force barrier by reducing the force barrier potency of the cellular membrane. In this report, mainly methods of increasing the pressure are sought. Two methods that are based on already published methods of increasing the pressure are used (tapping and sedimentation), and a third method is also extensively tested (centrifugation). Some experiments also include efforts to reduce the force barrier, namely by osmotically swelling cells before centrifugation. Results presented here are also contrasted with results published by other scientists.

2 Theory

2.1 Molecular cell biology

'The central dogma' of cell biology describes how information flows in a cell between DNA, RNA and protein, and states that information in general flows from DNA to RNA to protein [1]. During DNA replication information flows from DNA to DNA, and in some special circumstances information can flow from RNA to RNA or RNA to DNA (e.g. during viral infections). The cellular regulation of interactions between DNA, RNA and proteins define the state of the cell, and the understanding of how this process is regulated has increased substantially since it was first formulated in 1958 [12]. The process is shown in some more detail in figure 5.

Double-stranded DNA holds all the genetic information needed to direct the embryonic development of an organism, and to sustain life in changing conditions after development is completed. This information is encoded in a sequence of four nucleotides: adenine (A), cytosine (C), guanine (G), and thymine (T). During *transcription* mRNA strands are synthesized from DNA, and hold the complementary set of bases to the gene that served as a template, and with the base thymine exchanged for uracil (U). The first RNA strand formed during transcription is termed pre-mRNA, and is further processed in several steps before being exported as mRNA to the cytoplasm. These processing steps include:

- 5'-cap addition, where modified guanine nucleotide is added to the part of the RNA-strand first transcribed (the 5'-end),

- splicing, where non-coding parts of the RNA strand (introns) are removed to join the protein-encoding sequences (exons), either by joining all exons, or by joining only a subset of exons in a process termed 'alternative splicing', and

- polyadenylation, where a chain of adenylyl residues are added to the 3'-end of the RNA strand.

The process of alternative splicing allows one gene to encode several different mRNA transcripts.

From the mRNA strand, triplets of the four nucleotides A, C, G and U are *translated* into corresponding amino acids in the protein by ribosomes located in the cytoplasm. Ribosomes are complex molecular machines composed of both RNA and protein, and can be either membrane-bound in the endoplasmic reticulum, or freely moving around in the cytoplasm.
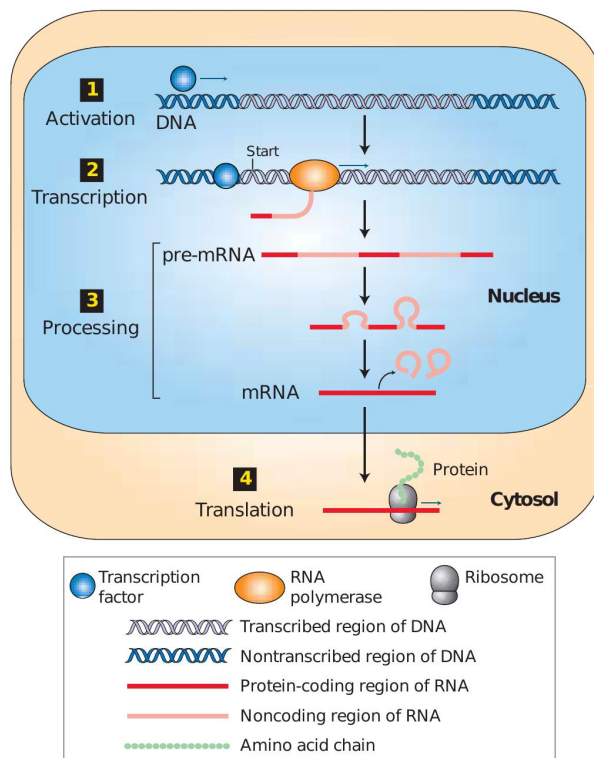
Figure 5: The central dogma states that information, in general, flows from DNA to RNA to protein. In the image the process is shown, where 1) transcription factors bind the regulatory regions of their target genes, 2) followed by the assembly of a multi-protein initiation complex bound to DNA. RNA polymerase, a part of this complex, then begins transcription of the target gene, and the polymerase moves along the DNA linking nucleotides into a single-stranded pre-mRNA transcript using one of the DNA strands as a template. 3) The transcript is processed inside the nucleus, removing non-coding regions and thus forming messenger RNA (mRNA), which subsequently is transported from the nucleus to the cytoplasm. 4) In the cytoplasm ribosomes bind mRNA, and the nucleotide sequence directs the assembly of amino acids in a process where triplets of nucleotides correspond to specific amino acids. Image is taken from reference [13].

All organisms have several ways to control when and in which amounts their genes should be transcribed, or *expressed*. This control is adamant to orchestrating the development of an organism, and to enable the organism to adapt to ever changing environments. Transcription factors provide one layer of gene expression regulation, and function in binding DNA and then activating or repressing transcription of target genes. Typically transcription factors recognize short DNA sequences about 6-12 base pairs long, and with four possible bases at each position this means that a DNA strand of 10 base pairs can have 4^{10} possible sequences (slightly over 1 million).

Transcription factors work in concert as part of multi-protein complexes, where some are responsible for recognizing a particular gene, and others are responsible for initiating or blocking transcription.

More details on the molecular basis of cell biology, including transcription, translation and gene regulation, can be found in reference [13].

2.2 Transfected cell arrays and high-throughput cell perturbation

The understanding of biology at the molecular level is advancing rapidly, partly as a consequence of the fact that the number of newly discovered proteins has increased rapidly over the last decades. However, the function of many genes and proteins is still unknown, and the understanding of how these genes and proteins participate in signal transduction and in gene regulatory networks is in its infancy. One way to elucidate how gene regulatory networks are constructed is by removing a gene one by one: Based on total genome analysis after each perturbation experiment, hypotheses about how the gene regulatory network is wired can be made. siRNAs and shRNAs are central molecules to these gene knockdown/knockout experiments [14], and based on such experiments gene regulatory networks can be reconstructed. One example is the reconstruction of a transcriptional network that provides dendritic cells (an integral part of the immune system) with the ability to distinguish between different classes of pathogens, i.e. viruses, bacteria, fungi and parasites [2]. Understanding cells and diseases from a networks perspective is however still in its infancy [15]. Reverse transfected cell arrays, using RNAi perturbation in an array format, allows many cell phenotypes to be investigated in parallel [5, 16], thus probing many hypotheses about the wiring of intracellular regulatory networks in a single experiment. RNAi microarray analysis is one type of high-throughput functional genomics studies. The use of reporter plasmids with fluorescence intensity as output data is one way to study the perturbation of many cells in parallel [17, 18, 19].

Introducing genetic material to a cell in order to change its genome or expression profile is termed transfection. Reverse transfected cell arrays were first described by Ziauddin and Sabatini, and are based on first printing genetic material on confined areas of a slide, followed by growing cells on the slide [5]. Cells will only take up the genetic material directly under it, and these cell arrays can be used to create spots of cells transfected with a specific nucleic acid sequence within a lawn of non-transfected cells, as seen in figure 6.
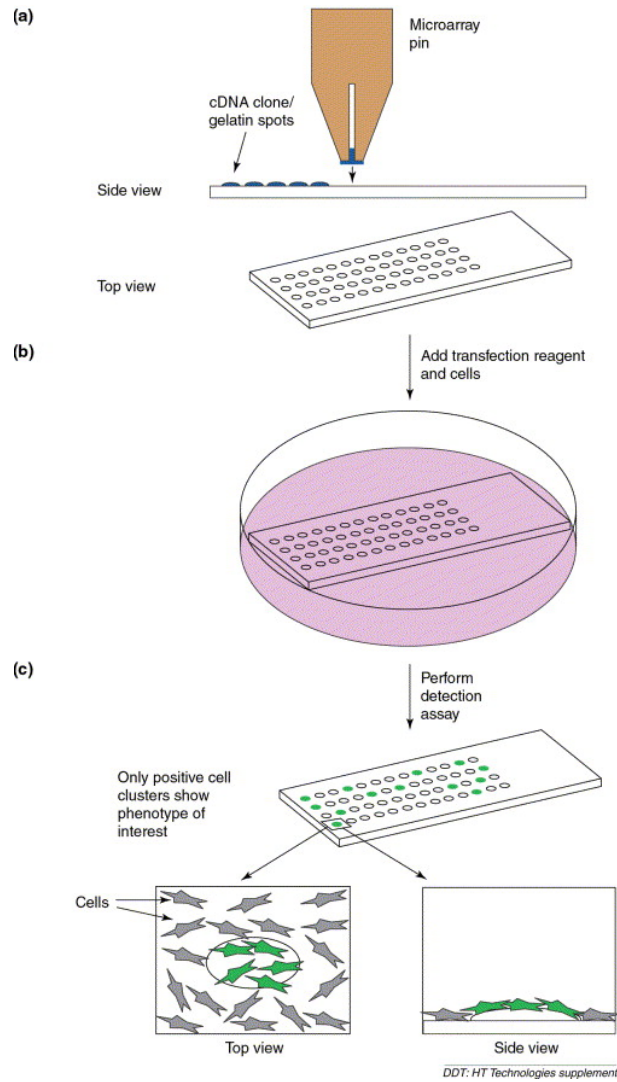
Figure 6: Reverse transfected cell microarrays use a) a robotic printer or a handheld printing device to transfer small amounts of genetic material to defined spots, b) then transfection reagents and cells are added, and c) only cells grown on the printed spots will be transfected with the nucleic acid it is grown on top of. Image is taken from reference [20].

2.3 Transfection

Many techniques have been employed in transfecting cells, i.e. the process of deliberately introducing foreign genetic material in a cell in order to change the genome or gene expression profile. All these techniques have to overcome the same set of barriers:

- The cellular membrane: The cellular membrane is a protective lipid bilayer surrounding the cell, protecting the interior from the exterior. Since the cell

has to communicate with the exterior, and gain nutrients from the outside world, several mechanisms to transport both larger and smaller molecules exist. Receptor-mediated endocytosis is one transport mechanism often targeted.

- Intracellular trafficking: After uptake through endocytosis, endolysosomal escape is important to avoid degradation of nucleic acids. Genetic material and other bioactive molecules escaping the endolysosomal system must then avoid degradation in the cytoplasm. Plasmids containing DNA must successfully be transported to the nucleus, cross the nuclear membrane, and interact with the transcriptional machinery, whereas siRNA molecules targeting mRNA transcripts only need to reach the cytoplasm to affect gene regulation, through RNA interference.

2.3.1 RNA interference

RNA interference (RNAi) is a quite newly discovered layer of gene expression regulation [21, 22], previously also known by the descriptive term post-transcriptional gene silencing (PTGS) [23]. RNA interference utilizes partial or complete base pairing between a shorter RNA molecule, and its target RNA that is degraded. These shorter RNA molecules can have both endogenous and exogenous origins, and the most common types of RNAs include siRNAs (short interfering RNAs), micro RNAs (miRNAs) and shRNAs (short hairpin RNAs). Several variations over RNA interference exist, and the one unifying theme between all RNAi-related pathways is the involvement of the Argonaute protein, which executes cleavage of a target mRNA in the cytoplasm of the cell, thus reducing the level of mRNA available for translation, and in effect reducing the level of a specific protein [24]. The specificity of RNAi is obtained through the complementary base pairing between siRNA and mRNA. The mRNA targeted for silencing is degraded, explaining the potency of RNAi. The relationship between siRNAs and miRNAs is illustrated in figure 7.

RNAi was originally believed to be an evolutionary ancient mechanism of defense against foreign genetic material, especially viruses, but today it is becoming evident that RNAi is part of the regulation of gene expression through the regulation of miRNA-levels and levels of target RNA molecules [26, 27, 28].

Introducing double-stranded siRNA precursors is one way to use RNAi for gene silencing in an experimental setting. Double-stranded RNA (dsRNA) molecules are artificially produced with a sequence based on the mRNA of the target gene. One of the two strands will have the same nucleotide sequence as a portion of the target
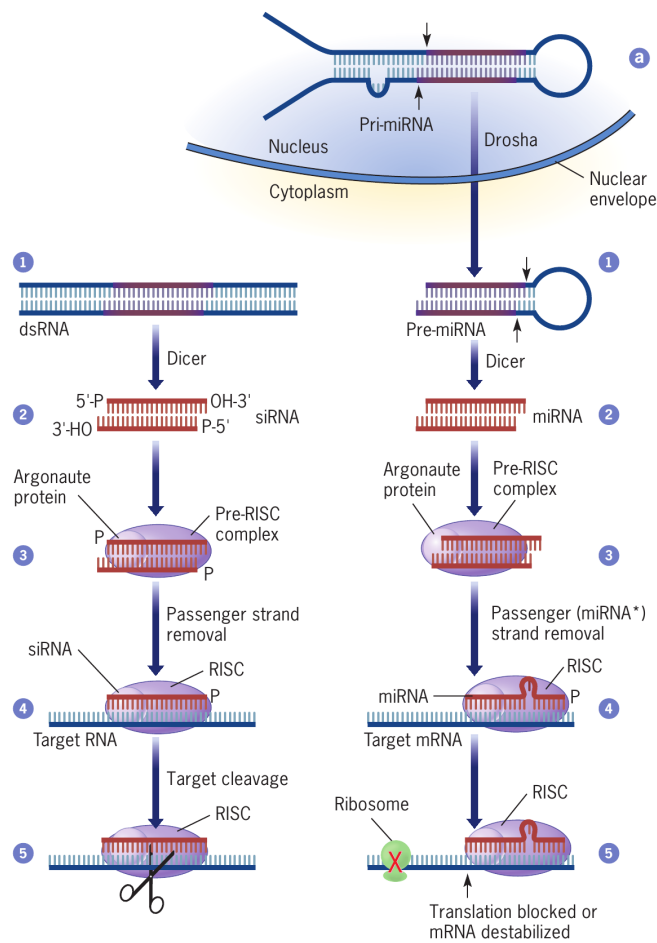
Figure 7: siRNA and miRNA follow similar processing pathways. 1) siRNA is introduced as a dsRNA, whereas miRNA is transcribed from a gene located in the nucleus. Both are cleaved by Dicer, 2-3) loaded in the RISC complex, and 4) bind target RNA molecules through complementary base pairing that is then 5) degraded through cleavage by the Argonaute protein. Image is taken from reference [25].

mRNA, and the other strand will have the complementary nucleotide sequence. dsRNAs are processed to shorter nucleotide strands of 21-25 nucleotides in length by the enzyme RNase III Dicer. Single-stranded siRNAs are then incorporated in the RNA-induced silencing complex (RISC). Argonaute is a core component of RISC, and directed by the siRNA molecule it will execute cleavage of target mRNAs in the cytoplasm of cells [29, 30].

Another common technique for silencing specific gene products is through the use of plasmid transfection of short hairpin RNAs (shRNAs) that are then constitutively expressed by the cell. These shRNAs are processed into shorter RNA strands that utilize RNAi, in order to silence target mRNAs [31, 32, 33, 34]. siRNA molecules

are reported to be rapidly degraded, with less than 1% of the introduced duplex remaining in the cell after 48h, whereas shRNAs are continuously expressed by stably transfected host cells [34].

Single miRNAs or siRNAs are known to be able to silence several targets, and in varying degrees, depending on the extent of base-pairing with its target RNA [32]. Also targeting one of the RNAi pathways, i.e. the siRNA-targeted or the miRNA-targeted pathway, can result in changed activity in another pathway, as a competition between the pathways does exist [24].

2.3.2 Viral transduction

Using viruses to deliver foreign genetic material to cells has been studied for decades, and historically viral delivery systems represent the bulk of effort in DNA delivery systems [35]. Viruses are composed of proteins, lipids, and genetic material, and are highly efficient in high-jacking the transcriptional and translational machinery in a cell for producing replicates of itself. The most common types of viruses used are adenovirus, adeno-associated virus (AAV), herpes simplex and retrovirus (including lentivirus). Of these, all classes but retroviruses carry the genetic material as DNA, which can be incorporated in the host's genome. Retroviruses represent a class of viruses that carry their genetic information in a single-stranded RNA molecule, which is transcribed into DNA using the enzyme *reverse transcriptase* before being integrated in the host's genome.

Viruses can be exploited to insert specific genes by modifying or exchanging the DNA/RNA they carry, and this is the basis of viral transduction. Viruses come with a full set of features to facilitate cellular uptake, avoid degradation and to be transported to the nucleus. Viral transduction of genetic material has been sought as a cure for many diseases, including cystic fibrosis, severe combined immunodeficiency, HIV/AIDS, cancer and malaria, but adverse reactions in clinical trials, including death, has reduced the enthusiasm that once surrounded this area of research [36]. Due to these severe reactions to viral transduction, non-viral transfection techniques are being researched for clinical use.

2.3.3 Chemical transfection

Chemical transfection uses complexes of genetic material with chemicals such as lipids, polymers, peptides, or combinations of these. The main advantage over viral transduction is low immunogenicity, low toxicity, and applicability to large-scale pro-

cessing. Negatively charged nucleic acids (DNA or RNA) are electrostatically bound to positively charged carrier molecules. Some of these complexes reuse mechanisms learnt from viral transduction, and could for instance include viral proteins that enhance passing the cargo over the cellular membrane. However, chemical transfection techniques display a lower efficiency than viral transduction [36].

2.3.4 Physical transfection

Physical transfection is based on the delivery of genetic material to a cell, without using viruses or chemicals to facilitate transfection. *Naked DNA* is an expression used for the delivery of naked, or free, DNA, and has been shown to be useful in gene transfer to skeletal muscle, liver and heart muscle, albeit with low transfection efficiency [35]. Microinjection is based on a simple mechanism, where genetic material is injected in a cell using a nanoneedle/nanosyringe or nanowire. Thus, microinjection efficiently bypasses the cellular membrane - and possibly also the nuclear membrane can be penetrated. Other common physical transfection techniques include electroporation, biolistic particle delivery, laser-irradiation, sonoporation and magnetic nanoparticles [37].

Methods, techniques and molecular components of viral, chemical and physical transfection techniques can also be combined and integrated in the process of finding new ways to transfect cells.

2.3.5 Synthesis of one-dimensional high aspect-ratio nanostructures for transfection

Nanowires can be used in physical transfection techniques. Nanowires are nanostructures where two dimensions are on a length scale less than 100 nm, as in round cylinders with a diameter of less than 100 nm, and are often referred to as one-dimensional (1-D) structures. The aspect ratio is the length to width ratio, and can be over 1000:1. Nanowires can be used in a similar way as microinjection, but in contrast to microinjection, using arrays of nanowires one can deliver genetic material to many cells in parallel. Nanowire-mediated transfection through impalement has been termed impalefection [38]. Nanostructures can generally be synthesized by either a top-down or a bottom-up approach. Some examples from the literature are provided in figure 11, in chapter 3.

Bottom-up approach: Catalyst-grown nanowires

There are several catalyst-grown one-dimensional nanostructures being studied with respect to impalefection. Two of the most established catalyst-grown nanowires in this respect are vertically aligned carbon nanofibers, and catalyst-grown silicon nanowires. Indium-arsenide nanowires and gallium-phosphide nanowires will also be briefly presented.

Vertically aligned carbon nanofibers (VACNFs) was the first method of reverse transfection using nanosized structures to be published [39, 38]. VACNFs are grown in parallel on a flat substrate, and are linked to genetic fragments, e.g. plasmids, either trough adsorption or through covalent bonding. Covalently bound plasmids can interact with the cells genetic machinery as long as the cells are grown on the transfection array, and genetic elements are not inherited to progeny cells, whereas adsorbed genetic material can be inherited. Adsorbed material will interact with the cell until the genetic material is broken down, while covalently linked plasmids are protected from degradation [39].

VACNFs can be synthesized in a variety of ways. In the works by McKnight et al. nickel particles with a diameter of 500 nm are used as catalysts. The nickel particles are spatially organized, using photolithography to define spots for nickel deposition using physical vapor deposition (PVD). The VACNFs are grown on n-doped silicon wafers, and the growth is achieved using plasma-enhanced chemical vapor deposition (PECVD) from a mix of acetylene and ammonia. The dimensions of the fibers are somewhat heterogeneous, and fibers are 6-10 µm in length with tip diameters of 20-50 nm and base diameters of approximately 1 µm [39]. Catalytic plasma-enhanced CVD (PECVD) allows precise control over location, alignment, size, shape and structure of each individual nanofiber during synthesis, using lithographically patterned catalysts [40].

The dimensional properties of the VACNFs can to some extent be controlled by the experimental setup, and Cassell et al. obtained VACNFs with a uniform diameter in the range 30-100 nm, depending on the PECVD conditions, and lengths of ~700 nm, controlled by growth time [41, 42]. VACNFs are inferior in electrical and mechanical properties compared to the regularly structured multi-walled carbon nanotubes (MWCNTs) [42], but MWCNTs have proven difficult to be grown vertically and spatially controlled on a substrate using CVD, even with patterned catalyst features with strictly controlled spot sizes.

Transfection efficiency, i.e. the ratio of the number of expressing cells over the total number of cells on the chip, was variable, and efficiency for fibers with a diameter of 200 nm was less than 5% [38].

Silicon nanowires (SiNW) are more recently characterized with respect to impalefection and reverse transfection [43, 44]. SiNW can be grown from silicon wafers using CVD with gold nanoparticles as a catalyst [45], and as discussed later they can also be formed through etching of silicon wafers [46].

Hochbaum et al. used gold nanoparticles for nanowire synthesis by the vapor-liquid-solid (VLS) growth mechanism, using $SiCl_4$ as the precursor gas in a CVD system. Precise growth and epitaxial alignment of the SiNWs has only been achieved using lithographically defined regions of SiNW growth by thin film evaporation, and these methods employ expensive processing techniques with limited control over nanowire size and areal density [45, 47]. VLS growth by chemical vapor deposition can produce epitaxially aligned, single-crystalline silicon wires from thin gold films. Metal thin film does however not allow for good diameter control of the resulting wires due to the randomness of the film breakup at reaction temperatures [45]. Hochbaum et al. used a thin polyelectrolyte layer to attract and immobilize gold colloids on the substrate, which then act as seeds for silicon nanowires grown using the VLS-CVD method. The position of the SiNW is random, due to the random deposition of the gold colloids. Spatial control of grouped SiNW growth can be achieved by patterning regions of seed particles, using a PDMS stamp for microcontact printing, while the position of each individual SiNW is still random within the region of seed particles [45].

To obtain a true spatial control of the SiNWs the location and size of the gold catalysts can be defined using lithography [44]. From a (111) Si wafer the SiNW will be grown as a single crystal in the ⟨111⟩ direction. Hochbaum et al. used $SiCl_4$ as the precursor molecule for SiNW growth in the CVD system, using a temperature between 800 and 850°C [45]. The diameter of the colloids controls the nanowire diameter, and colloid solution concentration controls the areal density of growth. The thinnest vertically grown nanowires had an average diameter of 39 nm ± 3.7 nm, grown with 20 ± 2.1 nm diameter gold colloids, and the size distribution of the nanowires is attributed to the size distribution of the seed particles. Hochbaum et al. obtained an areal density of ~0.1-1.8 μm^{-2}. Kim et al. made silicon nanowires on a similar setup and obtained nanowires with a diameter of 90 nm and a length of 6 µm [43]. When adjusting the areal density so that each cell was pierced by 2-3 nanowires, they showed that cell viability increases with decreasing diameter of the nanowires, and this is thought to be a general phenomenon for impaled cells [48].

Indium-arsenide (InAs) nanowires and gallium-phosphide nanowires have been studied by Berthing et al., in order to probe electrical properties of neurons [48].

These nanowires were created with the semiconducting capabilities of InAs in mind, and not to deliver drugs. They are mentioned here because they were fabricated with another bottom-up technique, using gold particles as catalyst. The InAs nanowires were created using molecular beam epitaxy (MBE) growth, where the InAs wafer was exposed to gold atom bombardment. The gold atoms condense and aggregate into nanosized particles on the surface, and the gold particles then serve as a catalyst to grow InAs nanowires when the substrate is continuously exposed to molecular beams of In and As_2 at a temperature of 430-440°C. A similar setup was used by Hällström et al. [49], for creating gallium phosphide nanowires, using deposited gold particles as catalysts for a VLS-based synthesis of nanowires, and they could show better survival of neurons grown on nanowires than neurons grown on a flat glass substrate.

Top-down approach: Etching and focused ion beam milling

Etching: Ovchinnikov et al. used self-organizing gold-chromium nanodots as an etching mask [46, 50] to control spatial distribution of the SiNWs. Etching is generally considered a top-down approach, but the self-organizing mask can be regarded as a bottom-up approach. As with other types of etching there is a limit to how steep the structures can be (i.e. high aspect ratios are difficult to obtain). Ovchinnikov et al. used sequential depositions of gold and chromium films on a (100) p-type silicon substrate, followed by annealing, using electron-beam evaporation under high vacuum at room temperature, and then heating to 900°C for 5 s in nitrogen, to form a self-organized mask by coalescence of gold-chromium layers. A reactive-ion etching (RIE) reactor was then used for anisotropically etching the silicon wafer, directed by the self-assembled mask. The nanowires created are spatially disordered. By varying the thickness of the layers the particle diameter can be adjusted between 55 and 80 nm, and the height between 7 and 12 nm. Thinner films give bigger islands, probably due to the anticoagulant influence of chromium, which decreases with decreasing thickness of the chromium layer. Three different pillar shapes are created: straight sidewalls, conical and overcutting. Big mask erosion takes place during the RIE process, so a thick mask layer is needed for deep etching, and after optimizing the rf-power and pressure Ovchinnikov et al. were able to obtain a maximum pillar height of 600 nm with a mean pillar diameter of 60 nm.

Focused ion beam milling: Xie et al. used focused ion beam (FIB) milling to create nanowires of platinum [51] and then cultured neurons on these nanowires. Platinum was chosen because of the possibility to directly measure the electrical

activities of attached neurons, and they did not investigate if these wires could be used for transfection. FIB gives a precise control over the spatial arrangement of the nanowires, and is based on bombardment with ions, resulting in physical sputtering of the sample material (milling). Xie et al. tested nanowires with a diameter of 75-400 nm, and a height of 700 nm to 2 µm and, in contrast with Kim et al. [43], found that cell survival was not correlated to the size of the pillars in the tested range.

The main obstacle to the currently researched methods of nanowire fabrication is the time-consuming process, with relatively expensive materials and expensive setups required, thus rendering these approaches less suitable to high-throughput experiments, where cost per experiment should be as low as possible.

Certain materials can be used to create one-dimensional nanostructures in air, through thermal oxidation of a metal film, without the need for catalyst particles. This is already shown for materials such as copper[52], iron [53] and zinc [54].

Thermal oxidation

Jiang et al. have shown that CuO nanowires can be grown by a simple procedure where a copper surface is cleaned, dried and then heated in air to 400-700°C for 4 hours, at ambient pressure [52]. Jiang et al. were able to grow nanowires with a diameter of 30-100 nm, and a length of 15 µm, the height being controlled by growth time (growth rate of ~3 µm/hour). Because of the relatively simple steps needed for synthesis, CuO nanowires can thus be used in high-throughput nanowire-mediated transfection experiments.

2.3.6   The cellular and nuclear membrane barriers

The cellular membrane

Chemical transfection reagents (i.e. cationic complexes/lipofection) are thought to enter cells by endocytosis [55, 56, 57, 58, 59]. Nanowire-mediated transfection seeks to bypass endocytosis and other cellular uptake mechanisms by simply pushing the genetic material through the cellular membrane.

Experiments where nanowire tips on AFM probes are inserted into cells provide an indication of the force barrier that has to be overcome in order to penetrate the cellular membrane. In one experiment it was shown that cylindrical silicon nanoneedles with a diameter of 200 nm penetrates a cell when a force of 0.65 ± 0.28

nN was applied (92% insertion probability), with an indentation depth of 610 ± 270 nm before penetration. For cylindrical nanowires with a diameter of 800 nm the force required was similar (0.67 ± 0.37 nN), but with a higher indentation depth of 1900 ± 810 nm [60]. This system has also been used to transfect single cells, with a transfection efficiency of 74% [61].

The nuclear membrane

The nuclear membrane is the barrier separating the DNA replicating and transcribing machinery from genetic fragments introduced to the cytoplasm. The process of nuclear entry of plasmid DNA is only scarcely known, and increased understanding of this barrier is considered important to non-viral gene delivery [62]. It is however probably not mandatory to reach the nucleus by physically pushing the plasmid into the nucleus, as reports on microinjection show that DNA complexed with cationic lipids directly injected to the nucleus are expressed at a lower level than DNA complexed with cationic lipids injected to the cytoplasm [58]. Other reports have shown a higher transfection of DNA-cationic lipid complexes injected to the nucleus than the cytoplasm [63].

It is thought that the nuclear barrier is passed in dividing cells during mitosis, since the nuclear membrane is degraded in this process [62, 64], but also non-dividing cells can be transfected, albeit at lower transfection efficiencies [65, 66]. Based on these considerations, DNA that reaches the cytoplasm of dividing cells, and which can desorb from the nanowire, should be expressed by the impaled cell. Successfully transfected cells would thus be rendered fluorescent, if a plasmid encoding a fluorescent protein is delivered. Fluorescent reporter proteins can then be observed by scanning confocal microscopy, as well as other techniques (e.g. flow cytometry and fluorescence microscopy).

2.4 Scanning confocal microscopy

Scanning confocal microscopy is a fluorescent light microscopy technique, where a confocal aperture (such as a pinhole) is inserted in the path of the image forming beam to reject all light collected from out of focus planes, giving an image of a thin plane only [67]. Fluorescent light is used to image the focal plane, and due to the Stoke's shift the emitted light has a higher wavelength than the excitation light, allowing for separation of source light and fluorescence light based on inserting filters in the optical pathway. Stoke's shift is the difference in wavelength/frequency

between maximum absorption and emission of the same electronic transition. Stoke's shift occurs because the excited molecule loses a small amount of the absorbed energy as thermal energy/vibrational relaxation before releasing the rest of the energy as a photon with higher wavelength, termed fluorescence. The sample is scanned in a raster pattern. The schematics of a confocal microscope is shown in figure 8.
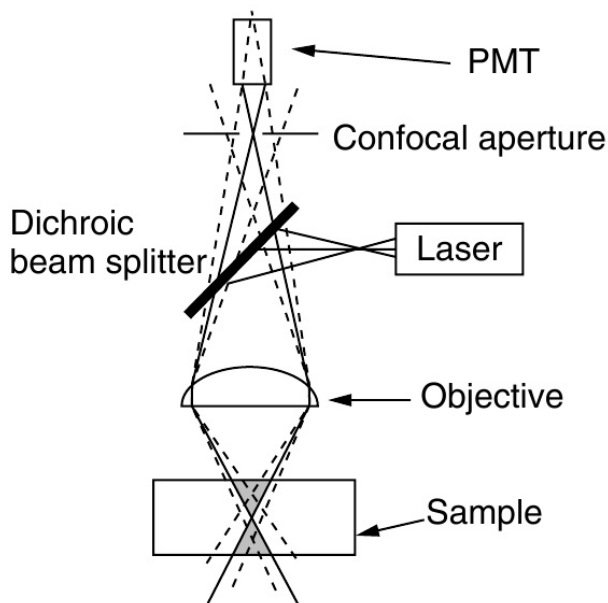
Figure 8: The figure shows a confocal microscope with a laser for excitation of fluorophores, a confocal aperture to remove light collected from out of focus planes, and a photo-multiplier tube (PMT) for detecting light and to convert the amount of light to an electrical signal. In this figure the microscope is set up in a reflection system, and the objective lens therefore also functions as a condenser lens. Image is taken from reference [67].

The most important settings that need consideration when using confocal laser-scanning microscopy can be summarized as:

- Excitation wavelength: The excitation wavelength is determined by the laser used, and should be chosen to match the absorbance wavelength range for the fluorophore used.

- Detector range: The fluorophore will emit light with a longer wavelength than the excitation wavelength (due to the Stoke's shift), and the range should be chosen so that as much of the light emitted is collected, while avoiding cross-talk with the emission spectra of other fluorophores and the excitation wavelength.

- Detector gain: Changing detector gain determines the sensitivity of the detector by setting the maximum intensity limit. This should be set so that the brightest spots sampled will have a maximum digital intensity (a numeric value of 255 for an 8-bit sensor).

- Amplifier offset: Changing the amplifier offset determines the minimum intensity limit recorded by the detector. The amplifier offset should be set so that the spots of interest with lowest intensity are just detected (a numeric value close to zero).

- Pinhole: Changing the size of the pinhole will affect the height of the scanned volume. A larger pinhole will allow light from a larger depth range to enter the detector, thus decreasing resolution in the z-direction. A smaller pinhole will allow less light to pass, and the choice is usually set to 1 Airy unit to give an optimal compromise between depth discrimination and efficiency (1 Airy unit is the diameter of the first intensity minima circle in an Airy disc).

Several types of fluorophores are available. Some endogenous fluorophores, like NADPH and flavin are autofluorescent, and can be used to image cells. Exogenous fluorophores are usually small organic molecules with conjugated aromatic cyclic structures, and these can be functionalized to only bind specific targets (e.g. proteins, DNA). Detection of fluorescence should be optimized and controlled so that fluorescence from exogenous fluorophores exceeds autofluorescence.

A common problem encountered in fluorescence microscopy is photobleaching. Photobleaching generally refers to chemical degradation of a fluorophore, leading to reduced excitability and reduction of fluorescence.

A commonly used fluorophore in biology is the green fluorescent protein and its variants.

2.5 Fluorescent reporters

2.5.1 Green fluorescent protein (GFP)

Green fluorescent protein was first discovered and characterized from the jellyfish *Aequorea victoria* [68, 69]. GFP is a green fluorescent fluorophore encoded by the primary amino acid sequence of the GFP gene, and it forms spontaneously without the requirement of cofactors or external enzymes, other than molecular oxygen, through a self-catalyzed protein folding mechanism [70]. In 1996 the crystal structure

of GFP was determined [71], revealing that the cyclic tripeptide fluorophore is buried in the center of a cylinder formed by a tightly interwoven eleven-stranded "β-barrel" structure, as seen in figure 9.
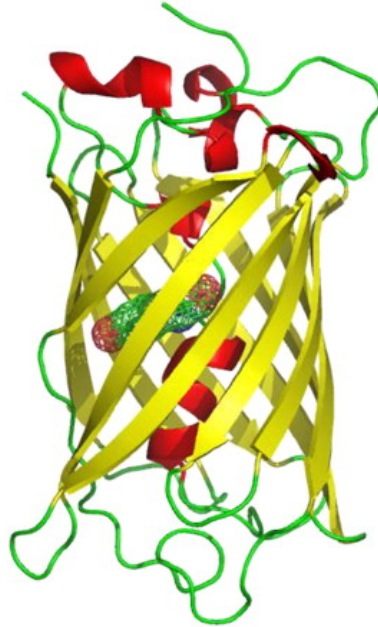
Figure 9: The protein structure of GFP, showing the "β-barrel" surrounding the fluorophore. Image is taken from reference [72].

Many variations of GFP has been made, with different colors [73], pH insensitivity, enhanced photostability, and fluorescence intensity [74]. Wild-type GFP has an intracellular half-life of approximately 26 hours in cultured mouse cells (LA-9) [75]. Destabilized versions of EGFP exist, one being encoded by the plasmid pEGFP-d2-N3 (Clontech) with a defined protein half-life of 2 hours [16].

The absorbance and emittance spectra of GFP is illustrated in figure 10. EGFP, which is the most commonly used variant of GFP, has an excitation peak at 488 nm, and a red-shifted emittance with a peak at about 509 nm.

2.5.2 The fluorescent dye YOYO-1

Oxazole yellow homodimer YOYO-1 is a fluorescent dye that is used to stain DNA, and binds DNA by reversibly intercalating between base-pairs [76, 77, 78]. It binds DNA with a high association constant, and exhibits a strong fluorescence enhancement when interacting with double-stranded DNA, and thus provides a high signal-to-noise ratio. Also YOYO-1 is quite resilient to photobleaching, which makes YOYO suitable for long-time imaging [79]. YOYO-1 has an excitation peak of

34
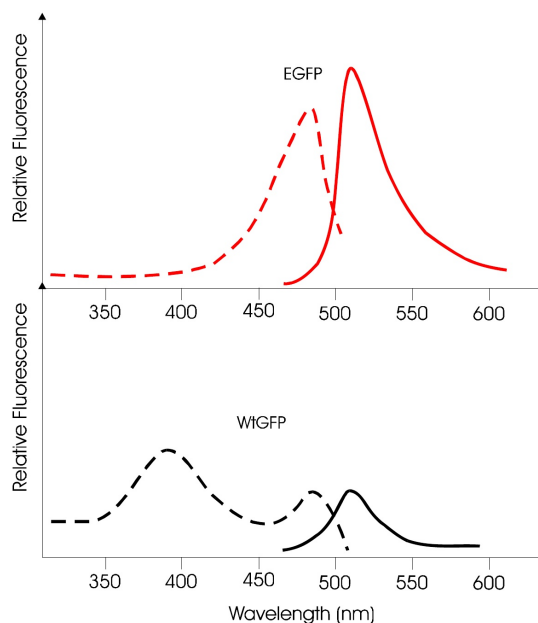
Figure 10: EGFP and wild-type GFP absorbance and emittance spectra. The red-shifted variants, like EGFP, have a single excitation peak centered at about 488 nm, with an emission peak wavelength of 509 nm. The wild type like variants have their primary excitation peak centered on 395 nm, with an emission peak at 509 nm. The image is taken from the BioTek website (http://www.biotek.com/resources/articles/green-fluorescent-proteins.html).

491 nm, and emission peak of 509 nm [79].

2.6   Image analysis using ImageJ

ImageJ is a multi-platform Java-based software application commonly used in image analysis in the scientific community [80]. The first version was released in 1997, and since then many extensions (i.e. plugins, filters, macros etc) have been added to address specific needs of scientists investigating a particular area of research. Among the huge amount of possibilities offered by ImageJ, only a few are used for the work described in this report. ImageJ allows measuring fluorescence intensities for a whole image or subsections of it, as well as offering simple and sophisticated tools to remove background signal/noise.

ImageJ allows 3D stacks to be built from sets of images, each image spanning an area in the xy-plane, and representing a given focal plane in the z direction. A three-dimensional stack then allows reconstructions of xz- and yz-planes, and this

can be used to investigate protrusions from a surface extending to the inside of a cell.

2.7 Fluorescence spectroscopy

Fluorescence spectroscopy, like scanning confocal microscopy, uses a light source to excite a fluorophore. A detector is placed at a 90°angle to the axis of the incoming light, and the fluorescent spectrum emitted by the fluorophore can be analyzed. By measuring the fluorescence intensity of a few reference samples, the unknown concentration of a fluorophore in a fluid can be determined.

The Beer-Lambert law for light absorbance shows how the intensity of the detected light I is related to the intensity of the incoming light, I_0, the thickness of the the the specimen x, and the concentration of the light absorbing molecules c:

$$\frac{dI}{dx} = -I\sigma c \tag{1}$$

where σ is known as the molar extinction coefficient. For $x = 0$ no light is absorbed, i.e. $I = I_0$:

$$ln\frac{I_0}{I} = \sigma cd \tag{2}$$

where d is the thickness of the sample. The same general relationship holds for fluorescence emission, since light must be absorbed to generate fluorescence. The intensity of the detected light thus has a logarithmic relationship to the concentration, and for low concentrations the relationship is almost linear. For further discussion of fluorescence spectroscopy see reference [81].

2.8 Centrifugation

A centrifuge will be used to in order to increase the sedimentation rate of cells, and thus increase the force applied to the interface between nanowire tips and cellular membranes, to increase the probability of perforation. The basic theory of centrifuges will be presented here, for a further discussion of centrifuges see reference [82].

A centrifuge is based on inertia mimicking a gravitational field, where the moment of inertia (and thus the fictional gravitational constant) can be controlled by adjusting the rotating speed of the centrifuge. The relative centrifugal force (RCF)

is traditionally used to indicate the acceleration relative to earth's gravitational constant. RCF is calculated from the angular speed ω, the radius of rotation r, and the gravitational field constant g:

$$RCF = \frac{\omega^2 r}{g} \tag{3}$$

As can be seen from equation 3 RCF is a dimensionless quantity. It is common to indicate the acceleration in terms of multiples of 'g', or '× g', and that tradition is followed in this work, i.e. the RCF that we experience when walking around in earth's gravitational field is 1 × g. Centrifuge speeds are commonly measured in rotations per minutes (rpm), which can be converted to angular speed measured in radians per second:

$$\omega = rpm \times \frac{2\pi}{60} \tag{4}$$

Two forces will govern the movement of a sphere in a centrifuge: The gravitational or centrifugal force, and the buoyant force. The buoyant force can be combined with the gravitational or centrifugal force by using the effective mass of a spherical particle:

$$m = V \times (\rho_P - \rho) \tag{5}$$

where m is the mass of a spherical particle, V is the volume of the particle, ρ_P is the density of the particle, and ρ is the density of the surrounding medium.

The effective centrifugal force F_C on the spherical particle with effective mass m and diameter D_P is:

$$F_C = ma = V(\rho_P - \rho) \times a = \frac{\pi}{6}D_P^3(\rho_P - \rho)r\omega^2 \tag{6}$$

The viscous drag force F_D is the frictional force that a particle will experience when moving in a fluid, and has the opposite direction of F_C. The viscous drag force is dependent on the viscosity η of the surrounding fluid and the radial speed $\frac{dr}{dt}$ of the moving spherical particle:

$$F_D = 3\pi D_P \eta \frac{dr}{dt} \tag{7}$$

When the centrifugal, buoyant and viscous drag force balance each other, the particle will move with constant radial velocity $\frac{dr}{dt}$ known as the *terminal velocity*:

$$F_C = F_D \tag{8}$$

$$\frac{\pi}{6} D_P^3 (\rho_P - \rho) r \omega^2 = 3\pi D_P \eta \frac{dr}{dt} \tag{9}$$

$$\frac{dr}{dt} = \frac{D_P^2}{18\eta} (\rho_P - \rho) \omega^2 r \tag{10}$$

These equations form the basis for the transfection experiments where a centrifuge is used to increase the force of penetration, described in chapter 4.7.4.

2.9 Shear stress

For some of the results presented in this thesis shear stress can explain observed results, and the basic theory of shear stress in fluids will be presented here. Fluid physics in microcosmos is dominated by laminar flow. When the inertia of a fluid is low compared to frictional forces (i.e. the viscosity of a fluid) there will be no turbulent flow, and fluid flow can be seen as thin sheets of fluid sliding next to each other.

When fluids move along a solid object, the border of the object will be subjected to a shear stress. The no-slip boundary condition says that the fluid immediately next to the border will be stationary relative to the wall. Two objects moving in non-perpendicular directions of each other will thus cause the fluid to move between these objects, as the no-slip boundary condition will be applicable to both objects. If two plates in parallel orientation are immersed in a fluid, and moving in opposite, parallel directions, the viscosity of the fluid gives rise to a frictional, viscous force. Both plates will be subjected to a dragging force in the direction the opposite plate is moving. This force f will decrease with distance d between the two plates, and increase with speed v_0:

$$f = -\eta v_0 A / d \tag{11}$$

for Newtonian fluids at small speeds, where η denotes the viscosity of the fluid, and A denotes the area of the plates. The quantity $\frac{f}{A}$ is defined as the shear stress, and for non-Newtonian fluids this will equal $-\frac{\eta v}{d}$.

The fluid can be seen as infinitesimally thin parallel sheets, each of thickness dx, where each sheet will obey the no-slip condition, and the shear stress between neighboring sheets in the z-direction can thus be described as

$$f/A = -\eta \frac{dv_z}{dx}, \tag{12}$$

where dv_z denotes the relative velocity of two neighboring sheets of fluid. Since all sheets move uniformly (do not accelerate), each sheet must exert on its neighbor above the same force as exerted on it by the neighbor below (Newton's Law of Motion), which translates to $\frac{dv_z}{dx}$ being constant, and the shear stress experienced by objects in moving fluids is proportional to the speed of movement. For a further discussion of shear stress see reference [83].

The shear stress experienced by cells will cause the cell to deform, and due to the visco-elastic nature of cells this deformation will only partly be reverse when the speed of fluid flow approaches zero.

2.10 Osmolarity and osmotic pressure

Osmotic swelling of cells is used to deplete cell membrane reserves in some of the experiments presented, in order to reduce the capability of a cell to reorient its cellular membrane upon indentation by nanowires. Osmolarity, or osmotic concentration, is the number of dissolved moles of ions per liter of solution, and is measured in osmoles/liter (Osm/L). Example: 1 molar of NaCl will give 2 osmoles in water, since each each NaCl molecule will give two ions (Na^+ and Cl^-), given that all of the salt dissolves.

If two compartments of liquid are separated by a semipermeable membrane, through which only water can pass, and a solute is added to one of the compartments, water will move from the compartment with no solute to the compartment with solute (and thus diluting the solute), and the extra pressure needed to stop water from entering the compartment with solute is defined as the osmotic pressure. This process can be viewed as an entropic process, where the entropy of the entire system (both compartments) is maximized. If no pressure is applied to the compartment with the solute then all water will enter this compartment. For a further discussion of osmotic pressure, including definitions from an entropic perspective, see reference [84].

Ions are allowed to pass cellular membranes through ion channels, in a process under strict regulation by cells. This results in a charge separation over the cell membrane, and both potential related to concentration difference and the electric potential must balance at equilibrium. Cells are optimized to live with an extracellular osmolarity of ~300 mOsm/L, and reducing the osmolarity of the extracellular

fluid will cause water to cross the cellular membrane and enter the intracellular compartment, which causes swelling of cells.

3 Survey of performance of published nanowire transfection experiments

Several articles have been published on transfection mediated by arrays of nanowires, since the first article was published in 2003 by McKnight et al. [39]. These will be reviewed here, and this survey forms a basis for discussing results obtained with the silica-coated cupric oxide nanowire device investigated in this project. For an overview of the techniques used to synthesize nanowires see chapter 2.3.5. Some examples of final nanowire devices with cells, from published experiments, are provided in figure 11.
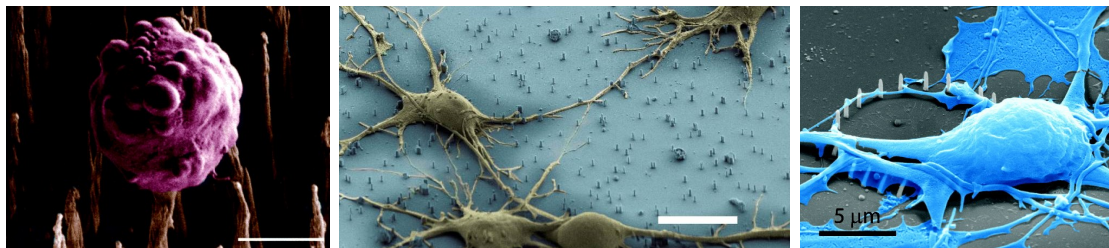
Figure 11: A few examples of cells grown on nanowires, from published experiments. The left image shows a mouse myeloma cell growing on vertically aligned carbon nanofibers (scalebar is 5 µm) [39]. The middle image shows rat hippocampal neurons grown on silicon nanowires (scale bar is 10 µm) [44], and the right image shows embryonic cortical neurons from rats grown on platinum nanowires [51].

There are several ways to assess and compare the efficiency of nanowire-mediated transfection. The essence of a reporter plasmid lies in the reporter plasmid containing a regulatory sequence that, upon introduction to cells, provides an easily detectable signal. A straight-forward way to assess transfection efficiency would be to transfect cells with a reporter plasmid, and then count cells expressing this reporter plasmid, compared to the total number of cells. Plasmids encoding proteins affecting phenotypes that can be assessed by fluorescent microscopy techniques, such as the enhanced green fluorescent protein (EGFP), are commonly used in such experiments, and many other varieties of reporter proteins exist [85]. A requisite is that the plasmid interacts with the internal machinery of a cell, as the plasmid itself can not be the source of a detectable signal; only the gene product encoded by the plasmid will give a detectable signal.

Efficiency can also be assessed by measuring total fluorescence intensity from a collection of cells. In knock-in experiments, i.e. experiments with reporter plasmids,

this would then be seen as an increase in the amount of detected signal from all cells combined. In knock-down experiments, e.g. using RNAi to knock down a gene for a reporter protein, detected signal will decrease, and this knock-down can be assessed at the single cell level, or for a population of cells. When the detected signal is integrated over all cells, variation from cell to cell will affect results. Also, a transfection efficiency of 50% could both mean that all cells have a lowered reporter protein expression to a level of 50% of the initial value or control experiment, or that half of the cells have a complete knock-down of expression of the reporter protein. In the literature, both assessing transfection efficiency by measuring an integrated response, and as a fraction of cells exhibiting the intended response, are used.

Also, delivery of fluorescent cargo is used to indicate that a given system is suitable to enhance transfection. An important difference from reporter plasmids is that fluorescent cargo is inherently fluorescent, and interaction with the internal machinery of a cell is thus not required for a positive signal.

Many different techniques have been tested to permit and improve efficiency of nanowire-mediated transfection. These can be grouped into a few categories, and a schematic overview can be seen in figure 12:

- Experiments where cells sediment out of a solution onto nanowires, and where gravity and cell membrane-nanowire interactions should facilitate membrane penetration. A centrifuge could also be used to increase the sedimentation rate.

- Experiments where a force is applied to the cell membrane-nanowire interface, to increase the chance of membrane penetration. This could be done by depositing cells on a nanowire surface, and then sandwich the cells between the nanowire surface and a supporting surface.

- Experiments where the membrane barrier is partly compromised, to increase the likelihood of membrane penetration, e.g. by adding a membrane destabilizer to the system.

These different approaches to increase the efficiency of transfection could also be combined.

In one of the early experiments with nanowire-mediated transfection McKnight et al. used vertically aligned carbon nanofibers (VACNFs), grown in a plasma-enhanced vapor deposition (PECVD) process [39]. Nanowires were spaced 5 µm apart, had a length of 6-10 µm, a tip diameter of 20-50 nm, and base diameters
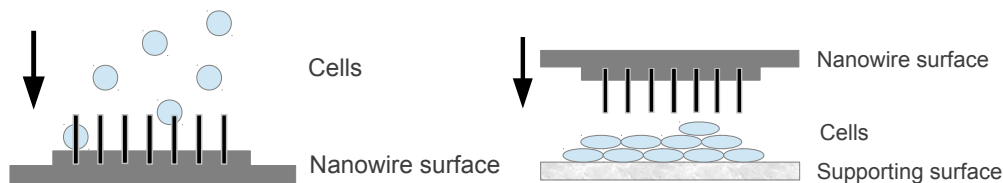
Figure 12: Schematic overview of nanowire penetration of cells. In the left image cells are in suspension, and gravitation will pull cells onto a nanowire surface, and cellular membranes will spontaneously be penetrated. In the right image a force is applied to the cell membrane-nanowire interface by pressing a nanowire surface against a supporting surface, trapping cells in between.

of approximately 1 µm. 0.5-1 µL of 5-500 ng/µl of the plasmid pGreenLantern-1 was deposited on the surface and was allowed to dry, or was covalently linked to the VACNFs. The plasmid pGreenLantern-1 encodes an enhanced green fluorescent protein (EGFP), and if a cell is successfully transfected this will easily be seen in fluorescence microscopy. Chinese hamster ovary (CHO) cells were centrifuged down on the nanowire surface at $600 \times$ g, and then, optionally, the chip was gently pressed against a flat, wetted surface. When the pressing step was skipped, EGFP expression was very low ($<1\%$). With the pressing step EGFP expression could reach ~50% of the cells in local regions (~1mm^2). When the plasmid was covalently linked to VACNFs, pressing gave 81, 198, 65 and 102 transfected cells on a 3x3mm^2 chip (total number of cells on chip is not reported).

McKnight's group has later published several follow-up articles [38, 86, 87, 88, 89]. In an article from 2004 [38] 50 µL of 200,000 CHO cells/ml are sandwiched between a PDMS surface and VACNFs with a yellow fluorescent protein (YFP)-plasmid (pd2EYFP-N1) covalently attached to the VACNFs. VACNFs have diameters of 200 nm, and efficiency was <5% after 36 hours. It was found that covalently attached plasmids are not inherited to progenitor cells. A follow-up article [87] finds that both *in vitro transcription*-kits and polymerase chain reaction (PCR) enzymes are able to access pd2EFYP-N1 plasmids covalently linked to VACNFs.

In 2008 a variant of these experiments was published by the same group [86]. VACNFs were 10-17 µm tall, with tip diameters of approximately 100 nm. CHO-K1-cells stably transfected with a cyan fluorescent protein (CFP)-plasmid and a TetR-plasmid are used. The TetR-plasmid represses the expression of CFP-silencing shRNA in the absence of tetracycline. When tetracycline is added to the system repression of CFP is inhibited. Two plasmids are delivered using VACNFs: YFP (pd2EYFP-N1) and CFP-silencing shRNA (pCFPQuiet). YFP is used to iden-

tify successfully transfected cells, and CFP-silencing shRNA expression can then be tested by adding tetracycline. Of YFP-expressing cells, 53.1%±10.4% could also be successfully silenced by the inducible CFP-silencing shRNA, which means that cells that were transfected with YFP would have a ~50% probability of also being transfected with the other plasmid (co-transfection). In the same article it is referred to an experiment where two plasmids, pd2EYFP-N1 and pd2ECFP-N1, are simultaneously delivered to cells, with an efficiency of 76.7%±3.9% for co-delivery of both plasmids to the total number of impalefected cells, but data for this experiment is not included in the article. Also, the term 'impalefected cells' is ambiguous: Is it the number of successfully transfected cells in an impalefection experiment, identified by the cells expressing either one of the two plasmids delivered, or the total number of cells subjected to an impalefection experiment (including both transfected cells and non-transfected cells)?

A later article pertaining to transfection of plasmids using the VACNF delivery system was published in 2009 [88], where immobilized and releasable DNA was compared. In this article nanofibers have a length of 15 µm, a tip diameter of 250 nm, and base diameters of 0.8-1.0 µm. A cell pellet is formed, and the nanowire surface is gently pressed against this pellet. The plasmid pd2EYFP-N1 is delivered to cells, and with 20 replicates they are able to obtain YFP-expression in 75.8 ± 55.7 cells/mm^2 when using a cleavable linker (3-[2-aminoethyl]-dithio)propionic acid (AEDP)), and 73.2 ± 55.6 cells/mm^2 when using thiol-modified dsDNA (17 replicates). The density of cells in this experiment is unknown, and therefore the proportion of successfully transfected cells is also unknown. Since cells are transferred to the nanowire surface by pressing the nanowire surface against a cell pellet this suggests that the cell density is indeed high, and thus the transfection efficiency low.

In the last article by McKnight et al. [89] a similar setup with VACNF are used, but now with the nanowires protruding from a transparent PDMS membrane. A cell pellet was formed, deposited on a concave glass surface, and a nanowire surface (5x5 mm^2) was pressed against the glass surface. The transfection efficiency is not quantified, but described as 'low'[2], and it is suggested that many cells were first transfected, but that many of these are lost due to poor adherence to the substrate.

Kim et al. have interfaced silicon nanowires with mouse embryonic stems cells (mES) and human embryonic kidney cells (HEK293T) [43]. Cells are cultivated on the nanowire surface, and penetration of SiNW into individual cells is thought to

---

[2]Original author's expression

happen spontaneously. The nanowires have lengths of 3-6 µm and diameters of ~30, 90 and 400 nm. Each cell is on average pierced by 2-3 nanowires. Cell viability on nanowires with a diameter of 400 nm was low. 2 µg of plasmid DNA (0.2 µg/µL) encoding GFP under the cytomegalovirus promoter was deposited on the nanowire surface, and then HEK293T cells were cultured on top. After one day some cells express GFP (<1%).

Shalek et al. have also used silicon nanowires to deliver plasmids and fluorescently labeled biomolecules [44, 90], and in both papers many experiments are presented. Here only some of the results pertaining transfection and biomolecule delivery will be addressed. Synthesis of the wires is described in a paper by Hochbaum et al. [45], and nanowires have controllable dimensions, with a smallest average diameter of 39 nm, and an areal density of 0.1-1.8 nanowires/µm^2. In the second paper dimensions are optimized for different immune cells, with lengths typically in the range 1-3 µm, diameter <150 nm, and areal density 0.15-1 nanowire/µm^2, and as a general rule it was found that areal nanowire density and, to a lesser extent, diameter needed to be scaled to the size of the cell type investigated.

In the first paper by Shalek et al. [44] a comparison between cells grown on nanowire surfaces, with fluorescently labeled cargo adhered to the nanowire surface, is compared to flat silicon surfaces without any cargo, but with fluorescently labeled cargo added to the culture medium at two time-points. Adding cargo to the solution does not favor delivery. A variant of this experiment, with two fluorophores used in the same experiment, was also done, where one of the fluorescently labeled cargos would be associated with the surface, and the other cargo would be added to the solution. In this instance only the fluorescently labeled cargo adhered to the nanowire surface would be delivered, and if both types of fluorescently labeled cargo were associated with nanowire surfaces, both would be delivered to cells. However, the delivery seen on nanowire surfaces could be a surface effect, and a comparison with flat silicon surfaces, with cargo adhered to the surface similarly as for the nanowires, could have been compared to elucidate the effect of nanowires. Also, showing delivery of fluorescent cargo to the cell's interior does not necessarily mean that the cellular membrane was breached, as the cargo inside a cell could be isolated from the cytoplasm and/or nucleus, e.g. in endosomes. A plasmid that has to be transcribed and translated into a fluorescent reporter protein would indicate that the cargo reaches the cellular machinery (however, this experiment would not distinguish between cargo that directly enters the cytoplasm, and cargo that enters a cell through endocytosis and subsequently escapes the endosome). In the supple-

mentary information for the same paper by Shalek et al. a comparison of nanowire and flat silicon surfaces coated with siRNA directed against vimentin is done, and in this experiment the flat silicon surface performs much worse than the nanowire surface, indicating that nanowires could deliver siRNA more efficiently than a flat surface. The proportion of cells where siRNA was successfully delivered is however not reported.

In the second paper by Shalek et. al [90] fluorescently labeled biomolecule delivery was again investigated, and it was found that biomolecules were delivered to 'nearly every cell'[3]. siRNAs targeting RNAi was also delivered, and it was found that nanowires were able to reduce levels of targeted mRNA >69%. However, no comparison was done with siRNA delivered from a flat but otherwise chemically similar surface.

Two papers, by Peer et al. [91] and Park et al. [92], use one-dimensional, hollow nanostructures to deliver biomolecules to cells. In the paper by Park et al. carbon nanosyringes coated with an amphiphilic polymer are used to deliver both plasmid (pEGFP) and quantum dots to fibroblast cells (NIH3T3) and human mesenchymal stem cells (MSC), and green fluorescence intensity and expression was 30% and 34% for the two cell lines respectively, as opposed to 57% and 42% respectively for a commercial non-viral gene delivery vector (Lipofectamine 2000). The same surface chemistry without nanosyringes was however not tested, so the effect of the nanosyringes is unknown. Also, it is not specified if the percentages relate to the proportion of transfected cells, or the combined intensity of EGFP expression for all cells. For the delivery of inherently fluorescent cargo (quantum dots), uptake was seen in 'many cells'[4]. Cells were seeded on the nanosyringes, with no external force favoring penetration.

In a more recent paper, by Peer et al. [91], hollow silica nanoneedles are used to deliver biomolecules to HEK293 and NIH3T3 cells, where cargo is loaded in a reservoir separated from the cells by a membrane with hollow silica nanoneedles. Cells are cultured on the nanoneedle array, with no external force to facilitate penetration. A membrane permeation promoter, saponin, is added to the reservoir when biomolecules are administered, at a concentration of 3 µg/mL. With this setup fluorescently tagged dextran is delivered to 70%±15% of cells in direct contact with nanoneedles that are again in direct contact with the reservoir. Increasing the concentration of saponin to 4 µg/mL gives uptake in a higher proportion of cells, but

---

[3]Original author's expression
[4]Original author's expression

also causes uptake in cells not in contact with the reservoir. A control experiment is done with a flat silicon surface, where no uptake is seen. However, it is not specified whether saponin was administered or not in the control experiment, so how much of the delivery that can be attributed to the membrane destabilizer is unknown (saponin has previously been implicated in enhancing cellular uptake of chemicals [93]). A plasmid encoding red fluorescent protein (plsRes2-RFP-dsExpress) was also added to the reservoir, together with saponin, and 'most of the cells'[5] that grew on nanoneedles in direct contact with the reservoir exhibited red fluorescence. Some RFP-expressing cells were also seen in other areas where nanoneedles were not in contact with the reservoir, either indicating uptake of naked plasmid, or migration of transfected cells.

A summary of these articles is presented in table 1, which includes method, biomolecule, how delivery was assessed, and results.

---

[5]Original author's expression

Author(Year)	Material	Method	Biomolecule	Assessment	Results
McKnight (2003) [39]	VACNF	Tapping	Plasmid pGreenLantern-1 (EGFP)	Proportion of expressing cells	<1% (~50% in small areas)
McKnight (2004) [38]	VACNF	Tapping	Plasmid pd2EYFP-N1	Proportion of expressing cells	<5%
Kim (2007) [43]	SiNW	Sedimentation	Plasmid	Proportion of expressing cells	<1%
Mann (2008) [86]	VACNF	Tapping	Co-transfection of YFP and inducible shRNA silencer	Ratio of co-transfected cells out of only transfected cells, and similarly ratio of cells with successful knockdown	76.7±3.9% and 53.1±10.4% respectively
Park (2009) [92]	CNSA	Sedimentation	a) Plasmid pEGFPC1, b) quantum dots	a) Flow cytometry, b) fluorescence microscopy	a) 34%, b) not reported
Peckys (2009) [88]	VACNF	Tapping	Plasmid pd2eYFP-N1	Number of expressing cells (total density of cells not reported)	75.8±55.7 cells/mm^2
Shalek (2010) [44]	SiNW	Sedimentation	a) shRNA against Na$^+$-channel Nav1.1, Nav1.2, Nav1.3 and Nav1.9, b) siRNA, c) fluorescently labeled molecules (DNA, RNA, IgG etc)	a) Altered voltage reading, b) knockdown of vimentin, assessed by immunostaining and real-time PCR, c) fluorescence	a) 'Substantial', b) 'substantial', c) 95-100%
Peer (2012) [91]	Si NNA	Saponin	a) Plasmid plsRes2-RFP-dsExpress, b) fluorescently stained dextran	a) Proportion of expressing cells, b) proportion of cells	a) 'Most cells', b) 70±15%
Shalek (2012) [90]	SiNW	Sedimentation	a) siRNA, b) fluorescently labeled molecules (plasmids, siRNA, peptides, proteins)	a) qRT-PCR of mRNA, b) fluorescence	a) >69% reduction, b) 'nearly every cell'
Na (2012) [94]	SiNW	Sandwiching*	a) Fluorescently labeled peptides, b) metabolic substrate	a) Presence of fluorescent cytoplasm, b) metabolic changes	a) Not specified, b) not specified
Pearce (2013) [89]	VACNF	Tapping	Plasmid pVENUS-C1 (variant of YFP)	Number of transfected cells	'Low transfection rate'

Table 1: Published performance of nanowires on substrate for biomolecule delivery to growing cells. SiNW: Silicon nanowires, VACNF: Vertically aligned carbon nanofibers, CNSA: Carbon nano-syringe array, Si NNA: Silicon nano-needle arrays. *Cells are sandwiched between two nanowire surfaces. Expressions in quotation marks are quotes from the original article.

In published experiments, few comparisons between nanowire surfaces and flat surfaces, which are similar to the nanowire surfaces in all other respects than the nanowires themselves, have been done. Figure 13 illustrates the setup that should be used in comparing nanowire setups seen in figure 12, where all experimental parameters should be the same for the nanowire experiment and the flat control experiment, except for the presence of nanowires.
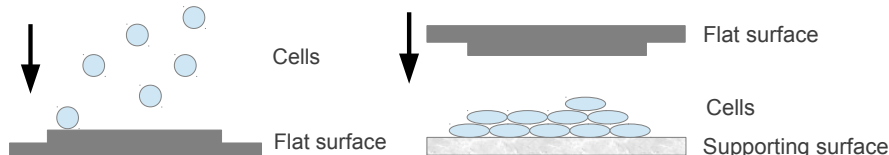
Figure 13: Schematic overview of control experiments for nanowire-mediated transfected. A proper control experiment for nanowire-mediated transfection experiments should keep all parameters identical except for the presence of nanowires. In the left image cells are in suspension, and gravitation will pull cells onto a flat surface which is chemically similar to the surface seen in the left part of figure 12. In the right image a force is applied to the cell membrane-flat surface interface by pressing a flat surface against a supporting surface, similarly to what is seen in the right part of figure 12.

Only one paper, by Shalek et al. [44], compare uptake of molecules that affect the phenotype (siRNA knockdown in this case) of a cell on nanowires versus flat surfaces, but unfortunately do not provide information on the proportion of cells transfected. One paper, by Peer et al. [91], where delivery of biomolecules to cells using nanoneedles was investigated, also compare nanoneedle surfaces with flat silicon surfaces, but don't specify whether the control experiment was identical in all other respects than the presence of nanoneedles, i.e. if they add the membrane destabilizer to the control experiment or not. Also this comparison is only done for fluorescently labeled biomolecules, and not with setups where delivered molecules must interact with the internal machinery of a cell.

Articles describing nanowire devices that give numbers of successfully transfected cells as a proportion of all cells all have low transfection efficiencies. Furthermore, it is often difficult to dissect the the true meaning of numbers published in the literature, as key parameters are often not reported, such as in experiments where the number of successfully transfected cells per area are reported, without reporting the total density of cells. In summary, published experiments on nanowire-mediated transfection should include:

- Proper controls: Identical control experiments, with flat surfaces that are

chemically identical to the nanowire surfaces, apart from the nanowires themselves, should be used for comparison to transfection mediated by nanowires.

- Transfection effectivity assessment: Number of transfected cells should be given as well as the total number of cells, to indicate what proportion of cell subjected to a transfection experiment are successfully transfected.

- Functional molecules: Delivery of functional reporter molecules that cannot diffuse over cellular membranes, and which must interact with the internal machinery of a cell to be detectable, should be be used to assess positive delivery, since the delivery of functional molecules is the overarching goal in transfection experiments. Labeled molecules give a positive signal even if it is isolated from the internal machinery.

4 Method

4.1 Nanowire synthesis

The procedure to synthesize nanowires is adopted from Mumm et al [95], and is summarized in figure 14. Cupric oxide nanowires are grown by thermal oxidation of copper foils. For cleaning the copper foil (25 µm, 99,98% purity, Sigma Aldrich) before thermal oxidation, the foil was ultrasonicated in 2M HCl (Merck Chemicals, Germany), deionized water, acetone, and 96% ethanol. The foil was then dried using Kimtech wipe pads, and bent around a glass slide. Thermal oxidation was done by heating the sample (Carbolite CWF1200 oven) to 450 °C for 4 hours if relative humidity was above 55%, or 5 hours for lower relative humidity.

The sample was then processed at the NTNU NanoLab facilities. SU-8 2 (MicroChem) photoresist was spun onto the sample at 5000 rpm for 90 s, and the sample then baked in a two-step process, first at 65 °C for 1 minute and then, after ramping the temperature, at 95 °C for 1 minute. The SU-8 2 was then exposed to an I-line (365 nm) mercury source at an energy density of 300 mJ/cm^2 for 30 s (Karl Suss MJB3 Mask Aligner). The sample was then post-exposure baked in a two-step process, first at 65 °C for 1 minute, and then, after ramping the temperature, at 95 °C for 1 minute.

After SU-8 processing the sample was plasma cleaned[6] using O_2 at a pressure of 0.04 mbar at 50W for 1 minute.

The sample was then sputter-coated with 30 nm SiO_x (Cressington 308R DC-magnetron sputter coater) at 0.01 mbar and a current of 80mA. The thickness of SiO_x was measured by a quartz crystal thickness monitor (Cressington MTM-10 thickness measurement system).

A solution of poly(dimethylsiloxane) (PDMS) (Sylgaard 184, Dow Corning) was made and dissolved to a concentration of 10% in tert-butanol, and then spun on the sample at 6000 rpm for 90 s. The sample was then plasma cleaned using O_2 at a pressure of 0.04 mbar at 50W for 12 s. SU-8 2 (MicroChem) photoresist was spun onto the sample at 3000 rpm for 90 s, and the sample then baked in a two-step process and the SU-8 exposed to an I-line mercury source, as described above. A new plasma cleaning step was performed at 100W for 5 minutes in an O_2 atmosphere

---

[6]Plasma cleaning introduces highly reactive oxygen species to the surface, which both removes organic compounds (C_XH_Y by the formation of CO_2 and H_2O) and modifies surface chemistry by introducing oxygen-containing groups such as hydroxy-groups to polymers, which gives a very hydrophilic surface.

of 0.08 mbar. CrystalBond 555, a water-soluble wax, was then heated to 95 °C and applied to the surface, to protect the nanowires protruding from the surface, and to help separating the nanowires from the copper foil. The sample was allowed to cool for 10 minutes before proceeding. Separation at the correct interface is observed in a light microscope.

The sample was glued to glass slide surfaces or 8-well Ibidi μ-slides using standard PDMS, and the sample cured over night at 45 °C. Before functionalizing the surface the wax was removed by immersing the sample in deionized water at 65 °C for 10 minutes with light stirring. Then the sample was rinsed in fresh deionized water at 65 °C and dried.

The nanowire surface was then functionalized using fresh 1% (3-trimethoxysilylpropyl) diethylenetriamine (DETA), which was applied to the surface for 10 minutes, before the sample was rinsed in deionized water, and then subsequently in 96% ethanol for 5 minutes. The sample was then dried.

A large batch of nanowire devices was created by the start of the master thesis project, and samples from this batch was used over a period of three months. Nanowire samples were plasma-cleaned and silanized immediately before cells were grown on the samples, due to an aging effect of the surface, as described in the results section.

The nanowires were optionally labeled using Alexa 633 (Invitrogen). If a transfection experiment was to be conducted, the nanowires were not labeled using Alexa 633.

4.2 Cell cultivation

4.2.1 Cultivation of HeLa cells

HeLa cells were grown in Dulbecco's modified Eagle's medium (DMEM) with 4.5 g/l glucose, 10% fetal bovine serum, 1% minimum essential medium non-essential amino acids, and 0.5% L-glutamate. The cell culture was splitted and regrown in a new flask at 70-90% confluence, typically twice per week. To detach cells from the flask surface growth medium was aspirated, and trypsin/EDTA (0.25%/0.02%) was added to the cells for 2-3 minutes. Trypsination was halted by adding DMEM to the solution, and a cell pellet formed by centrifugation of the cells at 1500 rpm for 5 minutes. The the supernatant was removed and a fraction of the cells were resuspended in fresh medium. For T25-flasks 500,000 cells were suspended in 5 ml of fresh medium, and for T75-flasks 2 million cells were suspended in 15 ml of fresh

CuO nanowire growth

Spin coating with SU-8

Spin coating with SiO$_x$, PDMS and SU-8 (second layer)

Casting of Crystalbond 555, substrate separation, and partitioning

Attachment to glass with PDMS and dissolution of Crystalbond 555

CuO	SiO$_x$	SU-8 (second layer)
Cu$_2$O	SU-8	Crystalbond 555
Cu	PDMS	Glass
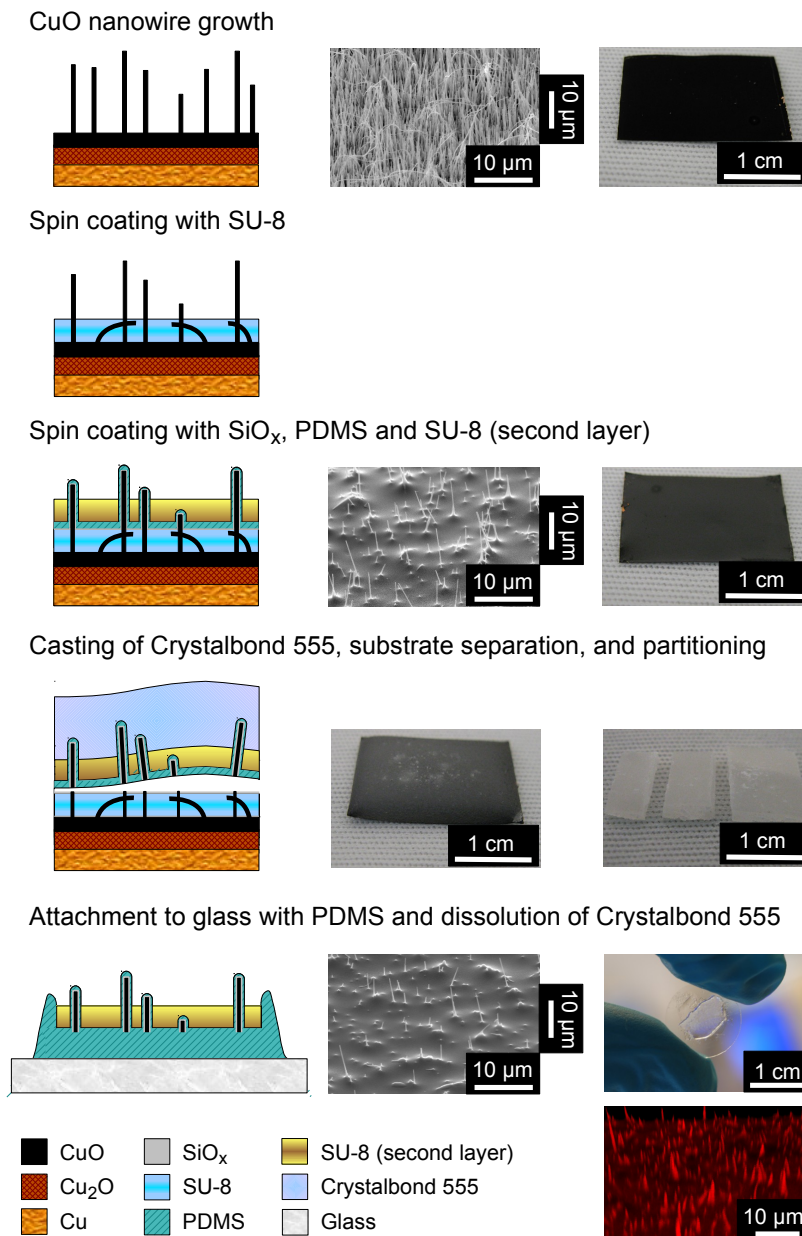
Figure 14: A schematic overview of the synthesis of nanowire devices. First CuO nanowires are grown from a copper foil by thermal oxidation. A layer of the photoresist SU-8 is spun on the foil, burying small nanowires, as well as some longer wires, and thus reducing the areal density of nanowires on the surface. After plasma cleaning a thin layer of SiO$_x$ is sputtered on to the nanowire surface, as well as PDMS, and a second layer of SU-8. Nanowires protruding from the second layer of SU-8 are embedded in wax, and will be part of the final device, whereas the PDMS layer helps separating the SU-8 membrane with nanowires in wax from the copper foil. After separation the SU-8 membrane with nanowires is attached to a glass surface by PDMS. The figure is modified from [95].

medium.

4.2.2 Cultivation of AR42J cells

AR42J [96] (ATCC number CRL-1492) (rat pancreatic acinar cell derived, ATCC, Rockville, MD) were grown in Dulbecco's modified Eagle's medium (DMEM) with 4.5 g/l glucose (Invitrogen, Carlsbad, CA), 15% fetal calf serum (FCS) (Euroclone Ltd, Devon, UK), 1 mM sodium pyruvate, 0.1 mg/ml L-glutamine (Invitrogen), 100 U/ml penicillin/streptomycin (Invitrogen), 1 µg/ml fungizone (Invitrogen) and puromycin 2 µg/ml.

AR42J cells used in this work has been stably transfected using a retrovirus to express a Puromycin resistance gene and GFP, encoded by the plasmid pMSCV-Puro2A-GFP-Empty. The plasmid is called "Empty" because it does not contain any shRNA, and was made as a control cell line for other shRNA-expressing clones. When included, the shRNA is directed against a specific cellular protein transcript, and GFP is used to validate that the cell is indeed transfected with the GFP/shRNA-containing plasmid. These cells were provided by dr. Tonje Strømmen Steigedal at the Department of Molecular Medicine and Cancer Research, NTNU, and cultured in the cell laboratory at the physics department, NTNU.

4.3 Cell growth experiments

Nanowire surfaces were glued to glass slides or 8-well Ibidi µ-slides, as described above. The sample was cleaned using 70 % ethanol when brought to the cell lab ventilation chambers, and then allowed to dry completely. A cell suspension with known concentration of cells was then deposited either directly on the nanowire surface, or added to the suspension in which the nanowire surface was immersed, depending on the type of experiment conducted. Growth medium was added to the well according to instructions, and the cells were incubated at 5 % CO_2 and 100% humidity.

4.4 Experiments with cells exposed to hypotonic environments

For some of the experiments cells were exposed to hypotonic environments, causing osmotic swelling of the cell with the intention of reducing membrane reserves, and possibly to cause distension of the cellular membrane. Two buffers were tested, one

at 50% hypotonicity (~150 mOsm/L), and one at 98% hypotonicity (~6 mOsm/L). The buffers were made based on reference [97], with the 50% hypotonicity buffer containing 1mM $CaCl_2$, 1mM $MgCl_2$, 10 mM glucose, 20 mM HEPES (4-(2-hydroxyethyl)-1-piperazineethanesulfonic acid), 10 mM KCl, and 58,5 mM NaCl. The 98% hypotonicity buffer consisted of 1 mM $CaCl_2$ and 1 mM $MgCl_2$. Exocytosis was blocked by keeping the buffer at a temperature <10°C. Cell swelling by hypotonic buffers at 10°C can typically cause four-fold volume increases[97]. At maximal swelling the lipid bilayer can be stretched by 3% to give an additional volume increase before the membrane ruptures [97].

4.5   Delivery of fluorescently labeled plasmids

YOYO-1-labeled plasmids (pcDNA) were used in investigations of nanowire-mediated uptake of biomolecules. YOYO-1 has en excitation wavelength of 491 nm, and an emission peak of 509 nm. A droplet of labeled pcDNA plasmid was added to the surface investigated, and allowed to dry completely before cells were added. The sample with cells was then placed in a 24-well plate in a growth chamber. Both imaging of cells directly on top of surfaces with adsorbed YOYO-labeled plasmid and imaging of cells that were trypsinated, resuspended and grown on a new glass slide, were tested. When cells were trypsinated, medium was aspirated, 0.5 ml of PBS was used to wash cells, and cells were immersed in 0.5 ml of trypsin for 5 minutes, until detachment was observed in an optical microscope. 1 ml of medium was then added to stop trypsination, and medium and trypsin was mixed in a pipette to loosen all cells. Cells were then centrifuged to form a pellet, the cells deposited on a new cover glass, and then placed in an incubator for 1 day before imaging. This experiment was repeated three times, with slight variations from experiment to experiment. In the first experiment 20 µL of labeled plasmid at a concentration of 100 ng/µL was used (2 µg in total). In the second experiment 10 µL of labeled plasmid at a concentration of 550 ng/µL was used (5.5 µg in total). In the last experiment 5.5 µg labeled plasmid was again used, but this time cells were deposited in a 10 µL droplet on top of the deposited plasmid for 60 minutes, before the rest of the medium was added to the well, whereas for the first to experiments medium was added to the well just after depositing the cells. The reason for using 5.5 µg labeled plasmid per experiment was that this amount has been used by other groups showing uptake of plasmid [44], and the reason for depositing a high-concentration droplet and then let it settle for 60 minutes was also done because this has been

used by other groups[7].

A stack of images with focal planes spaced 0.40 µm apart was recorded with confocal laser-scanning microscopy from an area of 246x246 µm^2, covering approximately 50-150 cells. The presence or absence of fluorescent spots in each cell was registered, and cells initially grown on nanowires and silanized glass were compared.

It was also investigated whether nanowires affect the number of fluorescent spots seen per cell. First a maximum intensity projection was created from the stack of images recorded for an area. For one of the areas imaged two cells were evenly fluorescent, and these were excluded from further analysis. The same intensity cut-off value was then used for all experiments, to exclude fluorescence intensity below a certain value (a numerical value of 46 was used as a threshold, where intensity is represented by a numerical value in the range 0-255). This cut-off value was chosen by finding a value that preserved most of the clearly bright spots, while not including the faint background fluorescence that was also recorded. In addition all spots with a size smaller than 4 pixels (or equivalently smaller than 0.23 µm^2) were excluded from further analysis. The particle analyzer of ImageJ was then used to count the number of spots for the entire slide, and the optical images were used to manually count the number of cells per slide. A smallest size of 9 pixels was also used, which excluded even more spots, but with the same overall trends observed, which are presented in the results section.

4.6   siRNA transfection experiments

Nanowire surfaces were glued to 8-well Ibidi µ-slides, as described above. The sample was cleaned using 70 % ethanol when brought to the cell lab ventilation chambers, and then allowed to dry completely. An siRNA solution was then made at the PDMS surface directly, for a total volume of 20-40 µ l, depending on surface area. First the correct volume of pure medium (without serum) was applied as a droplet to the surface, and then the corresponding volume of siRNA was applied by injecting the siRNA solution in the droplet on the nanowire surface. siRNA solutions were annealed at concentrations 50 µM. The amount adsorbed to the PDMS and nanowire surface was estimated in ng/µl (as done in similar experiments using reverse transfected cell arrays, as in references [18] and [14]), and a concentration of 50 ng/µl was used. The siRNAs used contain 22 base-pairs, and a molecular weight of

---

[7]Communication between Alex Shalek (Department of Chemistry and Chemical Biology, Harvard University) and Florian Mumm (our group)

14.000 g/mol (14 µg/nmol) was used for calculating the amount of annealed siRNA solution needed.

Example: To apply 50 ng/µl siRNA to a surface that needs 40 µl solution for covering the entire surface, one needs 50 ng/µl × 40 µl = 2000 ng = 2 µg siRNA. The siRNA was annealed at a concentration of 50 µM, and one therefore needs 2.9 µl of this solution, as shown in equation 13, and the remainder of the droplet as serum-free medium. 37.1 µl of serum-free medium would first be applied to the surface, and then 2.9 µl of 50 µM siRNA would be injected into the droplet on the surface. The droplet was then allowed to dry completely, before cells were grown on the surface, as described above.

$$V = \frac{n}{c} = \frac{m}{c \times Mm} = \frac{2 \times 10^{-6}g}{50 \times 10^{-6}M \times 14000g/mol} = 2.9 \times 10^{-6}l = 2.9\mu l \quad (13)$$

where c is concentration, n is number of moles, V is volume, m is mass and Mm is molar mass.

4.6.1 siRNA

Synthetic siRNA specific to EGFP (siEGFP): sense, 5'-GCAAGCUGACCCU GAAGUUCAU-3'; antisense, 5'-GAACUUCAGGGUCAGCUUGCCG-3' [16]. Control siRNA targeting CAT (chloramphenicol acetyl transferase) (siCAT): sense, 5'-GAGUGAAUACCACGACGAUUUC-3'; antisense, 5'-AAUCGUCG UGGUAUUCACUCCA-3' [16]. siEGFP and siCAT were obtained from the laboratory at The Department of Cancer Research and Molecular Medicine at NTNU, who obtained them from The Biotechnology Center, University of Oslo [98, 99]. Both siEGFP and siCAT were already annealed at concentrations 50 µM.

Using Sci Ed Central from Clone Manager Professional Suite v6.0, the presence of matching siEGFP target sequences in the EGFP plasmid expressed by AR42J cells was confirmed. The siEGFP and siCAT has been used in a previous study at NTNU against a HEK293 cell line transiently transfected with the plasmid pEGFP-N1 (BD Bioscience Clontech) [18], and using Clone it was also confirmed that the EGFP encoded by the plasmid pEGFP-N1 was indeed the same EGFP as expressed by the AR42J cell line stably transfected with the plasmid pMSCV-Puro2A-EGFP-Empty.

4.6.2 Transfection experiment with patterned surfaces

The aim of the first transfection experiment was to assess whether nanowires give a better transfection efficiency than a flat SU-8 surface when cells sediment onto the nanowires. To test this a patterned surface was used, with nanowires confined to some areas. Plasmid transfection in a similar scenario has been investigated, but with discouraging results (<1% efficiency). To test whether gravitational forces are enough to penetrate only the cellular membrane, and not the nuclear membrane, siRNA transfection was attempted with an siRNA knocking down a fluorescent reporter protein. A dummy siRNA, siCAT, was also included to elucidate any general siRNA effect. Nanowire surfaces were glued to the bottom of 8-well Ibidi µ-slides. Based on previous experiments [9] droplets of siRNA solution with a volume of 20-40 µl and a concentration of 50 ng/µl was first deposited on the nanowire surface, and then allowed to dry completely. The exact amount of siRNA solution deposited varied from well to well, to ensure that the entire SU-8 surface was covered in solution. Cells were then deposited on top of the adsorbed siRNA at a seeding density of 20.000 cells per well, and growth medium was added to a total volume of 300 µl per well. Cells were then cultivated in a growth chamber, as described above. Fluorescence from wells were recorded at 48h and 72h after transfection.

4.7 Plasmid transfection experiments

Nanowire surfaces were glued to glass slides or 8-well Ibidi µ-slides, as described above. The sample was cleaned using 70% ethanol when brought to the cell lab ventilation chambers, and then allowed to dry completely. Plasmids in solution were then deposited as a droplet on the nanowire surface, typically 20-40 µl depending on the size of the surface, at a concentration of 100 ng/µl, and allowed to dry completely. Cells and growth medium were then deposited on the surface.

4.7.1 DNA adsorption on nanowire surfaces

DNA adsorption to nanowire surfaces was studied using fluorescently labeled plasmids. 100 ng/µl plasmid was applied to the nanowire surface, typically 20-40 µL per surface, and allowed to dry completely. Samples were then investigated using confocal scanning microscopy, and both dried surfaces and surfaces immersed in warm PBS (37 °C) were imaged.

4.7.2 Sedimenting method

The cell sedimentation method for nanowire-mediated transfection is based on gravitational forces pulling cells towards a nanowire surface immersed in growth medium or buffer. When a cell meets the nanowires protruding from the SU-8 surface gravitational forces will further pull the cell towards the surface, hopefully with forces strong enough to penetrate the cellular membrane.

4.7.3 Tapping method

The tapping method is based on the nanowire transfection method described by McKnight and Mann [38, 86], where the nanowire surface is placed face-down on cells deposited on a piece of cleanroom paper, and the nanowire surface then tapped with a sterilized tweezer to increase the force of penetration. This approach to perforate cellular membranes is illustrated in figure 15.
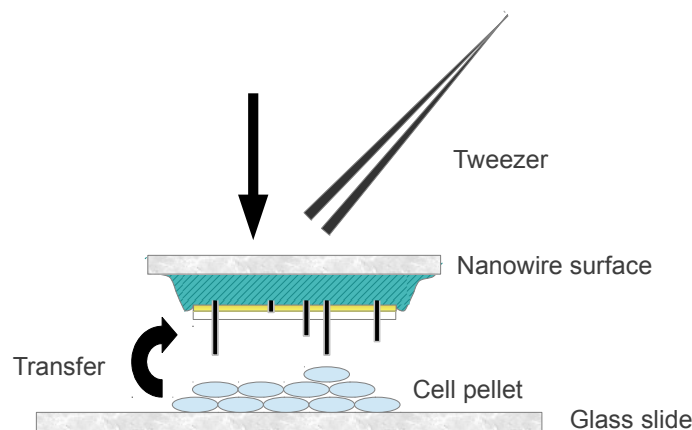
Figure 15: A schematic overview of the tapping method, where cells are deposited on a glass slide or a piece of cleanroom paper, and a nanowire surface is placed on top of the cells, with the nanowire surface facing the cells. A sterilized tweezer is used to tap nanowire surface, and upon contact with the cell pellet cells will be transferred to the nanowire surface. Cells that are transferred to the nanowire surface are thought to be perforated by nanowires when force is applied by tapping the surface. Both cells on the nanowire surface and cells on the supporting surface can then be cultured and checked for positive transfection of a reporter protein.

The cleanroom paper was sterilized in 70% ethanol in the cell ventilation chamber, and allowed to dry completely. Then 5x5 to 10x10 mm^2 pieces were cut out using sterilized scissors. Cells in suspension were prepared at a concentration of 2 million cells/ml. 100 µl of the cell suspension was gently applied to the cleanroom

wipe, and allowed to settle for 2 minutes. Then the nanowire surface was placed face-down on the cleanroom wipe, and tapped using a tweezer. The nanowire surface was then placed either face-up or face-down in a growth chamber with cell medium.

More recent papers from the same group [88, 89] was also used as a starting point, where cells were grown in large amounts, a cell pellet was formed, and the cell pellet was then deposited on a concave or flat glass surface, instead of a cleanroom wipe. The nanowire surface was then placed face-down on the cell pellet, and tapped using a tweezer. Both glass slides and flat SU-8 surfaces were used as controls.

It was also tested whether the tapping method could be applied to cells that had grown on a glass slide for one day. This experiments allows better control of number of cells that are tapped, since the seeding concentration is known, and 50,000 HeLa cells/cm^2 were used in this experiment. Two glass slides, two flat SU-8 surfaces and two nanowire surfaces were used, and all surfaces were silanized to ensure similar chemical surface properties. The SU-8 surfaces were prepared to have a comparable surface to the nanowire surface, both in terms of size, and to have a slight elevation from the supporting glass slide, as is the case for nanowire surfaces. After sterilization a droplet of 20 µL EGFP plasmid at a concentration of 100 ng/µL was deposited onto the surface and allowed to dry completely. After growing the cells on a glass slide for one day medium was aspirated, the surface with plasmid placed face-down on top of the cells, and tapped with a sterilized tweezer. Medium was immediately added, and the two surfaces where separated after 15 minutes, and both the supporting glass surface and the nanowire and control surfaces were then placed in a cultivation chamber for one day before the surfaces were investigated for successfully transfected cells.

4.7.4   Centrifugation method

The centrifugation method is based on the inertia of cells being slightly higher than the surrounding media, which allows centrifugation of cells onto a nanowire surface placed on the bottom of a centrifugation tube. This setup is illustrated in figure 16.

Two centrifuges were used in these experiments: Megafuge 1.0 (Tamro MedLab AS), which is used as a cell lab centrifuge with a maximal speed of 4000 rpm, and the ultracentrifuge Avanti J-30I High-Performance Centrifuge System (Beckman Coulter), with a maximum speed of 30,000 rpm.
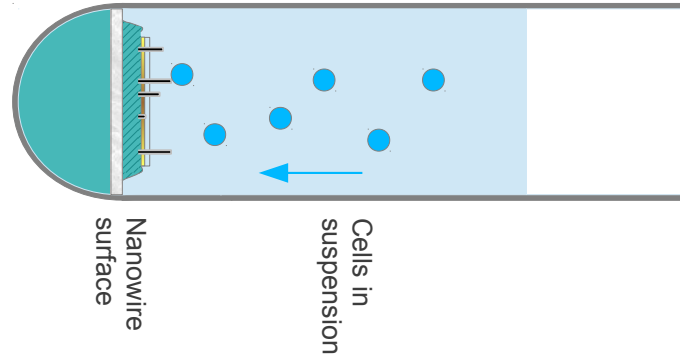
Cell Megafuge 1.0

Figure 16: A schematic overview of the centrifugation method. A nanowire surface is placed on the bottom of a centrifuge tube (the plane furthest away from the center of rotation), and cells in suspension will then sediment down on the nanowire surface when the centrifuge is rotating. In this figure the center of rotation lies to the right of the tube, and the arrow indicates the direction cells will travel when the centrifuge is rotating. The ultracentrifuge used in some of the experiments has a fixed angle rotor, and for those experiments the nanowire surface was tilted, so that the nanowire surface would stay perpendicular to the direction of cell sedimentation, as described in the text.

For the Megafuge 1.0 centrifuge cells were added to growth medium or hypotonic buffers deposited in wells in a 24-well plate, with nanowire surfaces at the bottom of the well. The radius of this centrifuge was 15 cm at the nanowire surface, which means that the relative centrifugal forces can reach 2680 × g (see equation 3). If it is assumed that each cell is impaled by ten nanowires, the volume of a cell on top of a single nanowire would be one tenth of the entire volume, which corresponds to a threshold relative centrifugal force of 5280 × g, based on force measurements from AFM experiments. The areal density of nanowires on a nanowire surface is however randomly distributed, and it can be assumed that some cells will only be impaled by 1-2 nanowires, which could allow a low, but significantly increased, transfection efficiency even in a centrifuge with a maximum RCF of 2680 × g.

For all Megafuge 1.0 centrifuge experiments cells were centrifuged down on nanowires located at the bottom of a well in 24-well plates with 1 ml of medium (37°C) or buffer (0°C). 100,000 cells were deposited as a 50 µL droplet, slightly decreasing the hypotonicity of the buffers used. The centrifuge was then run for 5 minutes at 4000 RPM. Buffer or medium was immediately exchanged for warm medium and the well-plate was incubated in a growth chamber for two days before the samples were investigated for expression of EGFP. Hypotonic buffers were used to deplete cell membrane reserves, and possibly also to distend the cellular mem-

brane, which could decrease the force barrier. Also the buffers were kept on ice until the experiment was run, to ensure that buffers were close to 0°C when the experiment was run. Exocytosis is inhibited in cool surrounding, and this could reduce the ability of a cell to reorient its cellular membrane when it interacts with nanowires, thus hopefully increasing the probability of penetration.

The Avanti J-30I centrifuge

The Avanti J-30I centrifuge was used together with the fixed-angle rotor JA-30.50 Ti and 50 mL polycarbonate tubes with lid. The polycarbonate tubes were filled with PDMS and cured at an angle of 42° to give an almost perpendicular surface when used in the rotor JA-30.50 Ti with a fixed angle of 56°, giving a surface that is tilted 5° outwards from a perpendicular line through the axis of rotation. PDMS surface area would then be 6.8 cm^2. The glass slide with nanowire surface was placed on the PDMS surface, growth medium added to the tube, and cells deposited in the solution. Typically 500,000 cells were deposited, which gives a seeding density of 73,000 cells/cm^2. After centrifugation the medium was aspirated, and the sample was then incubated in a 24-well plate with new medium. Between each experiment the polycarbonate tube was washed with 3-5 mL of PBS, and at the end of a series of experiments the tube was sterilized with 70% ethanol.

For the first series of experiments, where relative centrifugal forces less than 50,000 × g where tested, the PDMS surface in the polycarbonate tube was 6.0 cm from the center of rotation. For relative centrifugal forces up to 88,500 × g another set of PDMS-filled polycarbonate tubes were used, with the nanowire surface positioned 8.8 cm from the axis of rotation. The JA-30.50 Ti can be used up to 30,000 rpm (108,860 × g at bottom of tube).

4.8   Confocal laser-scanning microscopy

A Leica TCS SP5 confocal microscope was used for all imaging, and all image recording was done using the software application Leica Application Suite - Advanced Fluorescence, version 2.5.1.6757. For imaging fluorescence from EGFP the Argon laser was used, which has a peak excitation wavelength of 488 nm. Leica HyD detectors were used to detect signal, and the signal was filtered to only allow detection of wavelengths in the range 500-550 nm. For imaging fluorescence from Calcein Red, with a peak excitation wavelength of 577 nm, a 561 nm DPSS laser was used, and the signal was filtered to only allow detection of wavelengths in the

range 580-630 nm. Some cross-talk was seen where the 488 nm laser would also excite Calcein Red (the 561 nm laser was however not able to excite EGFP). Laser power was adjusted so that autofluorescence was low, and fluorescent cells were easily distinguished from autofluorescence.

A single image or a stack of images is taken for each well, covering as much of the SU-8 surface as possible for the overview experiments, where total number of transfected cells is the most interesting result.

4.9 Assessing transfection efficiency on patterned surfaces

4.9.1 siRNA transfection experiments

ImageJ is used for assessing siRNA transfection efficiency, based on measuring reduced fluorescent signal from cells grown on lanes of nanowires compared to cells grown on lanes of SU-8 (between the lanes of nanowires). The stack of images recorded is converted to a single image where each pixel is the sum of all corresponding pixel intensities in the slices. The area for measurement is outlined using the optical image, as the difference between the lanes is easily distinguished, see figure 17.

Figure 17: The lanes on patterned surfaces are easily distinguished in optically recorded images.

For each well a series of such lanes will be imaged, typically 12 to 13 lanes of alternating nanowire/SU-8 surfaces. Total fluorescence from an area covering al-

most the entire lane is measured, and for each well 12-13 measurements will be done, one for each lane. Total fluorescence intensity should then decrease for areas covering siEGFP covered nanowires, compared to cells growing on siEGFP without nanowires. Control experiments using dummy siRNA was also done in order to control for any other nanowire-mediated effects affecting fluorescence, as cytotoxicity.

4.9.2 Plasmid transfection experiments

Plasmid transfection efficiency is assessed first by a qualitative impression of efficiency, and if needed by estimating the number of successfully transfected cells, either by counting each cell for samples where only a few cells are successfully transfected, or, for samples where many cells are transfected, by counting the number of successfully transfected cells in a smaller area of the sample, and then calculating the proportion of successfully transfected cells by dividing the number of successfully transfected cells to all cells. Typically, samples with over 300 transfected cells on a slide were considered to have too many cells to count all cells, and instead only a smaller yet representative area would be investigated.

4.10 Fluorescence spectroscopy

To measure DNA release after adsorption to nanowire surfaces, DNA was complexed with the fluorescent intercalator YOYO-1. Five samples with known concentrations were prepared: 2000 ng in 2 ml PBS, 1000 ng in 2 ml PBS, 200 ng in 2 ml PBS and 20 ng in 2 ml PBS, and pure PBS, and the fluorescence emittance from these samples were measured with a fluorospectrophotometer, see figure 18. The maximum concentration corresponds to the amount of DNA normally adsorbed to the nanowire surface (20 µL of plasmid solution, at a concentration of 100 ng/µL). YOYO-1 has an excitation peak of 491 nm, and an emission peak of 509 nm. When DNA desorbs from the surface, both DNA desorbing from nanowires and the supporting surface will contribute to the DNA concentration in solution.

The Olis DSM 1000 CD Spectrophotometer was used to measure the concentration of fluorescently labeled DNA in a solution. A mercury lamp was used, and the excitation wavelength was set to 491 nm using the accompanying software Olis SpectralWorks version 4.3. A spectrum was recorded from a pure PBS solution, where the detected peak corresponds to the excitation peak, indicating that the excitation light was scattered in the solution. For low concentrations of plasmid (i.e. <20 ng/2ml) any fluorescent signal was lost in noise.

The detected signal F from the samples with known concentrations c were fitted to an exponential curve:

$$F = F_0(1 - e^{-c\epsilon}) + k \tag{14}$$

where F_0 is the fluorescent reading when no fluorescent dye is added to the solution, ϵ is a constant with inverse units of concentration, and k is a constant to account for any offset in the fluorescence volts reading. By rearranging equation 14 the concentration c of desorbed plasmid, when a nanowire surface with adsorbed plasmid was immersed in PBS, can then be found by recording fluorescence emittance over time:

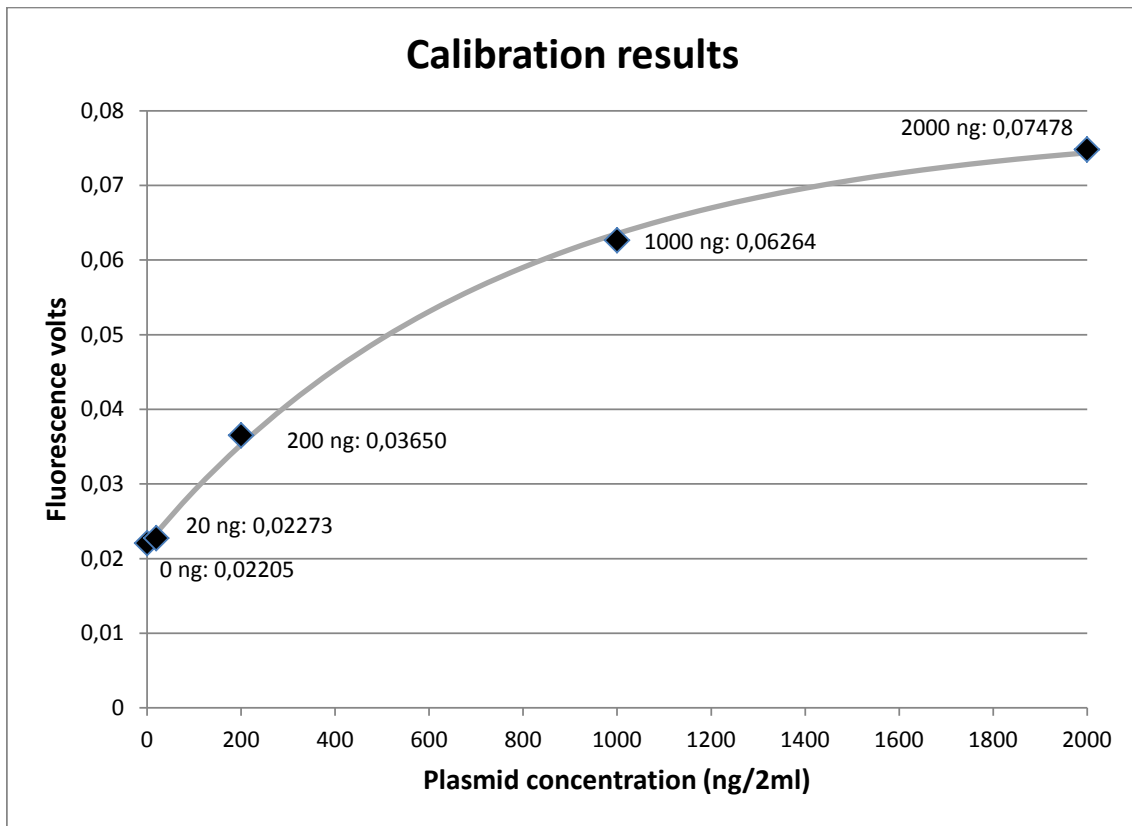$$c = -\frac{1}{\epsilon}ln\frac{F_0 + k - F}{F_0} \tag{15}$$

Figure 18: Results from calibrating the fluorospectrophotometer with 5 known concentrations of YOYO-1-labeled plasmid. The line shows the graph of equation 14, with the parameters found by a least square error optimization using the five known concentrations as reference points.

5 Results

5.1 Nanowire dimensions and areal density

After nanowire growth and processing some samples were imaged using scanning electron microscopy. The aim was to find average diameters and areal density, to be used when calculating forces necessary for membrane penetration. An example of the nanowire surface can be seen in figure 19, and four close-up examples of nanowires can be seen in figure 20. The diameters of 11 nanowires can be found in table 2. The average tip diameter is 119.9 ± 16.3 nm, and the average areal density of nanowires on the surface is $0.11 \ \mu m^{-1}$.
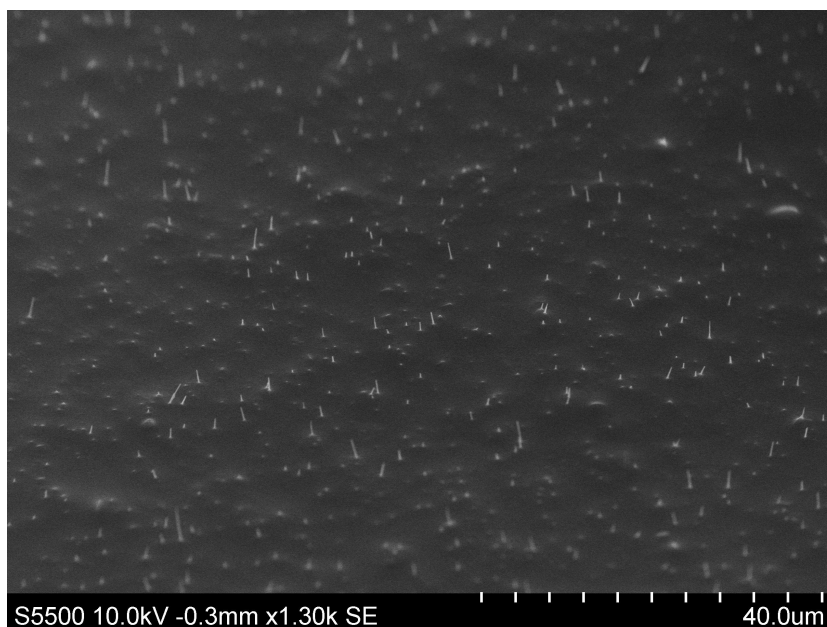
Figure 19: An example of the final silica-coated cupric oxide nanowire surface, after SU-8 and PDMS processing steps.

5.2 DNA release

DNA is electrostatically adsorbed to nanowires and the SU-8 surface through interactions with (3-trimethoxysilylpropyl) diethylenetriamine (DETA). In order to be able to deliver DNA to cells, DNA desorption should not complete within 10 minutes, and should reach appreciable levels within 24 hours (rough approximates). Two tests were done: Image YOYO-labeled DNA adsorbed to nanowire surfaces when the surface is immersed in PBS (37 °C) over time, and fluorospectrophotometric concentration measurements of YOYO-labeled DNA in PBS (20 °C) when

67
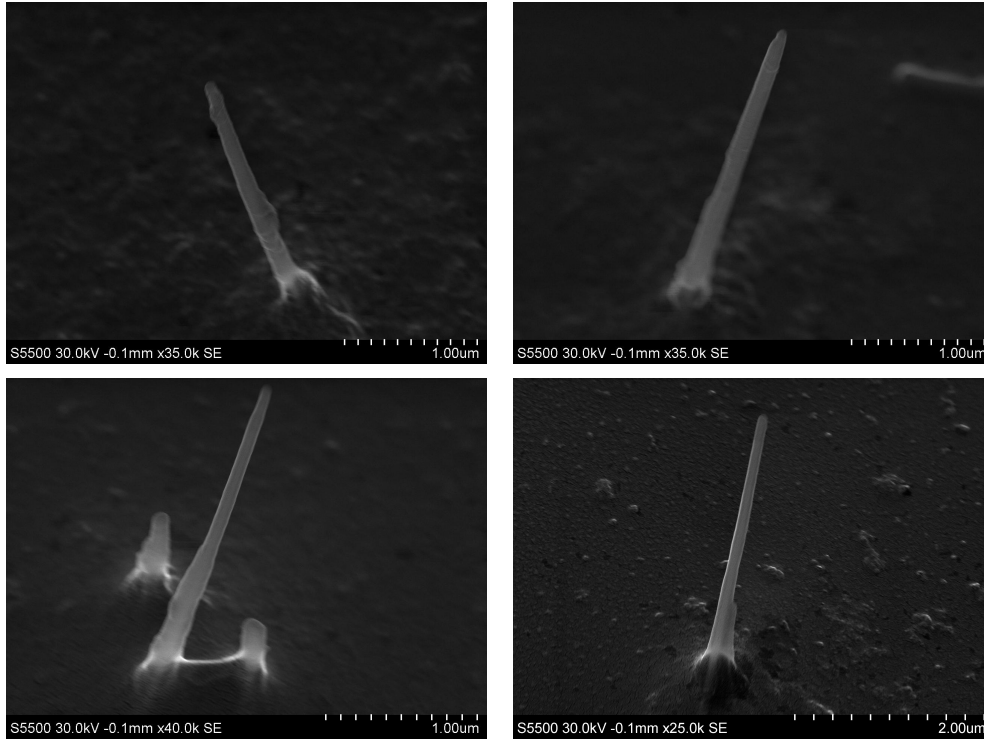
Figure 20: Nanowire tips

Tip diameter (nm)	Thickest diameter (nm)
119	222
148	217
121	142
122	162
121	188
126	164
86	155
110	144
111	100
135	213

Table 2: Nanowire diameters

desorbing from the nanowire surface. Note that the experiments presented here do not distinguish between desorption from nanowires or the supporting SU-8 surface, and the term 'nanowire surface' is used to describe the total surface of nanowire samples, including the SU-8 surface from which the nanowires protrude.

5.2.1 Results from investigations on DNA adsorption on nanowire surfaces

When YOYO-labeled DNA was imaged the fluorescent signal from the nanowire surface did not change over a period of 10 minutes, regardless of whether the surface was silanized with DETA or not, as seen in figure 21. This indicates that DNA adsorbed to nanowire surfaces is not immediately lost to the surrounding medium, which gives time for the cell to interact with the nanowire before DNA is desorbed.

| Dry surface | 0 minutes | 5 minutes | 10 minutes |
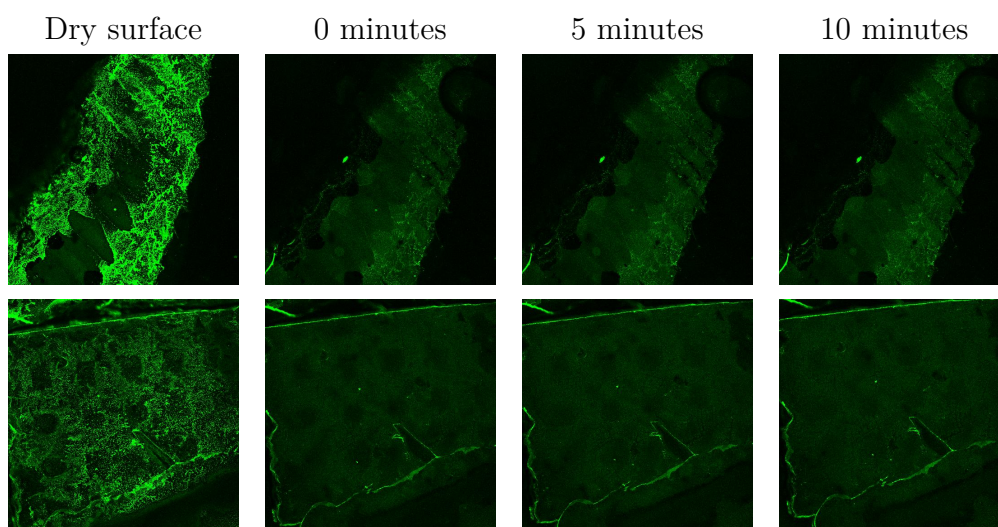
Figure 21: DNA does not desorb within 10 minutes from nanowire surfaces when the sample is immersed in warm PBS (37 °C). All images cover an area of 3.1x3.1 mm. The upper row shows images of surfaces that have been silanized, the lower row shows surfaces without silanization. Quantifying the fluorescent signal also showed that fluorescence did not decrease within 10 minutes, indicating that DNA adsorbed to the nanowire surface is not lost to the medium before cells are able to interact with the nanowires. The decrease in fluorescence from the dry surface to the same surface immediately after adding PBS can probably be attributed to solvent relaxation effects, and possibly also to immediate desorption of upper layers of dried plasmid. Note that the striped pattern in the upper row, and the rectangular pattern in the lower row of nanowire devices are attributed to a patterning of the nanowire surface, where only parts of the surface have nanowires, and other parts are chemically similar but flat.

5.2.2 DNA release determined using fluorospectrophotometry

DNA release was also investigated with the Olis DSM 1000 CD fluorospectrophotometer. The fluorescence from YOYO-1-labeled plasmid was detected from a PBS

solution in which a nanowire surface with adsorbed plasmid was immersed. The fluorescent emittance was registered over a period of 5.5 hours. Fluorescent detection increased over time, corresponding to a level indicating that half of the adsorbed plasmid was released to the solution in this time, as seen in figure 22. Concentrations less than 20 ng in 2 ml PBS gave too low fluorescence to be reliably recorded. The detected fluorescence was converted to a concentration value based on five reference samples and equation 15.
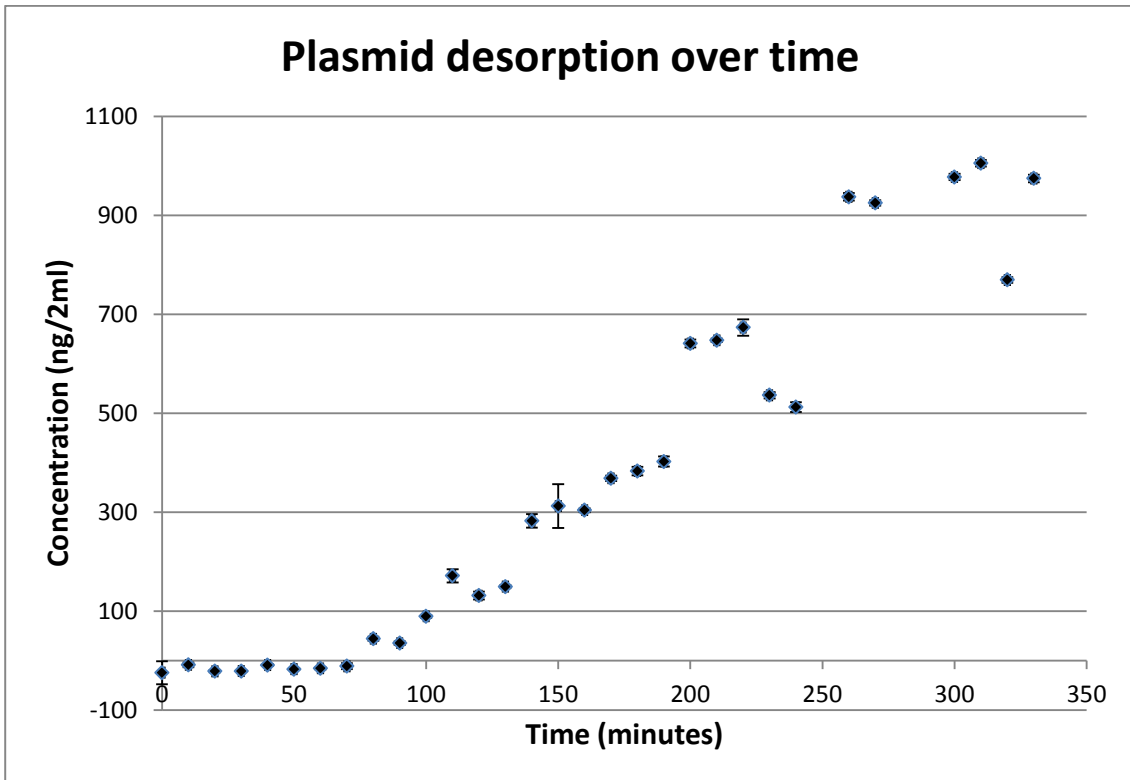
Figure 22: Results from the fluorospectrophotometer measuring fluorescence from a PBS solution in which a nanowire surface with adsorbed YOYO-1-labeled plasmid was immersed. After about 5 hours half of the adsorbed plasmid was released to the solution.

5.3 Cell growth on nanowire surfaces

Both HeLa cells and AR42J cells have previously been shown to grow and spread on nanowire surfaces [95, 100, 7, 9]. Cells grow and spread also on the surfaces used in this report, as seen in figure 23.

However, throughout the project it was found that cell growth deteriorated, and on nanowire surfaces over 7 weeks old almost no cells were able to grow. It was then found that nanowire surfaces can be refreshed by performing a new plasma
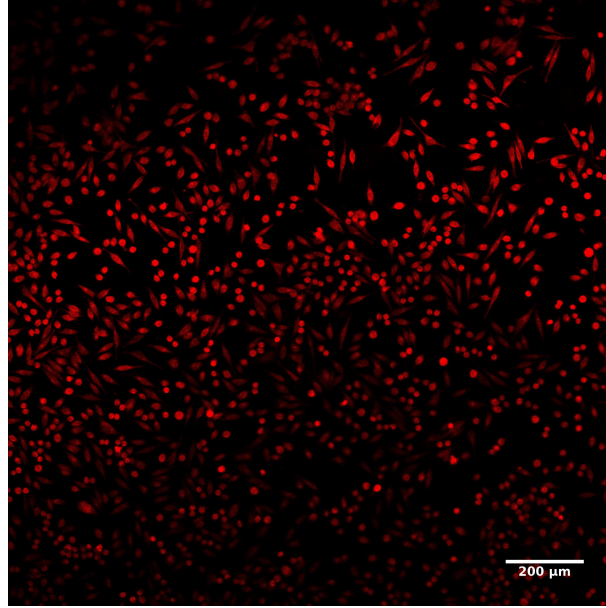
Figure 23: HeLa cells grow and spread on nanowire surfaces. The initial seeding concentration was 50,000 cells/cm^2, and cells were then grown for two days. Cells are stained with Calcein Red.

cleaning step (100% power of 100% O$_2$) for 30 seconds, and then silanizing the surface again, as described in the paragraph on nanowire synthesis. A comparison of old and refreshed nanowire surfaces (from the same batch) can be seen in figure 24. To avoid the deterioration of nanowire surfaces the final plasma cleaning step described in the standard nanowire synthesis (see chapter 4.1) protocol is now done just before using the surface for cell lab experiments. The cause of this deterioration is discussed in chapter 6.2.
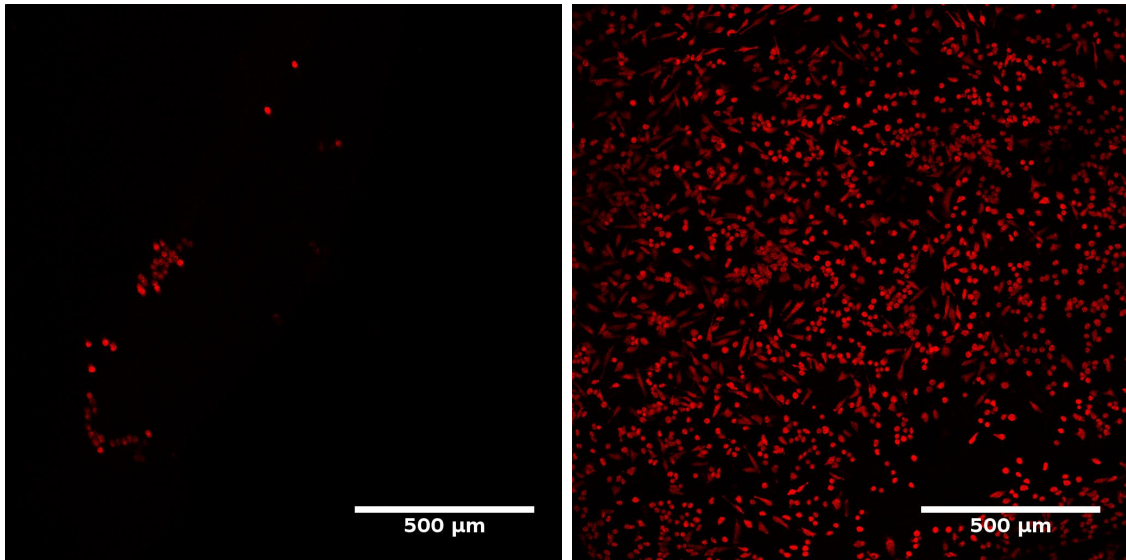
Figure 24: Growth of HeLa cells is impaired on nanowire surfaces that are older than a couple of weeks, as seen in the left image. Here HeLa cells are grown on a 7 week old nanowire surface, with a seeding density similar to what has been used throughout the current project. However, HeLa cells grow and spread well on old nanowire surfaces that have been refreshed by performing a plasma cleaning step and then silanizing the sample according to our standard protocol for nanowire synthesis, as can be seen in the right image. For both experiments the initial seeding concentration was 50,000 cells/cm^2, and cells were then grown for two days. Cells are stained with Calcein Red.

5.4 Results from labeled plasmid uptake experiments

YOYO-1-labeled plasmid (pcDNA) was used to investigate nanowire-mediated uptake of labeled molecules. Delivery of labeled cargo can be used to demonstrate that nanowire devices can serve as way to deliver biomolecules in general, and nanowire-mediated delivery has been demonstrated by other groups that investigate nanowire-mediated transfection systems. The delivery of fluorescently labeled cargo can quickly be assessed by fluorescence microscopy.

Imaging was done both with and without trypsination of cells. Washing, trypsination, and replating cells on a new glass slide ensures that all fluorescent spots that are not taken up by cells will be washed away, and thus not be included in further analysis. An example of a cell that has taken up fluorescently labeled cargo can be seen in figure 25. It was not possible to reliably discern YOYO-labeled plasmid taken up by cells from aggregates of YOYO-labeled plasmid just outside the cell in cells that were not trypsinated, when large numbers of cells were investigated. For trypsinated cells each cell was investigated for positive uptake from an area of 246x246 µm^2, with the area for each sample divided in four quadrants, each covering an area of 123x123 µm^2. For cells grown on nanowires and then trypsinated and grown on glass 86% $\pm$ 3% showed uptake of YOYO-labeled plasmid in these four quadrants in the first experiment. For cells grown on silanized glass and then trypsinated and grown on glass 32% $\pm$ 11% of the cells showed uptake of YOYO-labeled plasmid in the first experiment, as seen in figure 26. Nanowires thus initially seemed to facilitate uptake of labeled plasmid. Two follow-up experiments were conducted, where a higher amount of labeled plasmid was used: 5.5 µg plasmid per sample, vs 2 µg plasmid for the first experiment. In the second delivery experiment two replicates of nanowire and silanized glass samples were used, and delivery to cells were seen for 37% and 21% for cells grown on nanowires and glass respectively. In the third delivery experiment one replicate was investigated for nanowire and glass samples, with four areas imaged for each sample. Delivery was seen in 41% and 32% of cells grown on nanowires and glass respectively. These results are summarized in table 3. On average, for all experiments, 52% of cells grown on nanowires showed uptake of delivered cargo, versus 28% for cells grown on glass.

It was also investigated whether nanowires affect the number of fluorescent spots seen per cell. Results varied from area to area, and for cells grown on nanowires a range of 0.25-2.18 fluorescent spots per cell was seen, and for cells grown on glass a range of 0.12-0.90 spots per cell was seen. These results are summarized in table

4. On average cells grown on nanowires had 1.1 fluorescent spots per cell, and cells grown on glass had 0.53 spots per cell.

In all experimental settings many cells show uptake, including delivery from flat glass surfaces. Results were however highly variable from area to area, which reduces the strength of the results, considering the relatively low number of cells included in the experiment (a total of 964 cells were counted for all experiments combined). Even though positive delivery varies from experiment to experiment, the trend does indicate that nanowires could enhance delivery compared to flat surfaces, but experiments better suited for quantification are needed to fully elucidate and quantify the effects of nanowires.

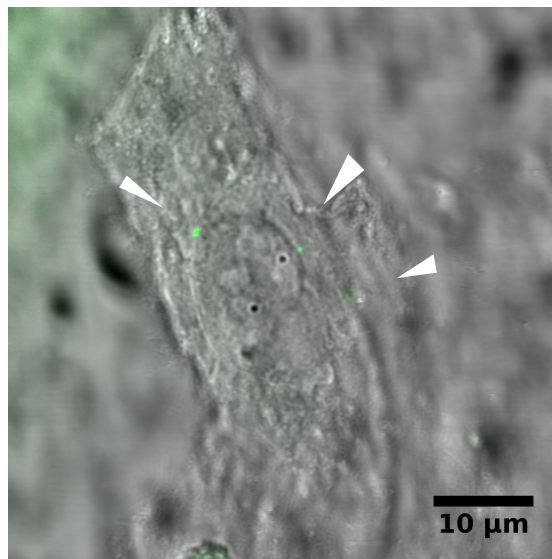Figure 25: Uptake of YOYO-labeled plasmid in a single cells is seen confined to small sections of a cell (arrows). This cell is still on a nanowire surfaces, and a stack must be recorded to ensure that fluorescent spots are truly inside cells, and not still outside. Since it was challenging to assess whether a spot was inside a cell or not, only single-cell investigations were performed for non-trypsinized cells.
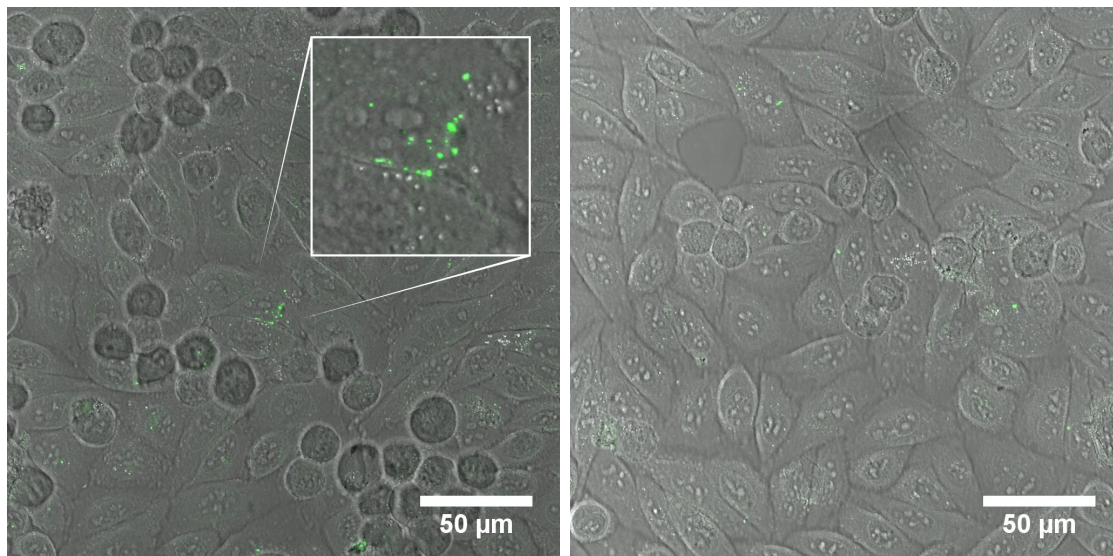
Figure 26: Uptake of YOYO-labeled plasmid in cells grown on nanowires versus cells grown on silanized glass. The left image shows cells grown for 1 day on nanowires, then 1 day on glass, before being imaged, and the right image shows cells grown for 1 day on glass (with plasmid), and then 1 day on a new glass slide, before being imaged. Green spots seen in some of the cells represent uptake of labeled plasmid. The left image includes a close-up image of a portion of the surface. Note that these images only cover 4 µm out of a stack covering ~25 µm in z-direction, and that many of the cells where no fluorescent spots are seen in this image could still have visible uptake in other focal planes.

No	Amount of plasmid	Nanowires	Glass	Cells	Comment
1	2.0 µg	86%	32%	255	1 replicate, 1 area
2	5.5 µg	37%	21%	323	2 replicates, 2 areas
3	5.5 µg	41%	32%	386	1 replicate, 4 areas

Table 3: Proportion of cells were fluorescently labeled plasmid was successfully delivered, with results for both cells grown on glass and nanowires. Also the total number of cells counted in each experiment, and the number of replicates are given, as well as number of areas per replicate.

No	Amount of plasmid	Nanowires	Glass	Cells	Comment
1	2.0 µg	2.2	0.21	255	1 replicate, 1 area
2	5.5 µg	0.89	0.39	323	2 replicates, 2 areas
3	5.5 µg	1.7	0.90	386	1 replicate, 4 areas

Table 4: Number of fluorescent spots per cell, with results for both cells grown on glass and nanowires. Also the total number of cells counted in each experiment, and the number of replicates are given, as well as number of areas per replicate. As can be seen the number of fluorescent spots varies from experiment to experiment, but with a trend towards higher number of fluorescent spots per cell for cells grown on nanowires compared to glass. For all experiments the same lower intensity cut-off values and minimum spot-size has been used for estimating the number of spots per cell. The number of cells was counted manually.

5.5 Results from siRNA transfection using patterned surfaces

To test the hypothesis that nanowires only facilitate the transfer of biomolecules to the cytoplasm of cells, and not to the nucleus, siRNA transfection was tested. siEGFP associates with its target mRNA, the transcript of the EGFP plasmid, in the cytoplasm of a cell, and instructs the degradation of its target mRNA. Successful delivery of siEGFP would thus be seen as a decrease of fluorescence from cells that stably express EGFP, even if siEGFP never reaches the nucleus of a cell.

Patterned surfaces, with alternating lanes of nanowires and flat SU-8, showed no convincing knockdown of EGFP expression when siRNA directed against EGFP mRNA was adsorbed to nanowire surfaces, and cells grown on top of these. The fluorescent recording from the same well as seen in figure 17 is shown in figure 27.
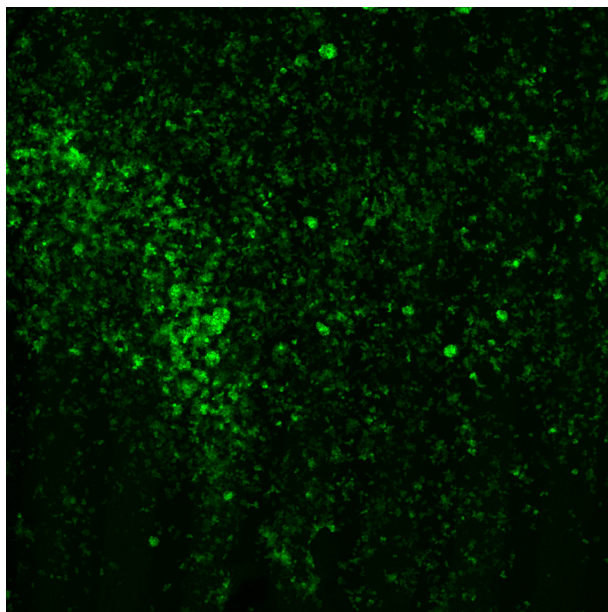
Figure 27: The fluorescent signal recorded from the same well as seen in figure 17. Cells are imaged 48 hours after being seeded on a patterned surface with adsorbed siEGFP. The lanes seen in the optical image in figure 17 are not distinguishable in the fluorescent image.

Total fluorescence intensity from cells growing on nanowires was generally slightly lower than from cells growing on flat SU-8, but this difference was found both in wells with siEGFP and wells with dummy siRNA. The results from one of the experiments is shown in figure 28.
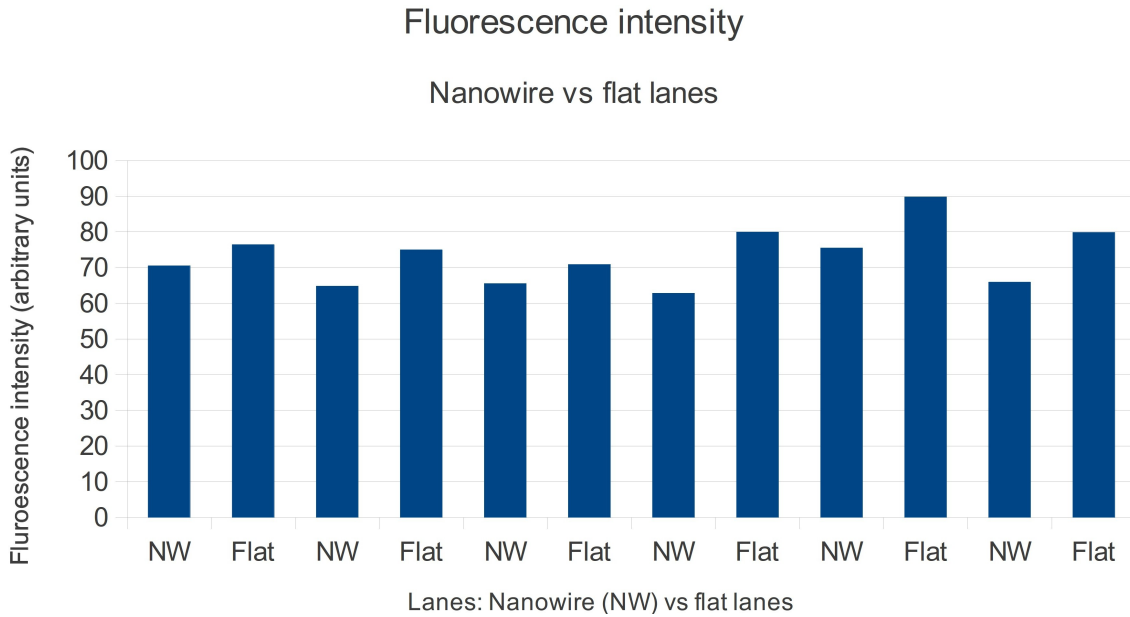
Figure 28: The graph height represents the total fluorescence from one lane, and these results are recorded as alternating lanes of nanowires or flat SU-8. Cells are imaged 48 hours after being seeded on a patterned surface with adsorbed dummy siRNA (siCAT). Fluorescence from lanes with nanowires are generally slightly lower than from neighboring lanes with flat SU-8. Some of the variations are the result of clustering of cells.

5.6 Results from plasmid transfection experiments with tapping method

The tapping method of transfecting cells is based on placing a nanowire surface with adsorbed plasmid face down on top of cells, and then tapping the surface to facilitate penetration of the cellular membrane. The reason for this approach is to increase the force of penetration. The method has been well described in the literature, with transfection efficiencies of <5% (cells expressing a reporter protein) to 53% (RNAi knockdown of selected cells) in some papers [38, 86, 39], and 76 ± 56 cells/mm^2 in a more recent paper by the same group [88][8].

In this work three variants of the tapping method were tested (see figure 15 for an illustration of the procedure in general):

- Depositing cells on a cleanroom wipe and then placing a nanowire surface face-down on top,

- forming a cell pellet that is then placed on a glass slide and then placing a

---

[8]The proportion of successfully transfected cells in [88] is unknown, since the density of cells is unknown, as discussed in chapter 3.

nanowire surface face-down on top, or

- growing cells for one day on a slide and then placing a nanowire surface face-down on top.

The last method, of growing cells for one day on a slide before tapping, has not been described in literature. With this method the amount of cells present on a surface can be quite well controlled, as the seeding density and growth time is known. Also control experiments with different surfaces can easily be compared, since the surface on which cells are grown will be the same for all experiments.

Transfer of cells from cleanroom wipe to a nanowire surface was generally very low in our experiments, and of those few cells that were transferred almost none were transfected (<1%). It was tested whether the hydrophilicity of the nanowire surface could contribute to the low transfer efficiencies. Freshly plasma cleaned surfaces were then tested without silanization, which gives a very hydrophilic surface. This did however not increase the efficiency of cell transference when used together with cells on a cleanroom wipe in our experiments, where 200,000 cells were deposited on a cleanroom wipe (5x5 to 10x10 mm^2).

New tapping experiments were then conducted, with a cell pellet deposited on a flat or concave glass surface. In these experiments high amounts of cells were transferred from the pellet to the nanowire surface upon placing the nanowire surface on top of the cell pellet, and then subsequently tapping the nanowire surface. The nanowire surface was then placed either face-up or face-down in medium. An optical microscope was used to get an impression of the number of cells transferred, and in cases of very high numbers (i.e. multiple layers of cells) medium was changed after 75 minutes, in order to wash away some of the more loosely adherent cells. The surface with cells was then placed in a growth chamber for two days. Positioning the nanowire surfaces face-up worked best, as many cells were lost on nanowire surfaces that were kept face-down. These experiments gave higher number of transfected cells than seen in our project previously. One of these results can be seen in figure 29, which had a transfection efficiency of ~5% in two areas of nanowire surface, or equivalently 62 cells/mm^2. A more commonly encountered result is shown in figure 30.

For most of the tapping experiments results were lower than seen in figure 29, and control experiments with glass surfaces were then done in order to see whether the good transfection efficiency seen occasionally in parts of nanowire surfaces could be attributed to nanowires.

79

Figure 29: A pellet was formed of 7-9 million cells, placed on a glass surface, and then a nanowire surface with pmaxEGFP adsorbed to it was placed face-down on top of the cell pellet. After tapping, the nanowire surface was placed in a growth chamber with medium for 2 days, and then imaged. Cells are stained with Calcein Red, and green cells are expressing EGFP. Good transfection efficiencies was confined to two areas of the nanowire surface, one in the middle of the surface and one around a corner, and could indicate that geometrical effects only allow tight contact between nanowires and cells in certain areas. In this part of the nanowire surface roughly 150 cells are transfected out of 3000 cells on an area of 2.40 mm^2 (total number estimated by counting five 155x155 µm^2 areas), or equivalently, ~5% or 62 cells/mm^2 of a total density of 1250 cells/mm^2 are successfully transfected. In other parts of the surface area transfection efficiency was <1%.
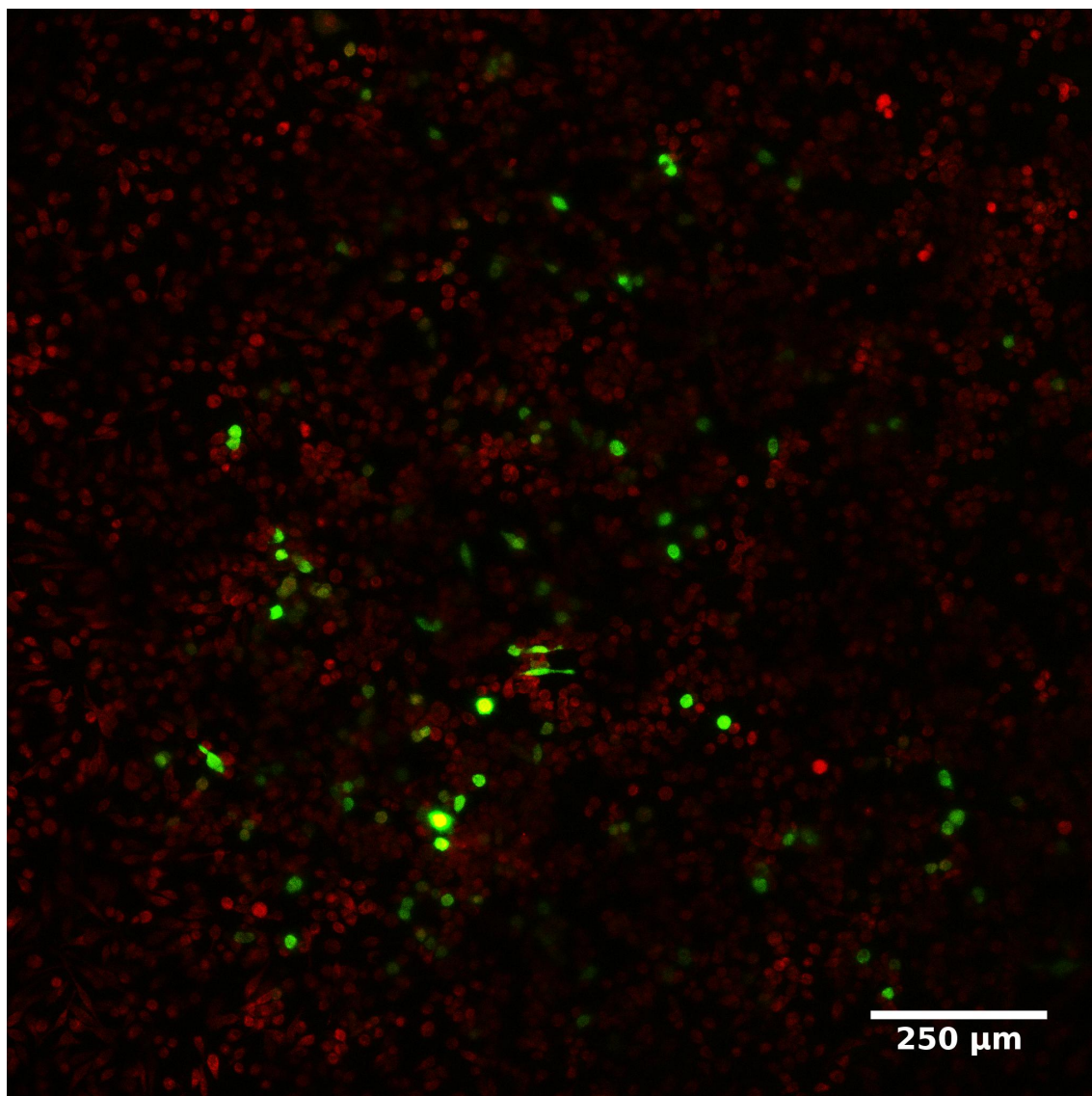
Figure 30: A pellet was formed of 7-9 million cells, placed on a glass surface, and then a nanowire surface with pmaxEGFP adsorbed to it was placed face-down on top of the cell pellet. After tapping, the nanowire surface was placed in a growth chamber with medium for 2 days, and then imaged. Cells are stained with Calcein Red, and green cells are expressing EGFP. In this image 10 cells are transfected out of 2400 cells, or equivalently, ~0.4% or 4 cells/mm^2.

For glass slides more transfected cells were generally found than on nanowire surfaces, and transfection efficiency also varied between different parts of a glass surface. An area of many transfected cells can be seen in figure 31, and a more typical result can be seen in figure 32.

In our standard procedure plasmid is adsorbed to a surface by depositing a droplet (typically 20 µL) of plasmid at a concentration of 100 ng/µL on the surface,

Figure 31: A pellet was formed of several million cells, placed on a glass surface, and then a glass surface with pmaxEGFP adsorbed to it was placed face-down on top of the cell pellet. After tapping the glass surface was placed in a growth chamber with medium for 2 days, and then imaged. Cells are stained with Calcein Red, and green cells are expressing EGFP. Good transfection efficiencies was confined to certain areas of the glass slide.

and then letting the droplet dry completely, which takes 30-60 minutes. It was also tested if the droplet should not dry completely, and tests where the droplet was deposited on the surface for 30 minutes were conducted, both for nanowire surfaces and glass controls. There was no apparent effect of using dry vs wet surfaces in terms of transfection efficiency.

These initial tapping experiments gave the impression of slightly better transfection efficiencies for glass controls compared to nanowire surfaces, but it was also
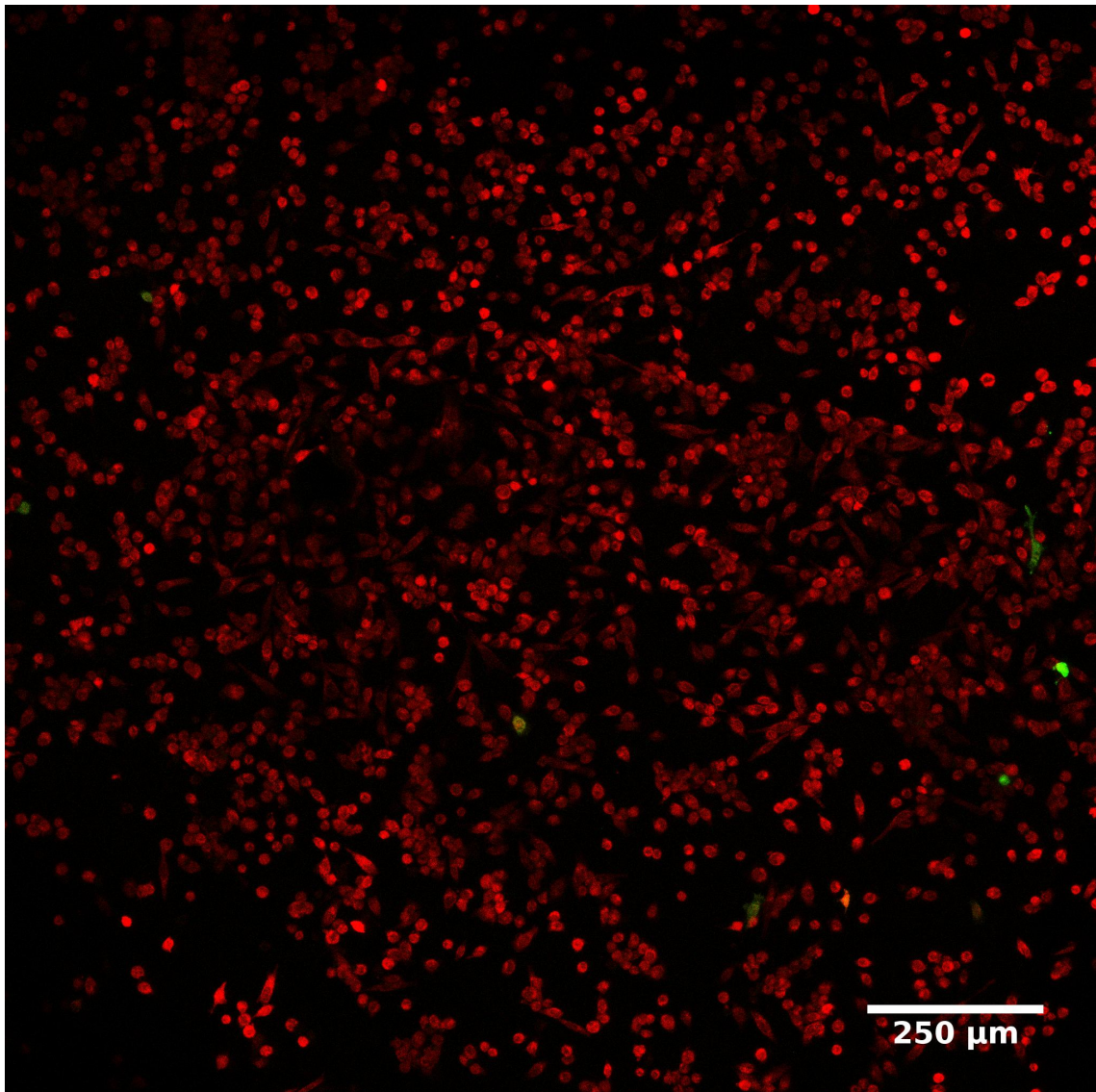
Figure 32: A pellet was formed of several million cells, placed on a glass surface, and then a glass surface with pmaxEGFP adsorbed to it was placed face-down on top of the cell pellet. After tapping, the glass surface was placed in a growth chamber with medium for 2 days, and then imaged. Cells are stained with Calcein Red, and green cells are expressing EGFP. In this image 51 cells out of 4700 are transfected, or equivalently ~1% or 22 cells/mm^2

found that cells grow and spread slightly better on glass surfaces than nanowire surfaces, which could indicate that a number effect contributes to our results. Two new control experiments were conducted to get around these issues: In the first control experiment nanowire surfaces were compared to equally sized (5x5 mm^2) flat SU-8 surfaces glued to glass slides using PDMS, so that surface chemistry and geometry would be very similar, apart from the nanowires found on the nanowire

surface. In the second control experiment cells were grown on a glass surface for one day before tapping, so that a known concentration of cells were deposited on all surfaces, to reduce the random fluctuations in seeding density often found with the tapping experiments. In this experiment flat SU-8 surfaces were compared to nanowire surfaces and glass surfaces, and for both control experiments two replicates of each experimental condition were done. Results were consistent between the two tapping experiments and between the two replicates: Flat SU-8 surfaces give the same number of transfected cells as nanowire surfaces, and glass surfaces give slightly higher transfection efficiencies than SU-8 surfaces.

In the first of these control experiments flat SU-8 surfaces were compared to nanowire surfaces when a pellet was tapped. For SU-8 and nanowire surface roughly 40-45 cells were transfected on the total surface area of 5x5 mm, or equivalently 1.6 cells/mm^2. The density of cells on both surfaces were similar, indicating that cells grow and spread equally well on a nanowire surface and a flat SU-8 surface. Figures 33 and 34 show typical results.

Finally, tapping of cells grown for one day on a glass slide were compared for nanowire surfaces, flat SU-8 surfaces and glass surfaces. 50,000 cells/cm^2 were seeded to a well with medium and a glass slide (diameter 13 mm) at the bottom, and then placed in a growth chamber. The next day medium was aspirated, the surface to be investigated placed face-down on top of the cells, and tapped with a tweezer. After 15 minutes the surfaces were separated, and both surfaces were then grown for one more day, before imaging. As expected, few cells were transferred to the top surface, since cells were already firmly attached to the glass slide. Interestingly, cells were evenly transfected on the entire glass slide, and not only in the central area that corresponded to the nanowire or flat surface. Replicate two of the glass slide tapping experiment was unproductive, since the two glass slide surfaces were to firmly adherent to be separated after 15 minutes, due to the high surface tension between these two flat surfaces. The results from this experiment are summarized in table 5. In conclusion transfection efficiencies on nanowire surfaces are comparable to flat SU-8 surfaces, and in this experiment an efficiency of ~1% was achieved. For glass surfaces a higher transfection efficiency of ~7% was observed in this experiment, which can not be attributed to a numbers effect, since the total number of cells were the same for all experimental conditions.

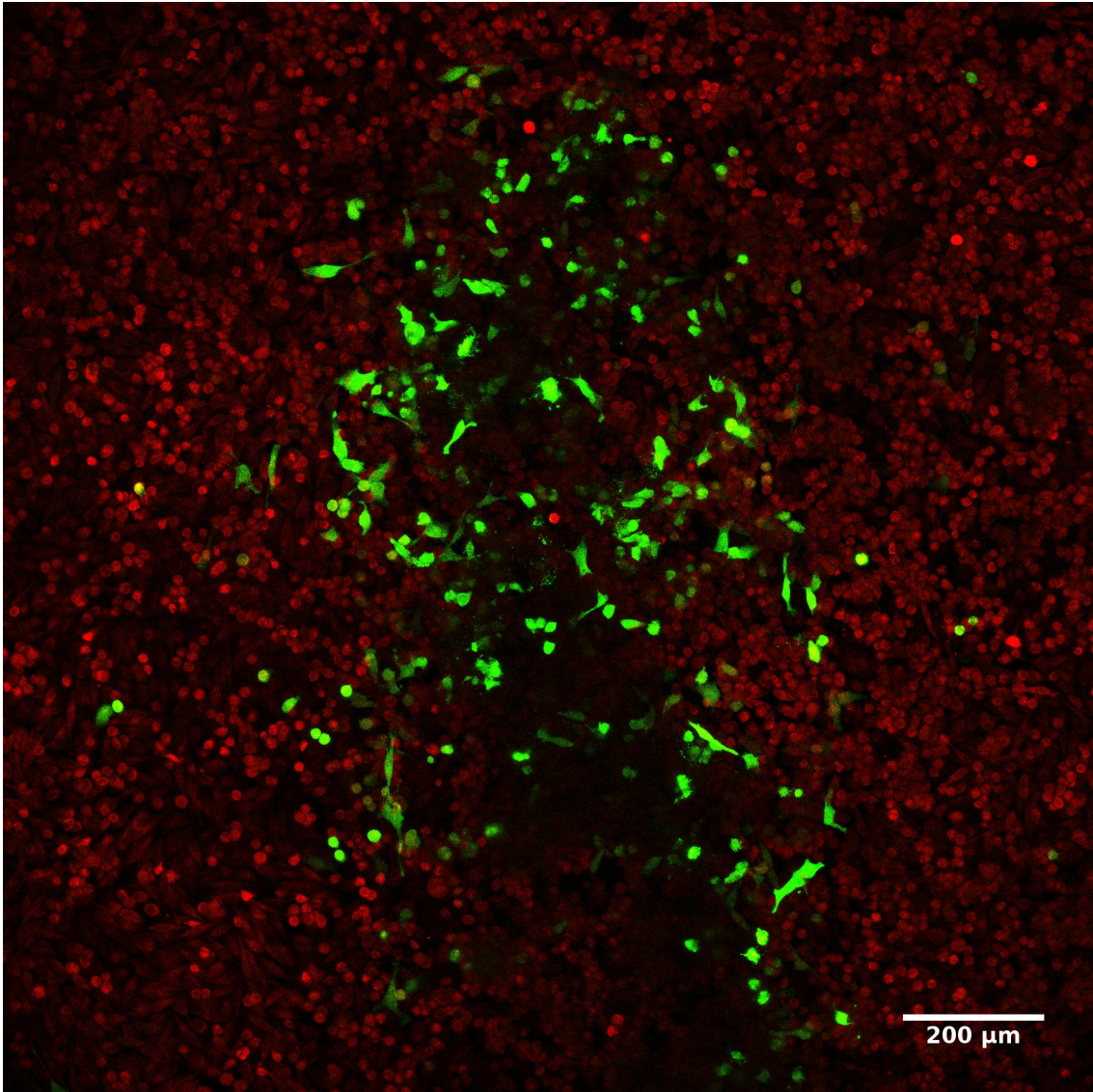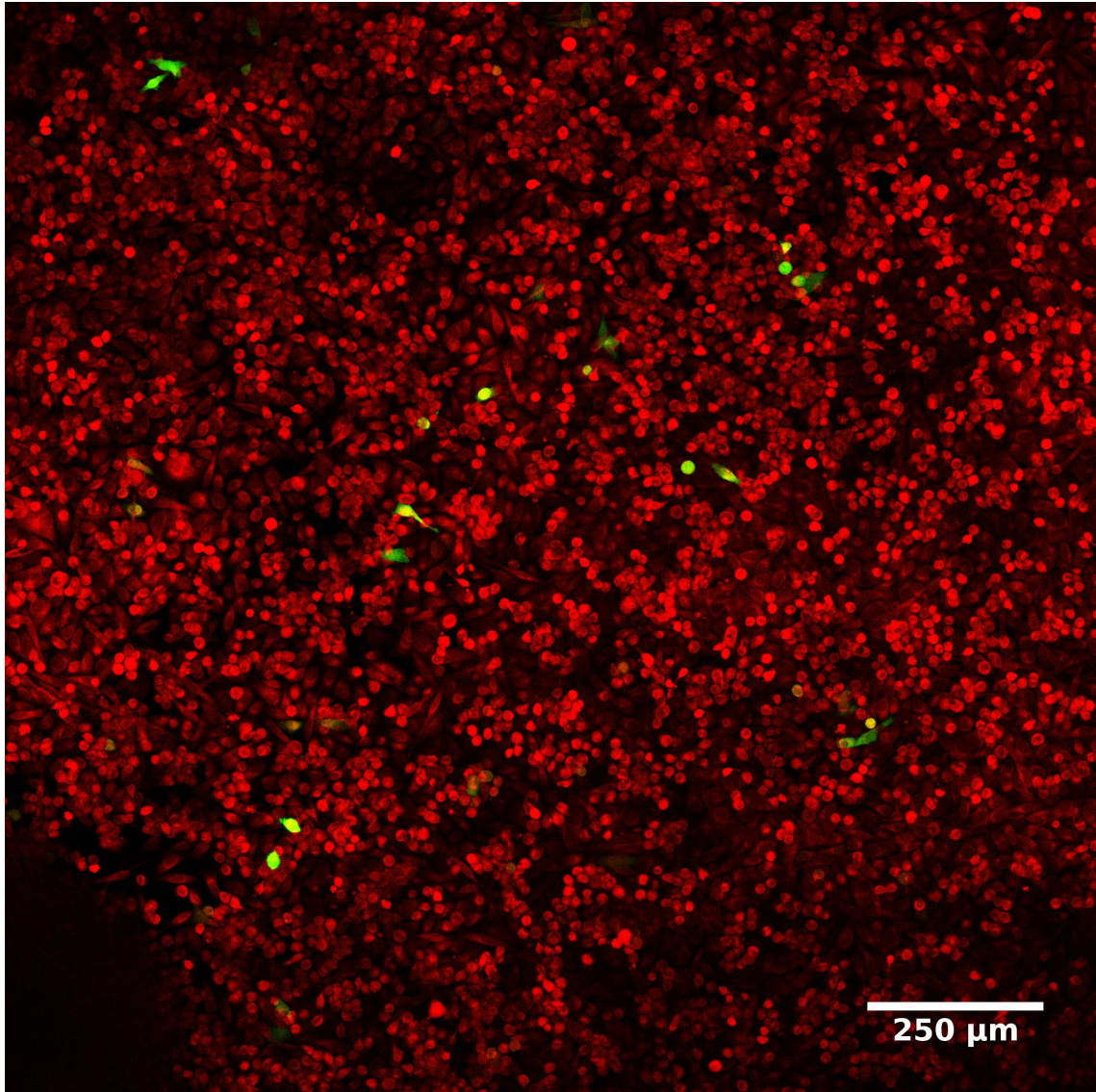The results for these experiments can be contrasted in figure 35.
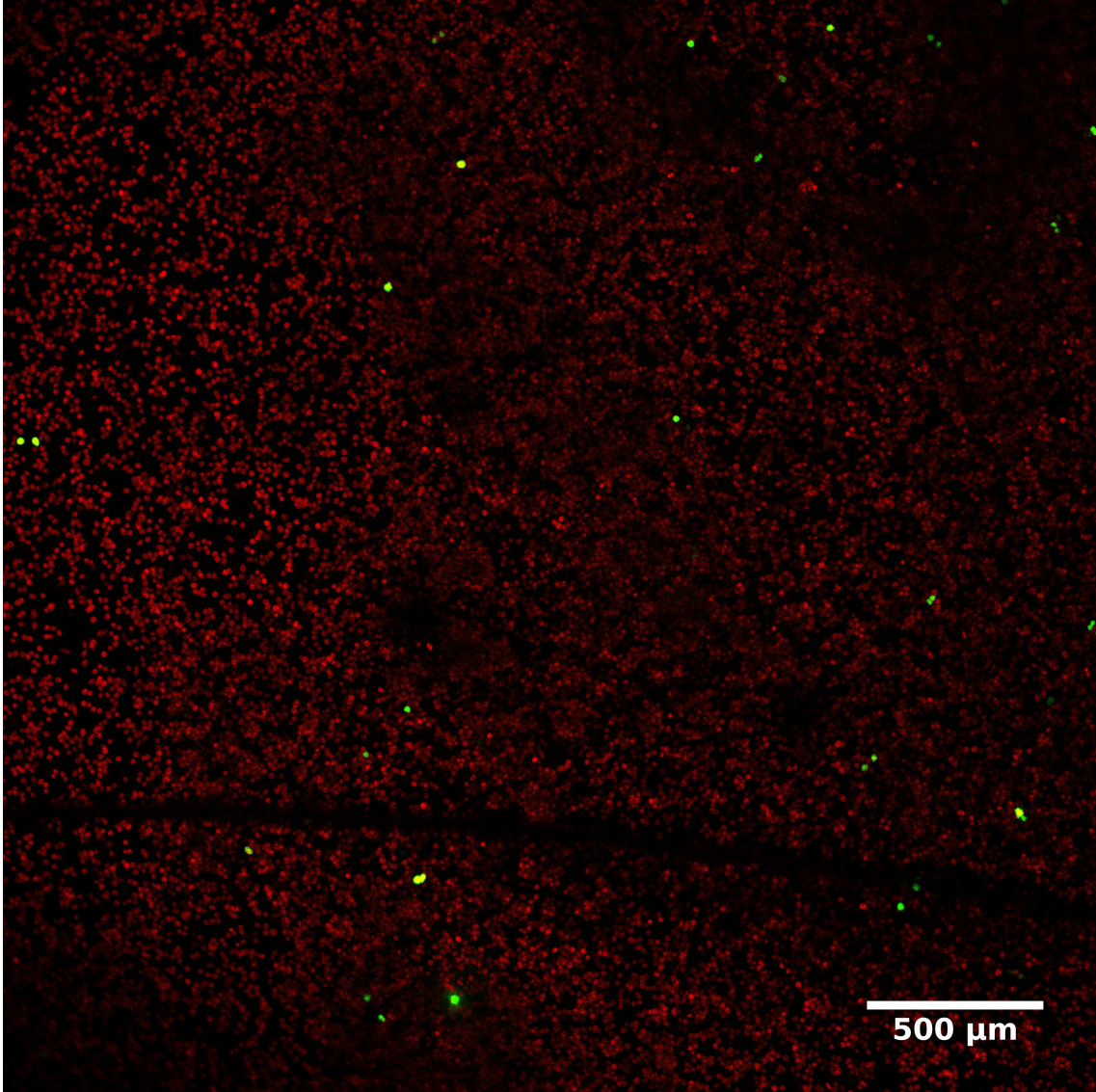
Figure 33: A pellet was formed of several million cells, placed on a glass surface, and then a nanowire surface with pmaxEGFP adsorbed to it was placed face-down on top of the cell pellet. After tapping, the nanowire surface was placed in a growth chamber with medium for 2 days, and then imaged. Cells are stained with Calcein Red, and green cells are expressing EGFP.
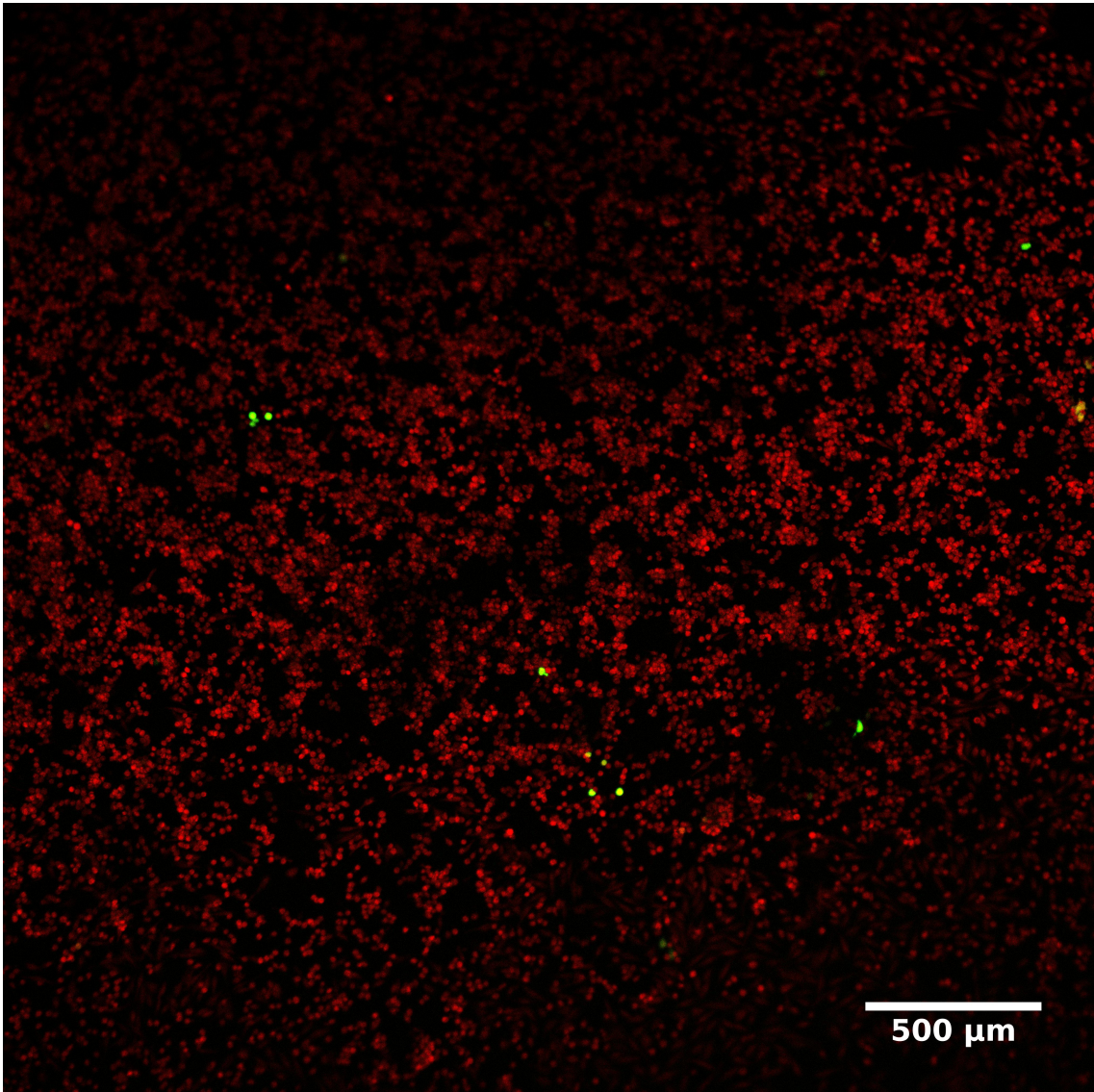
Figure 34: A pellet was formed of several million cells, placed on a glass surface, and then a flat SU-8 surface with pmaxEGFP adsorbed to it was placed face-down on top of the cell pellet. After tapping, the flat surface was placed in a growth chamber with medium for 2 days, and then imaged. Cells are stained with Calcein Red, and green cells are expressing EGFP.

Surface	Number of transfected cells	Efficiency (%)	Efficiency (cells/mm^2)
Nanowire surface 1	126	1.3%	13.1 cells/mm^2
Nanowire surface 2	130	1.4%	13.5 cells/mm^2
Flat SU-8 surface 1	82	0.85%	8.5 cells/mm^2
Flat SU-8 surface 2	95	0.99%	9.9 cells/mm^2
Glass surface 1	646	6.7%	67.2 cells/mm^2
Glass surface 2	-	-	-

Table 5: Transfection efficiencies in tapping experiments. Nanowire surfaces perform on par with flat SU-8 surfaces, and not as well as flat glass surfaces. Results for the second glass experiment are not included, as the two glass slides could not be separated, with the result that all cells died.
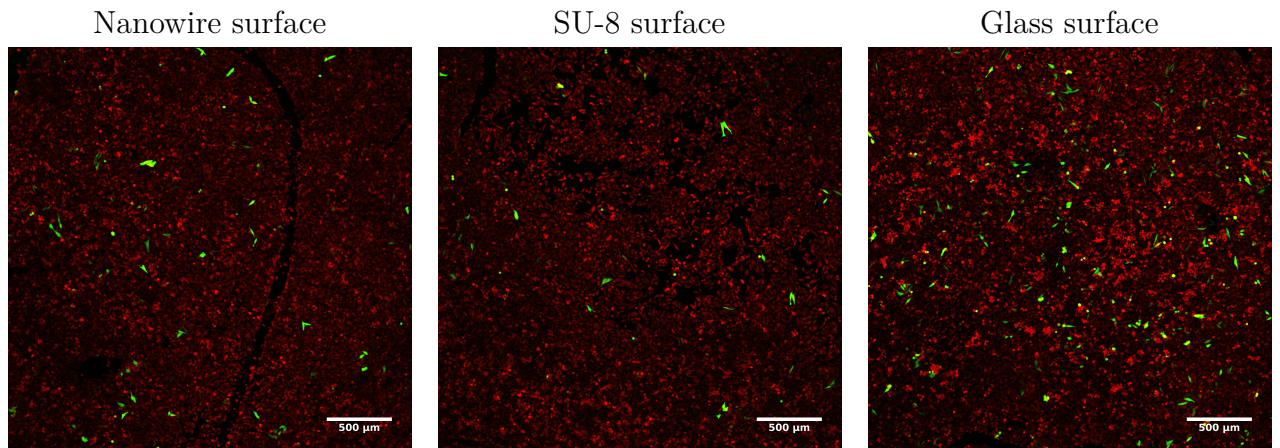
Figure 35: The three images show the results for tapping cells grown on glass for 1 day. 50,000 cells/cm^2 were seeded to a well with medium and a glass slide (diameter 13 mm) at the bottom, and then placed in a growth chamber. The next day medium was aspirated, the surface to be investigated placed face-down on top of the cells, and tapped with a tweezer. Transfection efficiency on nanowire surfaces is on par with flat SU-8 surfaces, and lower than on flat glass surfaces.

5.7 Results from plasmid transfection experiments with centrifugation method

Centrifugation experiments are based on the assumption that by increasing the relative centrifugal force the calculated force barrier that the membrane represents can be overcome.

5.7.1 Megafuge 1.0 experiments

The idea of penetrating the cellular and possibly also the nuclear membrane by centrifugation is based on the assumption that by increasing the relative centrifugal force the calculated force barrier that the membrane represents can be overcome. Cellular residues have a density of 1.078 g/cm^3 [101], and growth medium has a density of 1.006-1.008 g/cm^3. This gives the cell an effective mass of ~0.071 g/cm^3, and with a spherical diameter of 15 µm for trypsinized cells the gravitational force pulling cells down in a simple sedimentation experiment will be $F = m \times a = 1.2$ pN, which is almost three orders of magnitude lower than the force required empirically (0.65 nN) [60]. In addition, each cell is pierced by several nanowires. If the nanowire areal density is assumed to be 0.1 µm^{-2}, a trypsinized cell, covering a planar area of ~180 µm^2, will be impaled by 20 wires. Many wires will however not have the required length to perforate the cellular membrane, and for the following calculations it is assumed that each cell is impaled by 10 wires. With a nanowire diameter of 120 nm the combined surface at the end of the nanowires would be 0.011 µm^2. If a force of 0.65 nN is required to penetrate a cell with a single nanowire [60], this corresponds to a relative centrifugal force of 528G.

The relationship between relative centrifugal force (RCF) and terminal velocity is illustrated in figure 36, and the impalement force as a function of RCF is illustrated in figure 37.

In the Megafuge 1.0 centrifuge relative centrifugal forces up to 2680 × g can be reached. Two initial experiments yielded more transfected cells than previously seen by simply letting cells sediment on nanowire surfaces. Transfection efficiencies were compared between centrifugation in DMEM, and two hypotonic buffers (50% hypotonicity and 98% hypotonicity), as well as nanowire surfaces which were not silanized, and glass.

All surfaces covered an area of approximately 5x5 mm^2, and for these experiments transfection efficiencies of 2-40 cells were achieved. Initial seeding density was 50,000 cells/cm^2, and, with a lag time of close to 20h and a doubling time close to 24h,
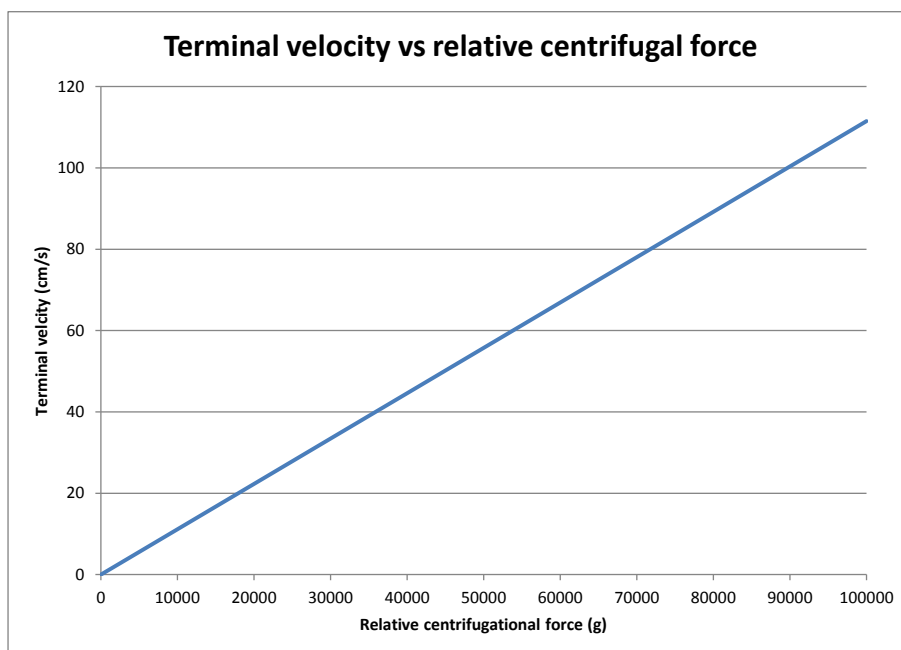
Figure 36: The relationship between relative centrifugal force and terminal velocity. As is evident from the graph cells will quickly sediment when centrifuged. For cells sedimenting by gravitation, the terminal velocity is 0.01 mm/s, or 10 cm in 15 minutes.
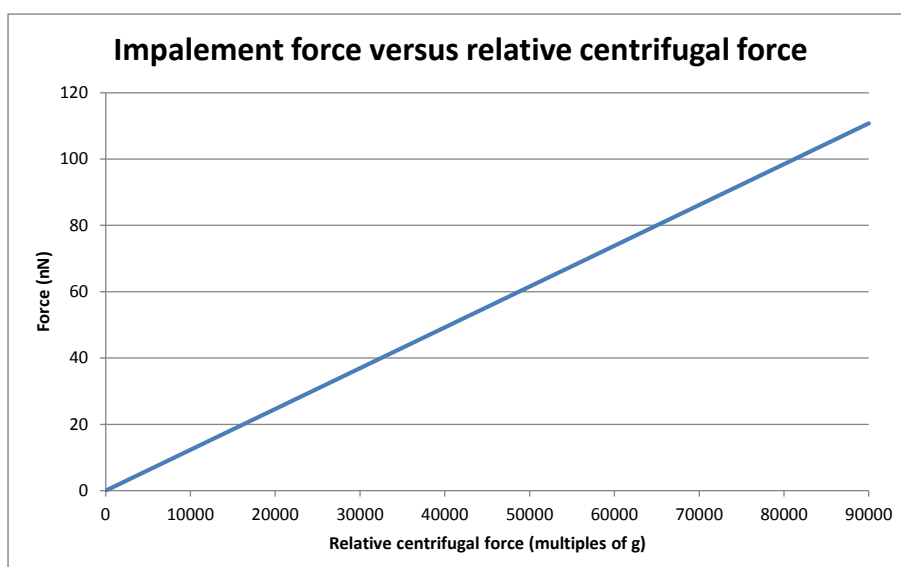
Figure 37: The relationship between impalement force and relative centrifugal force.

about 25,000 cells should be present on an area of 5x5 mm^2. Transfection efficiencies are very low, 40 transfected cells is equivalent to a transfection efficiency of 0.16%. Results were still considered encouraging as the ultracentrifugation experiments were planned. However, a final control experiment, with two nanowire surfaces and one glass surface, gave no transfected cells. These results are summarized in table 6.

Nanowires which were not silanized also gave poor results, with 2 and 6 transfected cells respectively (medium was used during the centrifugation). It was also tested if the nanowire surface with plasmid adsorbed should be left in medium for 5 minutes before centrifugation, to facilitate desorption of DNA, but this too was without any apparent effect on transfection efficiency.

Experiment no.	Medium	50% hypotonicity	98% hypotonicity	Glass (medium)
1	27	3	20	-
2	17	3	40	-
3	0	-	-	0

Table 6: Transfection efficiencies in Megafuge 1.0 centrifuge experiments. The numbers indicate the number of successfully transfected cells on a nanowire surface area covering 5x5 mm^2. Cells where seeded at a concentration of 50,000 cells/cm^2, and thus roughly 25,000 cells should be present on an area of 5x5 mm^2 after two days.

5.7.2 Ultracentrifuge experiments

Relative centrifugal forces of 5,000 $\times$ g, 10,000 $\times$ g, 15,000 $\times$ g, 20,000 $\times$ g, 30,000 $\times$ g, 40,000 $\times$ g, 50,000 $\times$ g, 60,000 $\times$ g, 80,000 $\times$ g and 88,500 $\times$ g (maximum) were tested. Several of these conditions were tested with two replicates, and 88,500 $\times$ g was tested with three replicates, and one glass control. Results were the same for all experiments: Cells are able to grow and spread after being subjected to high relative centrifugal forces, but are not transfected. An image of cells centrifuged at 88,500 $\times$ g can be seen in figure 38.

The behavior of nanowire surfaces when exposed to high relative centrifugal forces has not previously been described. Scanning electron microscopy reveals that wires are not affected by the high RCF, and also behave as previously described [95, 7], as seen in figures 39, 40 and 41.
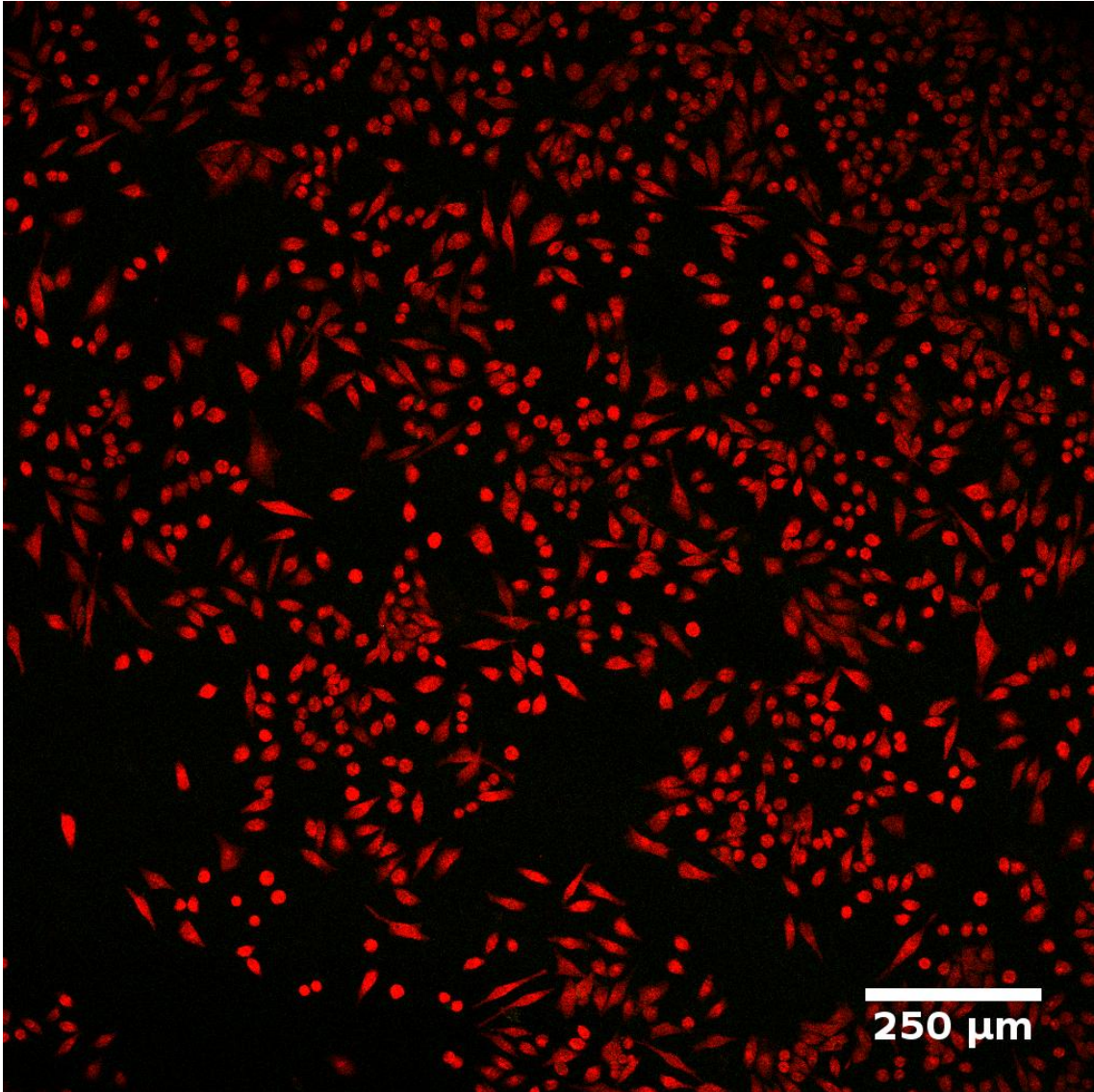
Figure 38: Cells grow and spread on nanowire surfaces after exposure to relative centrifugal forces of 88,500 × g. No cells are transfected.
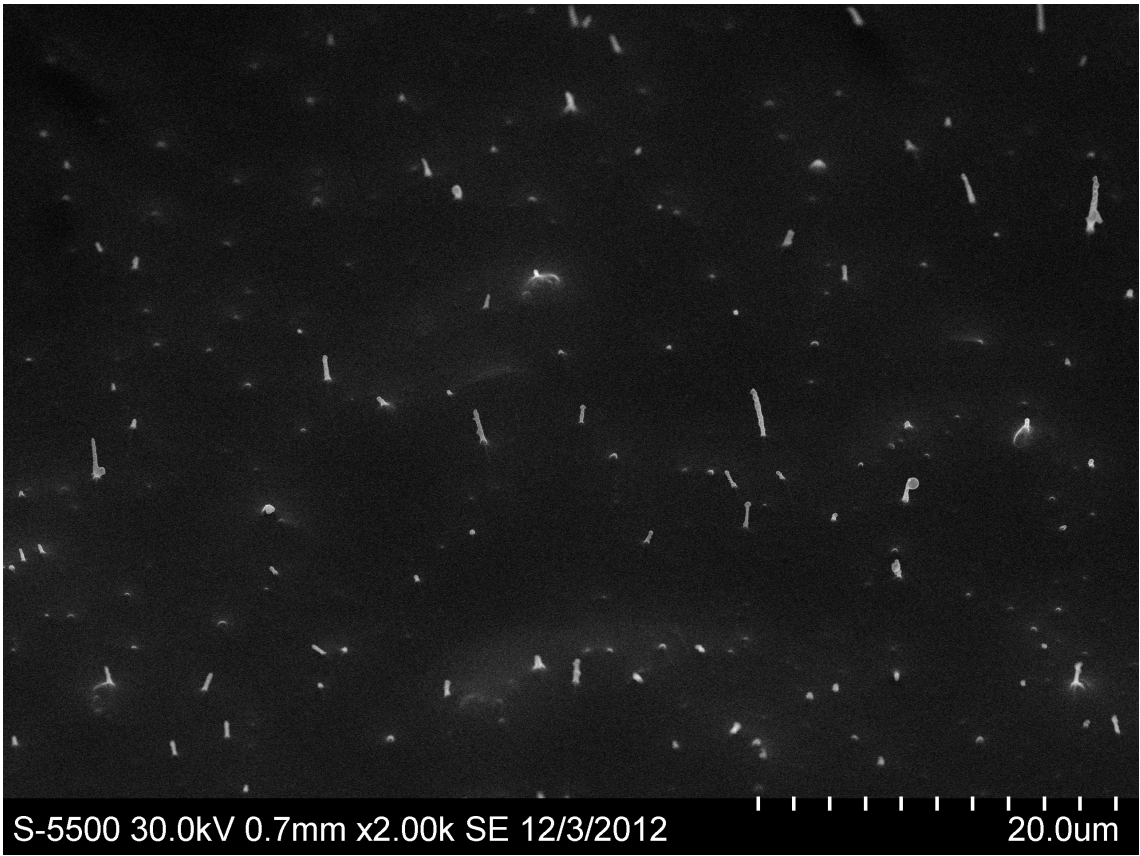
Figure 39: Nanowires are unaffected by 88,500 × g.

S-5500 25.0kV 0.6mm x2.00k SE 12/3/2012   20.0um
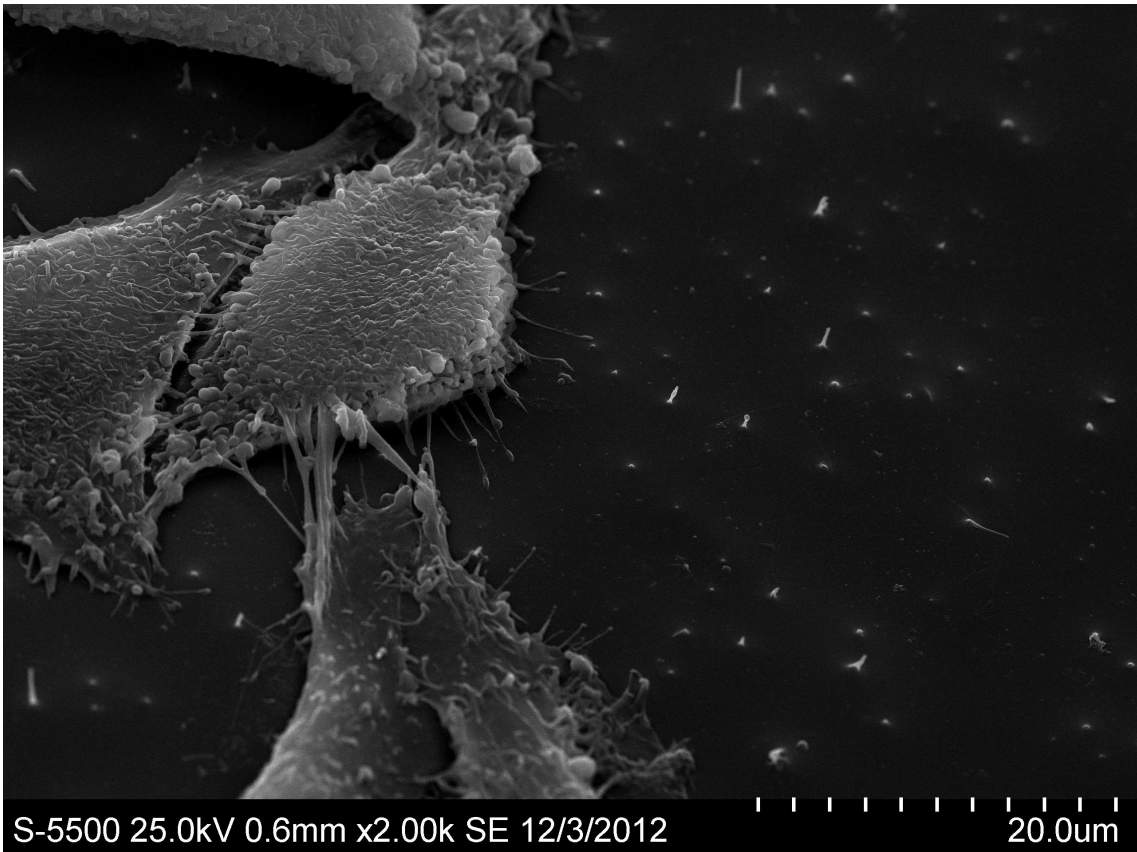
Figure 40: Cells are unaffected by 88,500 $\times$ g, and grow and spread in the same way as observed earlier, when investigated with scanning electron microscopy.
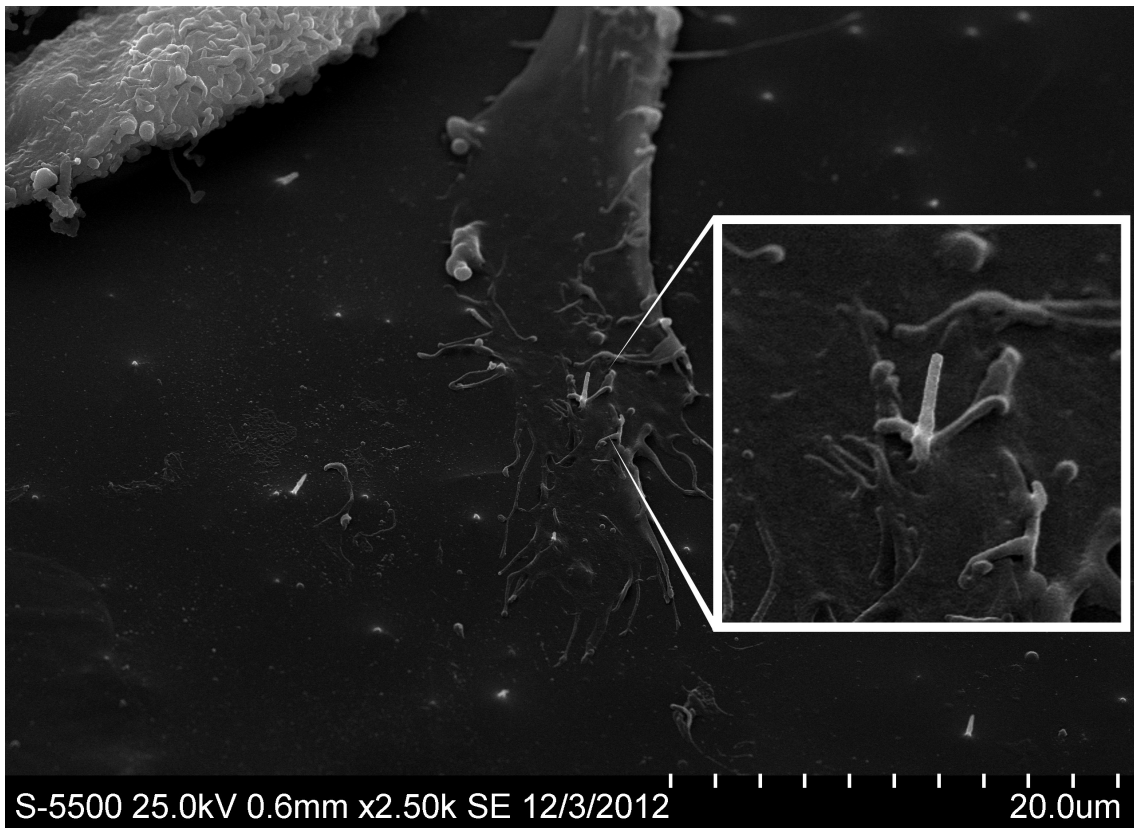
Figure 41: Structures that resemble nanowires can often be seen protruding from the surface of a cell, indicating that a cell is growing on top of a nanowire. The cell pictured was exposed to 88,500 × g.

6 Discussion

The goal of the current project was to test and optimize delivery of relatively large molecules to the cytoplasm and/or nucleus of cells. To test this, molecules that affect a cell's phenotype are used, and in this project both siRNAs, utilizing RNA interference, and plasmids, which encode easily detectable reporter proteins (EGFP), are used. Phenotypic changes are easily detected in a fluorescence microscope, through fluorescent reporter systems. In reaching this goal the cupric oxide nanowire delivery platform was further characterized with respect to DNA release, and dimensions of nanowires.

In summary, transfection experiments are disappointing, with low transfection efficiencies for both siRNA and plasmid transfection experiments. Similar results are obtained with flat surfaces, indicating that nanowires are not mediating the observed transfection. Given the number of experiments conducted these results are consistent, with only few, random examples that are more encouraging.

6.1 Nanowire dimensions and areal density

Results presented in this work regarding nanowire dimensions and areal density fit well with our previous experience of this delivery platform, indicating that the production of nanowire surfaces is largely reproducible, with similar dimensions and densities from experiment to experiment. It is however always a chance of random fluctuations, where parts of a nanowire surface might be dysfunctional. It can therefore not be excluded that some of the negative results obtained in this work could be attributed to non-functional parts of a nanowire surface. To reduce chances of this most results are tested with at least 2 replicates, often several more. Also it should be noted that surfaces where nanowires were largely missing have not been observed in the electron microscope when used throughout the project.

6.2 Aging of SU-8 surfaces

Aging effects, described in chapter 5.3, became apparent throughout the project. A large batch of nanowire devices were synthesized and assembled at the beginning of this project, and two parameters were found to change throughout the project: hydrophilicity of surfaces, as seen when depositing liquids on the nanowire surfaces, and cell growth. Hydrophilicity declined over weeks, with larger amounts of plasmid solutions needed to cover the entire nanowire surface: a 5x5 mm^2 initially needed

~10 µL of solution for complete coverage, and later ~40 µL were needed for similar surfaces. Repeating the final plasma-cleaning step in our nanowire synthesis procedure (chapter 4.1) was found to improve hydrophilicity, as well as the ability of cells to spread and survive on nanowire surfaces, and surface recovery could explain these observations.

Hydrophobic recovery of SU-8 after exposure to O_2-plasma is a known phenomenon, where wettability can go from $<5°$ to $30°$ within few days, and then steadily increase to $50°$ over a few months [102]. Storing SU-8 in dry conditions will decrease recovery rate compared to rewashed samples [103].

Surface recovery has been studied for many polymers used in biophysical systems. PDMS consists of repeating units of $-O-Si(CH_3)_2$-groups, which gives a hydrophobic surface. Upon treatment with oxygen plasma, silanol ($Si-OH$) groups are introduced to the surface, destroying methyl groups ($Si-CH_3$). This however also increases the surface free energy, and as low molecular weight (LMW) chains diffuse from bulk PDMS to the surface to decrease surface free energy, hydrophilicity is also lost [104, 105].

Surface recovery of PDMS surfaces, affecting biophysical usability, is a well described phenomenon, seen by both increasing contact angles [104] and reduced biocompatibility [106], and decreasing cell growth density has been described for other polymer surfaces when hydrophilicity is reduced [107, 108].

The SU-8 surfaces used throughout our work are silanized, giving a different surface chemistry compared to pure SU-8 surfaces. In our work a hydrophilic SU-8 surface was ensured by performing a plasma cleaning step with oxygen just before silanization and cell growth experiments. It seems likely that surface regeneration, as described above, could also explain altered surface chemistry over time for silanized SU-8 surfaces, although this has not been described in the literature.

6.3 DNA release

DNA release was assessed by imaging YOYO-1-labeled plasmids adsorbed to nanowire surfaces for 10 minutes, and by measuring release of adsorbed YOYO-1-labeled plasmid by spectrophotometry. These experiments show that adsorbed plasmids is not immediately lost to the solution, and that appreciable levels of DNA release is achieved within 5 hours. A silanization step is performed as part of the nanowire device synthesis, to electrostatically adsorb DNA to nanowire surfaces. It was however shown that DNA will not be immediately lost to the solution in the absence

of a silanization step, which is agreement with other reports that DNA can bind SU-8 directly [109]. For silanized samples roughly half of adsorbed DNA is released to solution, however, it is evident by the jumping nature of the graph from the spectrophotometric experiments that there is some uncertainty associated with the exact levels of plasmid release.

Also, in the experiments presented here, it is not distinguished between plasmid that desorbs from the surface of a nanowire, and plasmid that desorbs from the surface from which the nanowire protrudes. Results presented here on DNA desorption is a combination of desorption from both the surface of a nanowire, and the supporting surface. The area of one nanowire with radius r and height h can be calculated using the formula for the area of a one-sided cylinder:

$$A = 2\pi rh + \pi r^2 \approx 2\pi rh \tag{16}$$

With a diameter of 120 nm and a length of 2 µm the area per nanowire of is 7.5×10^{-13} m^2 ≈ 1 µm^2. Since the areal density of wires is 0.1 µm^{-2}, the active surface area for nanowire surfaces will be roughly an order of magnitude lower than the surface area from which the wires are protruding, if it is assumed DNA will bind the surface of nanowire at the same planar density as the supporting surface. DNA release from the supporting surface is thus probably the dominating effect in these experiments.

6.4 Results from labeled plasmid uptake experiments

Labeled plasmid uptake was assessed by fluorescence microscopy. Whenever a green fluorescent spot was seen inside a cell this was interpreted as delivery of cargo. Background fluorescence and noise could however influence these observations, giving false positives, even though care was taken to reduce such effects by using low laser intensities and by recording the intensity from each spot twice and taking the average, respectively. Also, since fluorescence microscopy was used to investigate delivery, only a limited number of cells could be observed, and the relatively low number of cells investigated adds to the uncertainty in the results. Other experiments could be done with flow cytometry to investigate a larger population of cells. Also such experiments allow for a cut-off to be chosen as a lower fluorescent intensity which signifies uptake, which guarantees a consistent assessment for all cells of whether a cells has taken up cargo or not.

Results from the labeled plasmid uptake experiments could indicate that nanowires

increase the uptake of plasmid, although results vary from experiment to experiment, which reduces the strength of this finding. However, in all experiments a substantial proportion of cells do show uptake of labeled cargo, which far exceeds the proportion of cells that are successfully transfected in similar experiments where reporter plasmids are delivered to cells. This clearly demonstrates that to show that nanowires can deliver fluorescent cargo does not guarantee that delivered cargo can interact with the internal machinery of a cell.

It was also investigated whether the number of fluorescent spots observed per cell was different for cells grown on nanowires versus cells grown on glass, and it was found that cells grown on nanowires had a higher number of fluorescent spots per cell compared to cells grown on glass (1.1 vs 0.53 spots per cell for cells grown on nanowires and glass, respectively). Here too results varied from experiment to experiment. All recorded images were treated the same way by the image analysis software, with the same cut-off and minimum spot-size necessary for a spot to be recorded, so these results could be less biased than experiments where the number of cells that show uptake are counted manually.

It is not known how this uptake happens, but it could be speculated that the uptake is through an endocytosis mechanism, since fluorescently labeled particles almost always seem confined to small spots, with diameters <0.5 µm. In other experiments on transport of DNA in endosomes, endosomes typically have sizes of 100-200 nm [110]. New experiments are planned to further characterize nanowire-mediated delivery of cargo and possible induction of endocytosis [111].

6.5   Results from siRNA knockdown experiments

siRNA knockdown experiments, where siRNA was adsorbed to a surface with alternating lanes of flat surfaces and nanowire surfaces, show no convincing knockdown of stably expressed EGFP in AR42J cells. A number of effects could contribute to reducing the contrast between nanowire lanes and flat surface lanes.

Clustered growth
Clustered growth could be a problem when assessing transfection efficiency using nanowires. For a cell to be successfully impaled, it has to be in close contact with the surface from which the nanowires protrude, or at least not be distanced further away than the length of the nanowire. In the current experimental setup nanowires have a length of 0.5-4 µm. Cells are seeded in a single cell fashion. In clustered

growth, as exhibited by AR42J cells, some cells grow on top of others, effectively protecting these cells from nanowire impalement. It could be speculated that these cells would nevertheless be exposed to siRNAs or other bioactive molecules adsorbed to the nanowires, as the adsorbed molecules would be delivered to the cytoplasm of the mother cell, and if stable enough these molecules would then be inherited to progenitor cells.

Wettability of surfaces affecting concentration of siRNA

Reference [18] was used as a starting point to find concentrations of siRNA for the final "printing solution". In the reference concentrations of 2-30 ng/µl of siRNA were used, and the size of the printing solution droplet was 15 µl before drying the slides. The amount of siRNA that is deposited and adsorbed to the surface will depend on the wettability of the surface: Surfaces with high wettability (small contact angle) will have a lower concentration of siRNA per area than surfaces with a low wettability, since a droplet covering a surface with high wettability will spread out more than a droplet on a surface with low wettability. This effect adds to the uncertainty in comparing the current experimental setup for nanowire-based transfection to transfection using conventional lipid-based transfection reagents in reverse transfected cell array setups. However, different concentrations of siRNA deposited on similar nanowire surfaces should still be comparable, as the wettability from well to well should be the same.

Long half-life of stably expressed EGFP

In this work conventional EGFP was used, and the stability of this protein could make the detection of loss of fluorescence difficult. Wild-type GFP has a half-life of approximately 26 hours [75], and EGFP has a similar half life [112]. EGFP has earlier been described as inferior to the destabilized version d2EGFP (Clontech) when assessing expression dynamics, due to its long half life [113, 114]. Successful siRNA mediated knockdown of EGFP expressed by AR42J cells has however been reported by our collaboratory group at The Institute for Cancer Research and Molecular Medicine (NTNU) [18] in a transiently transfected cell line (HEK293). AR42J cells used in the current project express EGFP incorporated in the genome, and to knock down a stably expressed protein could be more difficult than to knock down a transiently expressed protein, especially if a strong promoter is used, as is the case for the AR42J cells.

6.6 Results from plasmid transfection experiments

Plasmid transfection experiments presented here are disappointing, with consistently low transfection efficiencies. In sedimentation, centrifugation and tapping experiments nanowire surfaces perform similar to flat surfaces, when these are chemically and geometrically similar.

Tapping experiments

In the case of tapping experiments there were some experiments where nanowire surfaces gave higher transfection efficiencies in local parts of the nanowire surface (~5%, 62 cells/mm^2). It can not be excluded that the observed effect was mediated by nanowires. However, when nanowire surfaces were compared with chemically similar, flat surfaces, similar transfection results were obtained overall. Also, for glass surfaces, which are flatter than SU-8 surfaces (with or without nanowires), transfection efficiencies were sometimes even higher in local parts of the surface, discouraging the idea that nanowires are able to deliver plasmids and other biomolecules directly to the cytoplasm in our current experimental setup. Higher transfection efficiencies in local parts could be explained by an optimum geometry only in these parts, where the surface protrudes just enough to perforate cells in the pellet/on cleanroom paper, not killing them, and still reaching them. In one of the experiments with high local concentration of transfected cells this was found on one of the corners of the nanowire surface, and this could be such an area where nanowires are able to come into contact with cells on the opposing surface. Nanowires are generally shorter than 4 µm, and considering that this is about 1/1000th of the surface length and width, surfaces must be very flat for a large proportion of nanowires to be able to get in contact with an opposing flat surface. In the tapping experiment cells seemed to survive the procedure quite well, reducing the likelihood that cells are perforated and then die.

It is known that for cell membrane penetration to be successful, an actin meshwork must be present, even though insertion probability is not directly proportional to the Young's modulus of a cell [115]. Cortical rigidity varies with the state of the cell, and also trypsinized cells retain rigidity of the membrane [116]. It could still be speculated that trypsinized cells would behave differently than cells attached to glass, but no difference was observed when trypsinized cells were tapped, compared to cells attached to glass surfaces after one day growth.

Tapping experiments showed transfection efficiencies on nanowire surfaces com-

parable to flat surfaces, although some exceptions were seen. With tapping experiments the force applied to cells is largely uncontrollable, compared to centrifugation experiments. Another difference between the centrifugation and tapping experiments lies in how the force to breach the cellular membrane is transferred to the system. In the centrifugation experiments the force is based on the inertia of cells, and even after membrane rupture the cell will still experience a large force. In the tapping experiments the force is applied to the nanowires, and after a cellular membrane breaches, the energy transferred to the system would immediately be released, not further stressing the cell. A controllable force, applied through a technique similar to the tapping experiments, would thus be favorable, and would best mimic the AFM experiments where membrane perforation has been well documented.

Sedimentation and centrifugation experiments

Cells settling by gravity or centrifugation are similar, apart from that the forces acting on cells in a centrifuge can be much higher than gravity. AFM experiments have confirmed that nanowires can breach the cellular membrane, and directly deliver plasmids and other biomolecules to the cytoplasm of cells. The forces required for membrane penetration is in the range 0.7 ± 0.3 nN [60], which is almost three orders of magnitude higher than the gravitational pull experienced by cells in medium. This could explain why experiments where cells are settling on top of a nanowire surface by gravitation are generally unsuccessful.

In the centrifugation experiments, cells experience forces up to 109 nN, which is over two orders of magnitude higher than the empirically determined force barrier. This indicates that also other factors contribute to a lower transfection efficiency than expected. In the nanowire-on-AFM-tip experiments [60, 117, 61, 115, 118, 119, 120] a single nanowire is used when perforating the cellular membrane, as opposed to several nanowires in our experimental setup, where a cell is perforated by approximately 10 nanowires. It has been shown that nanowires with a diameter of 200 nm require the same force to perforate a cellular membrane as nanowires with a diameter of 800 nm [60], so the force required does not simply scale with the pressure (force/area) (even though this has been predicted by simulation [121]). Also, at a maximum force of 109 nN per cell, at least some cells should be perforated and transfected. Both centrifuges used require some time to reach the desired speed, and in the case of the ultracentrifuge, ~5 minutes is required to reach 88,500 × g. At a relative centrifugation force of 2680 × g cells move 3.0 cm/s (see equation 10), and therefore all cells will have settled by the time the centrifuge reaches the desired

speed. Perforation might be impossible once the cell has reached the surface, as the membrane is known to orient itself to the surface, and to wrap around nanowires [95, 122, 123, 51]. A possible variant of the experiments conducted here could be to a add a polymer to the medium, to increase viscosity, and thus reduce the terminal velocity proportionally. Reducing terminal velocity would cause the cells to reach the nanowires more slowly, and thus allow the centrifuge to reach the desired speed before the cells interact with the nanowires. Increasing the velocity, and thereby also the frictional drag on particles, does however not reduce the force by which the nanowires indent and perforate the cellular membrane, as this force is only dependent on the effective mass and relative centrifugal force (see equation 6 in chapter 2.8). Other experimental setups could also be considered, where cells were kept in a chamber separate from the chamber with a nanowire surface, only to be released when the centrifuge has reached its final speed. The different compartments could for instance be separated by a radio-controlled diaphragm, or by a membrane that breaks down over time. A membrane could be formed by letting medium freeze, and if the temperature of the entire system is optimized the melting could be delayed until the centrifuge has reached its final speed. These experimental approaches are however quite complicated compared to the experimental setup presented in this work.

6.7 Results in light of published performance

For a review of published nanowire-mediated transfection experiments, see chapter 3.

In the tapping experiments we get a transfection efficiency of 1%-5%, or 13-62 cells/mm². The tapping method is based on a series of papers described by McKnight et al. [39, 38, 86, 88, 89]. In published experiments that resemble our experimental setup (thus excluding one article [86]), similar results are obtained. In these articles, proper controls are almost invariably not included, and we show that we can also obtain these results on chemically similar surfaces without nanowires, indicating that transfection is not mediated by nanowires.

In the sedimentation experiments we get a lower transfection efficiency compared to the tapping experiments. Delivery of fluorescently labeled cargo has not been extensively studied with respect to silica-coated cupric oxide nanowires yet, but future experiments are planned to elucidate the apparent effect of nanowires. Our results are lower than similar experiments published by Shalek et al. [44], where 95-100%

of cells from different cell lines show uptake of fluorescently labeled cargo. When cargo delivery is investigated, we do however see delivery to a high proportion of cells, while at the same time we don't see expression of plasmids delivered by the same approach, and this indicates that simply delivering cargo to a cell does not guarantee that the cargo can interact with the cellular machinery, which is the ultimate goal of nanowire-mediated transfection devices. Experiments should therefore not only rely on delivery of labeled cargo, but also show that biomolecules can be delivered and interact with the cellular machinery, since this is usually presented as the ultimate goal.

Some published experiments show better results than we obtain, but these experiments are unfortunately not substantiated by proper control experiments with published data, where the proportion of cells transfected is quantified [86, 92, 44, 91, 90]. It would be beneficial to see published experiments repeated, with proper controls, as there are indications that arrays of nanowires are not able to penetrate cellular membranes, as is discussed in the next section.

6.8   Why is nanowire-mediated transfection unsuccessful?

Results presented here raise the question: Why is nanowire-mediated transfection unsuccessful? One answer could lie in how nanowires interact with cellular membranes. It has previously been implied that nanowires are not able to penetrate cellular membranes when cells sediment on a surface with nanowires protruding out of it, since a cellular membrane can be seen around nanowires in transmission electron microscopy sections [95, 123], and in confocal imaging when the cellular membrane has been fluorescently labeled [122]. Also, propidium iodide has been shown not to enter cells grown on nanowire surfaces [95, 94, 38]. This finding is by some groups seen as an indication that membrane perforation does not affect membrane integrity [94], but it could also be seen as an indication that cellular membranes are not perforated by nanowires [95], thus explaining why transfection is unsuccessful.

Together with results presented here, these observations raise the question: Why are cellular membranes not perforated by nanowires, and the follow-up question: If nanowires do not penetrate cellular membranes, how is delivery of fluorescently labeled cargo explained?

It has been suggested that nanowires are able to spontaneously penetrate cellular membranes when cells settle on top of nanowires, assessed by confocal microscopy

and scanning electron microscopy [43, 49], and is seen within 1 hour [44]. It is however questionable if confocal microscopy (without staining the cellular membrane) holds the resolving power needed to confirm that the cellular membrane is breached, and that the membrane is not simply indented. Also, drying artifacts can affect experiments when scanning and transmission electron microscopy is used to assess perforation of cellular membranes. From experiments where a single nanowire is attached to an AFM tip it is known that cells can be transfected by perforating the cellular membrane, by delivering attached plasmids. When silicon nanowires on AFM tips are used to transfect cells, 74% of human mesenchymal stem cells (MSC) are transfected with a plasmid expressing GFP, compared to 42% for lipofection and 8% for microinjection [124, 61]. Considering the level of control obtained when using AFM, an efficiency of 74% is probably close to the upper limit for transfection of this cell line, when using similar nanowires. In addition to give an estimate of the force barrier that must be passed, these experiments also show that nanowires can indeed penetrate cellular membranes. However, forces required to penetrate cellular membranes lies in the range 0.7±0.3 nN [60], which is almost three orders of magnitude higher than the gravitational pull experienced by cells in medium. It would therefore seem unlikely that cells are spontaneously perforated when settling on top of an array of nanowires.

In the ultracentrifugation experiments cells experienced centrifugal forces up to ~110 nN, and given the empirically based estimates, cellular membranes should be perforated at these forces. In the AFM experiments nanowires have been inserted into cells with an insertion speed of 1-4 µm/s [124, 61]. In the centrifugation experiments the centrifuge needs time to reach a given rotational speed, and ~5 minutes to reach the highest centrifugal forces. At a relative centrifugation force of 2680 × g cells move 3.0 cm/s, and it is therefore evident that all cells will have settled on the nanowire surface by the time the intended centrifugal speed is reached. This could allow cells to reorient the cellular membrane around nanowires, effectively blocking any perforation, as discussed previously.

Tapping experiments should allow much higher force loading rate than sedimentation and centrifugation, since cells and nanowires are (almost) at rest before the nanowire surface is tapped. Also the the energy input to the system would be released once the cellular membrane is breached, unlike the case for centrifugation. This approach is however much more sensitive to the planar geometry of the surfaces. Also, any fluid surrounding cells would probably dampen the effect of tapping the nanowire surface. In our experiments there are occasionally some areas with higher

transfection efficiencies compared to the rest of the surface, possibly indicating that these areas had an optimum geometry to allow penetration, while not killing cells. This has also been observed by others [39]. The high transfection efficiency seen in some areas could however probably also be explained by other factors, considering the high transfection seen in local areas of flat glass surfaces.

We observed consistently higher transfection efficiencies when flat glass slides where used, compared to flat SU-8 surfaces and nanowire surfaces. The reason for this effect is unknown, but it could be speculated that the very flat geometry, favoring adhesive capillary forces between the glass slides, somehow facilitate uptake of plasmid adsorbed to one of the surfaces. When the two glass slides were separated by the use of tweezers, this required a higher force compared to separating flat SU-8 or nanowire surfaces from the glass slide on which cells were deposited. The effect of shear stress and convective fluid flow has not been described in detail with respect to transfection, but is known to enhance transfection of liposome-entangled plasmids [125, 126]. According to theory, lipoplex delivery rate should increase substantially when convection is added to the system, and experiments have also shown higher lipoplex delivery rates in such scenarios, at least for modest increases in shear stress [126]. This increase in delivery rate is partly attributed to the increased probability of cell-liposome interactions in the presence of fluid flow. It is also speculated that frequently moving an incubated sample, when cells are in the process of being transfected, could contribute to convection and thus enhance transfection [126]. Thus, also the effect of convective flow and shear stress must be taken into account when considering proper control experiments. In our case, flat SU-8 surfaces behaved similarly to nanowire surfaces when separating the two slides in tapping experiments. Since the force required to separate two completely flat glass slides was higher, it could be speculated that the increased shear stress enhanced transfection even further for this system than for flat SU-8 or nanowire surfaces in tapping experiments. Over two decades ago, a method known has 'scrape loading transfection' [127] was been described for transfection, where a plasmid is added to cells adhered to a surface, and a rubber policeman used to scrape the cells. In such experiments transfection efficiencies were reported in the range 50%-80%. Experiments with scrape-loading was also showed to be able to deliver fluorescently labeled cargo to 40% of cells subjected to scrape loading [128]. The mechanism for delivery and transfection was thought to depend on the formation of transient openings of holes in the plasma membrane where the plasma membrane was tightly adhered to the plastic substrate [128]. A similar mechanism has been proposed

105

for transfection by thermal inkjet printing of cells [129] and by microfluidic devices [130], and a transient disruption in cellular membranes could be relevant to explain the transfection seen in the tapping experiments.

Finally, in experiments where labeled plasmid was delivered to cells, a significant proportion of cells showed uptake in all experiments (around 25-30% for cells grown on glass and 50% for cells grown on nanowires). In similar experiments where a reporter plasmid encoding EGFP was delivered <1% of cells where transfected, so simply to show delivery of fluorescently labeled cargo does not guarantee that the cargo is able to interact with the internal machinery of a cell, indicating that the delivered cargo is isolated from the rest of the cell. Delivery of fluorescently labeled cargo, without perforating cells, could be explained by a process where nanowires induce vesicular uptake, i.e. endocytosis. It has been suggested that other methods of inducing inward curving of the membrane could initiate vesiculation and uptake [131]. It is hypothesized that merely inducing a localized membrane deformation will result in a positive feedback loop that ends in hydrolysis of phosphatidylinositol-4,5-bisphosphate (PIP_2), an important part of endocytosis [132, 133]. A vesicular uptake also seems likely, as the delivered cargo is almost always confined to small sections of the cytoplasm in our experiments, and this is also seen in images presented by other groups [44, 90, 92]. If the cargo was delivered to the cytoplasm, it could be speculated that the cargo would distribute more evenly throughout the cell. Experiments to elucidate whether nanowires do induce endocytosis, and how this process happens, are planned [111].

6.9 How to proceed with high-throughput nanowire mediated transfection of cells

Some final thoughts on how to proceed with nanowire mediated transfection will be presented here. The cellular membrane represents a barrier which isolates the inside of a cell from the outside. It is mandatory to bypass this membrane if one is to interact with the internal machinery of a cell, such as for transfection. Nanowires do not spontaneously perforate cellular membranes, and in order to increase the probability of membrane penetration three factors are crucial: The strength of the cellular membrane (the force barrier), the force with which the membrane is indented, and the time over which the indentation takes place.

The force barrier of a membrane could be reduced by adding membrane destabilizers to experiments. It must however be taken into consideration that adding bioac-

tive chemicals to an experiment could in itself perturb cellular function. Saponin, an amphipathic glycoside, has already been mentioned in chapter 3. Saponin has been used in order to facilitate membrane perforation by nanoneedles [91], where a relatively small concentration range gave intended results. Multivalent ions are also thought to destabilize cellular membranes, and by changing the concentration of multivalent ions outside of cells the membrane could temporarily be destabilized [134]. Electroporation is another method to transiently destabilize membranes [135] that could enhance membrane penetration of nanowires, and experiments where the combination of nanowires and electroporation are currently being planned.

In order to increase the force of penetration other experimental setups could be considered. It is possible that the force applied to the nanowire-membrane interface by tapping method is dampened by fluid trapped between the nanowire surface and the supporting surface. If nanowires protruded from a porous membrane fluid could be allowed to pass between the nanowires, and thus not dampen the effect of tapping the nanowire surface.

As discussed previously the centrifugation experiments could be refined so that the centrifuge reaches its intended speed before cells interact with nanowires, in order to decrease the time over which the cellular membrane is allowed to reorient itself to the nanowire.

Also, centrifugation experiments and other approaches to increase the force, could be combined with approaches to decrease the force barrier, for instance by adding membrane destabilizers to the experiment.

7 Conclusion

Nanowire-mediated delivery of biomolecules to HeLa and AR42J cells has been extensively studied with respect to silica-coated cupric oxide nanowires. Nanowires are thought to mediate transfection of cells by penetrating the cellular, and possibly also the nuclear, membrane, thus directly delivering biomolecules to the cellular machinery located in the cytoplasm and/or nucleus. The cellular membrane represents a barrier that can be breached, either by applying enough force to the nanowires, or by decreasing the force barrier represented by the membrane.

It has been established that plasmid adsorbed to silanized nanowire surfaces will desorb in a PBS solution, and in 5 hours roughly half of the adsorbed plasmid will be released. It has also been confirmed that the method for synthesizing nanowire arrays works as intended, and resulting nanowires have diameters of ~120 nm, and protruding from an SU-8 surface at an areal density of 0.11 nanowires/µm². These properties should allow transfection from a theoretical point of view, based on published AFM experiments where the penetration of cellular membranes has been characterized.

Gravitational sedimentation of cells on an array of nanowires should not give transfection according to estimates from AFM experiments, and this was also found in our experiments, both in siRNA and plasmid transfection experiments. Two techniques to increase the force of penetration were tested: Centrifugation experiments, and placing the nanowire surface face-down on top of cells, and then tapping the nanowire surface. Centrifugation experiments yielded no transfection, even at relative centrifugal forces up to 88,500 × g, and this can possibly be attributed to the time needed to reach these high speeds, where cells will have settled on the surface long before the intended force is applied, which could give cells enough time to re-orient the cellular membrane to the nanowire. Tapping experiments gave a higher transfection efficiency than sedimentation or centrifugation, with ~1% of cells successfully transfected, and sometimes local areas were seen with higher transfection efficiencies (~5%). It was however shown that similar transfection efficiencies can be obtained with flat SU-8 surfaces, which are chemically similar to the nanowire surfaces used, apart from the nanowires themselves, when these surfaces were used in tapping experiments. Also, it was found that the transfection efficiency was even higher for completely flat glass surfaces, indicating that other effects pertaining to the surface geometry could also facilitate transfection, and it is speculated that the shear stress experienced by cells in tapping experiments could be part of this expla-

nation. A key finding is thus that proper controls are important to ascertain the effect of nanowires in nanowire-mediated transfection, and such control experiments are often lacking in published articles describing nanowire-mediated transfection.

Initial experiments have also been conducted to see if nanowires can deliver fluorescently labeled biomolecules. It was shown that both flat surfaces and nanowire surfaces are able to deliver fluorescently labeled plasmids to a significant proportion of cells (roughly one third of cells overall), and a trend was observed where nanowires perform better than flat surfaces in this respect. The same experimental setup does not facilitate transfection, indicating that the delivered biomolecules are not able to interact with the cellular machinery.

Results for published nanowire-mediated delivery of biomolecules and transfection systems has been reviewed, and it is found that, with few exceptions, our results are on par with published results. This emphasizes the need for proper control experiments when evaluating plasmid transfection efficiencies, as uptake of plasmid can happen without any facilitating factors, and other factors than nanowires could also have effects on transfection efficiencies (i.e. shear stress experienced by cells).

Published AFM experiments, where single nanowires perforate the cellular membrane, confirm that it is possible to directly deliver biomolecules to the interior of cells, and are encouraging in the quest to find ways to bypass the barrier represented by the cellular membrane. Currently, new experiments to elucidate any possible effects of nanowires on endocytosis are planned, and a set of possible approaches to breach the cellular membrane will also be investigated, in order to realize the potential of high throughput experiments that rely on nanowire mediated transfection.

References

[1] F. Crick. Central dogma of molecular biology. *Nature*, 227(5258):561–3, August 1970.

[2] I. Amit, M. Garber, N. Chevrier, A. P. Leite, Y. Donner, T. Eisenhaure, M. Guttman, J. K. Grenier, W. Li, O. Zuk, L. A. Schubert, B. Birditt, T. Shay, A. Goren, X. Zhang, Z. Smith, R. Deering, R. C. McDonald, M. Cabili, B. E. Bernstein, J. L. Rinn, A. Meissner, D. E. Root, N. Hacohen, and A. Regev. Unbiased reconstruction of a mammalian transcriptional network mediating pathogen responses. *Science*, 326(5950):257–63, October 2009.

[3] M. Stürzl, A. Konrad, G. Sander, E. Wies, F. Neipel, E. Naschberger, S. Reipschläger, N. Gonin-Laurent, R. E. Horch, U. Kneser, W. Hohenberger, H. Erfle, and M. Thurau. High throughput screening of gene functions in mammalian cells using reversely transfected cell arrays: review and protocol. *Combinatorial chemistry & high throughput screening*, 11(2):159–72, February 2008.

[4] A. J. M. Walhout, M. Vidal, and J. Dekker. *Handbook of Systems Biology.* Elsevier, Waltham, 1st edition, 2013.

[5] J. Ziauddin and D. M. Sabatini. Microarrays of cells expressing defined cDNAs. *Nature*, 411(6833):107–10, May 2001.

[6] F. Mumm and P. Sikorski. Oxidative fabrication of patterned, large, non-flaking CuO nanowire arrays. *Nanotechnology*, 22(10):105605, March 2011.

[7] K. M. Beckwith. A Study of Cultured Cells on a Nanowire-based Reverse Transfection Device, 2011.

[8] J. R. Masters. HeLa cells 50 years on: the good, the bad and the ugly. *Nature reviews. Cancer*, 2(4):315–9, April 2002.

[9] A. Flobak. Investigation of siRNA transient transfection of AR42J cells using silica-coated cupric oxide nanowires, 2012.

[10] J. K. Jaiswal and S. M. Simon. Imaging single events at the cell membrane. *Nature chemical biology*, 3(2):92–8, February 2007.

[11] M. Wong, S. Kong, W. H. Dragowska, and M. B. Bally. Oxazole yellow homodimer YOYO-1-labeled DNA: a fluorescent complex that can be used to

assess structural changes in DNA following formation and cellular delivery of cationic lipid DNA complexes. *Biochimica et biophysica acta*, 1527(1-2):61–72, July 2001.

[12] F. Crick. On protein synthesis. *Symposia of the Society for Experimental Biology*, 12:138–63, January 1958.

[13] H. Lodish, A. Berk, P. Matsudaira, C. A. Kaiser, M. Krieger, M. P. Scott, L. Zipursky, and J. Darnell. *Molecular Cell Biology*. W. H. Freeman, 2003.

[14] J. K. Rantala, R. Mäkelä, A.-R. Aaltola, P. Laasola, J.-P. Mpindi, M. Nees, P. Saviranta, and O. Kallioniemi. A cell spot microarray method for production of high density siRNA transfection microarrays. *BMC genomics*, 12(1):162, January 2011.

[15] D. Hanahan and R. a. Weinberg. Hallmarks of cancer: the next generation. *Cell*, 144(5):646–74, March 2011.

[16] S. Mousses, N. J. Caplen, R. Cornelison, D. Weaver, M. Basik, S. Hautaniemi, A. G. Elkahloun, R. a. Lotufo, A. Choudary, E. R. Dougherty, E. Suh, and O. Kallioniemi. RNAi microarray analysis in cultured mammalian cells. *Genome research*, 13(10):2341–7, October 2003.

[17] C. S. Fjeldbo, K. Misund, C.-C. Günther, M. Langaas, T. S. m. Steigedal, L. Thommesen, A. Laegreid, and T. Bruland. *RNA Therapeutics*, volume 629 of *Methods in Molecular Biology*. Humana Press, Totowa, NJ, 2010.

[18] C. S. Fjeldbo, K. Misund, C.-C. Günther, M. Langaas, T. S. m. Steigedal, L. Thommesen, A. Laegreid, and T. Bruland. Functional studies on transfected cell microarray analysed by linear regression modelling. *Nucleic acids research*, 36(15):e97, September 2008.

[19] R. Kumar, D. S. Conklin, and V. Mittal. High-throughput selection of effective RNAi probes for gene silencing. *Genome research*, 13(10):2333–40, October 2003.

[20] S. N. Bailey, R. Z. Wu, and D. M. Sabatini. Applications of transfected cell microarrays in high-throughput drug discovery. *Drug discovery today*, 7(18 Suppl):S113–8, September 2002.

[21] A. Fire, D. Albertson, S. W. Harrison, and D. G. Moerman. Production of antisense RNA leads to effective and specific inhibition of gene expression in C. elegans muscle. *Development (Cambridge, England)*, 113(2):503–14, October 1991.

[22] A. Fire, S. Xu, M. K. Montgomery, S. A. Kostas, S. E. Driver, and C. C. Mello. Potent and specific genetic interference by double-stranded RNA in Caenorhabditis elegans. *Nature*, 391(6669):806–11, February 1998.

[23] A. J. Hamilton and D. C. Baulcombe. A species of small antisense RNA in posttranscriptional gene silencing in plants. *Science (New York, N.Y.)*, 286(5441):950–2, October 1999.

[24] R. F. Ketting. The many faces of RNAi. *Developmental cell*, 20(2):148–61, February 2011.

[25] G. Karp. *Cell and Molecular Biology: Concepts and Experiments.* Wiley, 6th edition, 2009.

[26] D. P. Bartel. MicroRNAs: target recognition and regulatory functions. *Cell*, 136(2):215–33, January 2009.

[27] H. H. Seitz. Redefining microRNA targets. *Current biology : CB*, 19(10):870–3, May 2009.

[28] L. Salmena, L. Poliseno, Y. Tay, L. Kats, and P. P. Pandolfi. A ceRNA Hypothesis: The Rosetta Stone of a Hidden RNA Language? *Cell*, 146(3):353–358, July 2011.

[29] M. A. Matzke and J. A. Birchler. RNAi-mediated pathways in the nucleus. *Nature reviews. Genetics*, 6(1):24–35, January 2005.

[30] H. Kawasaki, K. Taira, and K. V. Morris. siRNA induced transcriptional gene silencing in mammalian cells. *Cell cycle (Georgetown, Tex.)*, 4(3):442–8, March 2005.

[31] D. Grimm and M. A. Kay. Therapeutic application of RNAi: is mRNA targeting finally ready for prime time? *The Journal of clinical investigation*, 117(12):3633–41, December 2007.

[32] S. Singh, A. S. Narang, and R. I. Mahato. Subcellular fate and off-target effects of siRNA, shRNA, and miRNA. *Pharmaceutical research*, 28(12):2996–3015, December 2011.

[33] X. Gao and P. Zhang. Transgenic RNA interference in mice. *Physiology (Bethesda, Md.)*, 22:161–6, June 2007.

[34] D. D. Rao, J. S. Vorhies, N. Senzer, and J. Nemunaitis. siRNA vs. shRNA: similarities and differences. *Advanced drug delivery reviews*, 61(9):746–59, July 2009.

[35] T. Azzam and A. J. Domb. Current developments in gene transfection agents. *Current drug delivery*, 1(2):165–93, April 2004.

[36] K. L. Douglas. Toward development of artificial viruses for gene therapy: a comparative evaluation of viral and non-viral transfection. *Biotechnology progress*, 24(4):871–83, 2008.

[37] T. K. Kim and J. H. Eberwine. Mammalian cell transfection: the present and the future. *Analytical and bioanalytical chemistry*, 397(8):3173–8, August 2010.

[38] T. E. McKnight, A. V. Melechko, D. K. Hensley, D. G. J. Mann, G. D. Griffin, and M. L. Simpson. Tracking Gene Expression after DNA Delivery Using Spatially Indexed Nanofiber Arrays. *Nano Letters*, 4(7):1213–1219, July 2004.

[39] T. McKnight, A. Melechko, G. Griffin, and MA. Intracellular integration of synthetic nanostructures with viable cells for controlled biochemical manipulation. *Materials Science*, 551, 2003.

[40] A. V. Melechko, V. I. Merkulov, T. E. McKnight, M. A. Guillorn, K. L. Klein, D. H. Lowndes, and M. L. Simpson. Vertically aligned carbon nanofibers and related structures: Controlled synthesis and directed assembly. *Journal of Applied Physics*, 97(4):041301, 2005.

[41] J. E. Koehne, H. Chen, A. Cassell, G.-y. Liu, J. Li, and M. Meyyappan. Arrays of carbon nanofibers as a platform for biosensing at the molecular level and for tissue engineering and implantation. *Bio-medical materials and engineering*, 19(1):35–43, January 2009.

[42] A. M. Cassell, Q. Ye, B. a. Cruden, J. Li, P. C. Sarrazin, H. T. Ng, J. Han, and M. Meyyappan. Combinatorial chips for optimizing the growth and integration of carbon nanofibre based devices. *Nanotechnology*, 15(1):9–15, January 2004.

[43] W. Kim, J. K. Ng, M. E. Kunitake, B. R. Conklin, and P. Yang. Interfacing silicon nanowires with mammalian cells. *Journal of the American Chemical Society*, 129(23):7228–9, June 2007.

[44] A. K. Shalek, J. T. Robinson, E. S. Karp, J. S. Lee, D.-R. Ahn, M.-H. Yoon, A. Sutton, M. Jorgolli, R. S. Gertner, T. S. Gujral, G. MacBeath, E. G. Yang, and H. Park. Vertical silicon nanowires as a universal platform for delivering biomolecules into living cells. *Proceedings of the National Academy of Sciences of the United States of America*, 107(5):1870–5, February 2010.

[45] A. I. Hochbaum, R. Fan, R. He, and P. Yang. Controlled growth of Si nanowire arrays for device integration. *Nano letters*, 5(3):457–60, March 2005.

[46] V. Ovchinnikov, A. Malinin, S. Novikov, and C. Tuovinen. Fabrication of silicon nanopillars using self-organized gold-chromium mask. *Materials Science and Engineering B*, 69-70:459–463, January 2000.

[47] L. Gangloff, E. Minoux, K. Teo, P. Vincent, V. Semet, V. Binh, M. Yang, I. Bu, R. Lacerda, G. Pirio, and Others. Self-aligned, gated arrays of individual nanotube and nanowire emitters. *Nano Letters*, 4(9):1575–1579, 2004.

[48] T. Berthing, S. Bonde, C. B. Sø rensen, P. Utko, J. Nygå rd, and K. L. Martinez. Intact mammalian cell function on semiconductor nanowire arrays: new perspectives for cell-based biosensing. *Small (Weinheim an der Bergstrasse, Germany)*, 7(5):640–7, March 2011.

[49] W. Hällström, T. Må rtensson, C. Prinz, P. Gustavsson, L. Montelius, L. Samuelson, and M. Kanje. Gallium phosphide nanowires as a substrate for cultured neurons. *Nano letters*, 7(10):2960–5, October 2007.

[50] V. Ovchinnikov, A. Malinin, S. Novikov, and C. Tuovinen. Silicon Nanopillars Formed by Reactive Ion Etching Using a Self-Organized Gold Mask. *Physica Scripta*, T79(1):263, 1999.

[51] C. Xie, L. Hanson, W. Xie, Z. Lin, B. Cui, and Y. Cui. Noninvasive neuron pinning with nanopillar arrays. *Nano letters*, 10(10):4020–4, October 2010.

[52] X. Jiang, T. Herricks, and Y. Xia. CuO Nanowires Can Be Synthesized by Heating Copper Substrates in Air. *Nano Letters*, 2(12):1333–1338, December 2002.

[53] Y. Fu. Synthesis of Fe2O3 nanowires by oxidation of iron. *Chemical Physics Letters*, 350(5-6):491–494, December 2001.

[54] B. Yao, Y. Chan, and N. Wang. Formation of ZnO nanostructures by a simple way of thermal evaporation. *Applied physics letters*, 81(4):757, 2002.

[55] D. S. Friend, D. Papahadjopoulos, and R. J. Debs. Endocytosis and intracellular processing accompanying transfection mediated by cationic liposomes. *Biochimica et biophysica acta*, 1278(1):41–50, January 1996.

[56] A. Rémy-Kristensen, J. P. Clamme, C. Vuilleumier, J. G. Kuhry, and Y. Mély. Role of endocytosis in the transfection of L929 fibroblasts by polyethylenimine/DNA complexes. *Biochimica et biophysica acta*, 1514(1):21–32, September 2001.

[57] I. S. Zuhorn, R. Kalicharan, and D. Hoekstra. Lipoplex-mediated transfection of mammalian cells occurs through the cholesterol-dependent clathrin-mediated pathway of endocytosis. *The Journal of biological chemistry*, 277(20):18021–8, May 2002.

[58] J. Zabner, A. J. Fasbender, T. Moninger, K. A. Poellinger, and M. J. Welsh. Cellular and molecular barriers to gene transfer by a cationic lipid. *The Journal of biological chemistry*, 270(32):18997–9007, August 1995.

[59] C. Liu, W. Yu, Z. Chen, J. Zhang, and N. Zhang. Enhanced gene transfection efficiency in CD13-positive vascular endothelial cells with targeted poly(lactic acid)-poly(ethylene glycol) nanoparticles through caveolae-mediated endocytosis. *Journal of controlled release : official journal of the Controlled Release Society*, 151(2):162–75, April 2011.

[60] I. Obataya, C. Nakamura, S. Han, N. Nakamura, and J. Miyake. Mechanical sensing of the penetration of various nanoneedles into a living cell using atomic force microscopy. *Biosensors & bioelectronics*, 20(8):1652–5, February 2005.

[61] S.-W. Han, C. Nakamura, N. Kotobuki, I. Obataya, H. Ohgushi, T. Nagamune, and J. Miyake. High-efficiency DNA injection into a single human mesenchy-

mal stem cell using a nanoneedle and atomic force microscopy. *Nanomedicine : nanotechnology, biology, and medicine*, 4(3):215–25, September 2008.

[62] J. D. Larsen, N. L. Ross, and M. O. Sullivan. Requirements for the nuclear entry of polyplexes and nanoparticles during mitosis. *The journal of gene medicine*, (September):580–589, September 2012.

[63] S. Cornelis, M. Vandenbranden, J.-M. Ruysschaert, and A. Elouahabi. Role of intracellular cationic liposome-DNA complex dissociation in transfection mediated by cationic lipids. *DNA and cell biology*, 21(2):91–7, February 2002.

[64] I. Mortimer, P. Tam, I. MacLachlan, R. W. Graham, E. G. Saravolac, and P. B. Joshi. Cationic lipid-mediated transfection of cells in culture requires mitotic activity. *Gene therapy*, 6(3):403–11, March 1999.

[65] I. S. Zuhorn and D. Hoekstra. On the mechanism of cationic amphiphile-mediated transfection. To fuse or not to fuse: is that the question? *The Journal of membrane biology*, 189(3):167–79, October 2002.

[66] S. Zou, K. Scarfo, M. H. Nantz, and J. G. Hecker. Lipid-mediated delivery of RNA is more efficient than delivery of DNA in non-dividing cells. *International journal of pharmaceutics*, 389(1-2):232–43, April 2010.

[67] P. N. Prasad. *Introduction to Biophotonics*. John Wiley & Sons, Hoboken, New Jersey, 1 edition, 2003.

[68] H. Morise, O. Shimomura, F. H. Johnson, and J. Winant. Intermolecular energy transfer in the bioluminescent system of Aequorea. *Biochemistry*, 13(12):2656–62, June 1974.

[69] O. Shimomura, F. H. Johnson, and Y. Saiga. Extraction, purification and properties of aequorin, a bioluminescent protein from the luminous hydrome-dusan, Aequorea. *Journal of cellular and comparative physiology*, 59:223–39, June 1962.

[70] R. N. Day and M. W. Davidson. The fluorescent protein palette: tools for cellular imaging. *Chemical Society reviews*, 38(10):2887–921, October 2009.

[71] M. Ormö, A. B. Cubitt, K. Kallio, L. A. Gross, R. Y. Tsien, and S. J. Remington. Crystal structure of the Aequorea victoria green fluorescent protein. *Science (New York, N.Y.)*, 273(5280):1392–5, September 1996.

[72] S. Bettati, E. Pasqualetto, G. Lolli, B. Campanini, and R. Battistutta. Structure and single crystal spectroscopy of Green Fluorescent Proteins. *Biochimica et biophysica acta*, 1814(6):824–33, June 2011.

[73] A. A. Pakhomov and V. I. Martynov. GFP family: structural insights into spectral tuning. *Chemistry & biology*, 15(8):755–64, August 2008.

[74] N. C. Shaner, G. H. Patterson, and M. W. Davidson. Advances in fluorescent protein technology. *Journal of cell science*, 120(Pt 24):4247–60, December 2007.

[75] P. Corish and C. Tyler-Smith. Attenuation of green fluorescent protein half-life in mammalian cells. *Protein engineering*, 12(12):1035–40, December 1999.

[76] A. D. Richards and A. Rodger. Synthetic metallomolecules as agents for the control of DNA structure. *Chemical Society reviews*, 36(3):471–83, March 2007.

[77] K. Günther, M. Mertig, and R. Seidel. Mechanical and structural properties of YOYO-1 complexed DNA. *Nucleic acids research*, 38(19):6526–32, October 2010.

[78] M. Reuter and D. T. F. Dryden. The kinetics of YOYO-1 intercalation into single molecules of double-stranded DNA. *Biochemical and biophysical research communications*, 403(2):225–9, December 2010.

[79] P. Tekola, J. P. Baak, J. A. Beliën, and J. Brugghe. Highly sensitive, specific, and stable new fluorescent DNA stains for confocal laser microscopy and image processing of normal paraffin sections. *Cytometry*, 17(3):191–5, November 1994.

[80] T. J. Collins. ImageJ for microscopy. *BioTechniques*, 43(1 Suppl):25–30, July 2007.

[81] J. R. Lakowicz. *Principles of Fluorescence Spectroscopy*. Kluwer Academic / Plenum Publishers, New York, 1999.

[82] P. C. Hiemenz and R. Rajagopalan. *Principles of Colloid and Surface Chemistry*. Marcel Dekker, Inc., New York, 3rd edition, 1997.

[83] P. Nelson. *Biological Physics - Energy, Information, Life*. W. H. Freeman and Company, New York, 1st edition, 2008.

[84] R. Phillips, J. Kondev, J. Theriot, and H. G. Garcia. *Physical Biology of the Cell*. Garland Science, New York, 2nd edition, 2013.

[85] C.-M. Ghim, S. K. Lee, S. Takayama, and R. J. Mitchell. The art of reporter proteins in science: past, present and future applications. *BMB reports*, 43(7):451–60, July 2010.

[86] D. G. J. Mann, T. E. McKnight, J. T. McPherson, P. R. Hoyt, A. V. Melechko, M. L. Simpson, and G. S. Sayler. Inducible RNA interference-mediated gene silencing using nanostructured gene delivery arrays. *ACS nano*, 2(1):69–76, January 2008.

[87] D. Mann, T. McKnight, A. Melechko, M. Simpson, and G. Sayler. Quantitative analysis of EDC-condensed DNA on vertically aligned carbon nanofiber gene delivery arrays. *Biotechnology and bioengineering*, 97(4):680–688, 2007.

[88] D. B. Peckys, A. V. Melechko, M. L. Simpson, and T. E. McKnight. Immobilization and release strategies for DNA delivery using carbon nanofiber arrays and self-assembled monolayers. *Nanotechnology*, 20(14):145304, April 2009.

[89] R. C. Pearce, J. G. Railsback, B. D. Anderson, M. F. Sarac, T. E. McKnight, J. B. Tracy, and A. V. Melechko. Transfer of Vertically Aligned Carbon Nanofibers to Polydimethylsiloxane (PDMS) While Maintaining their Alignment and Impalefection Functionality. *ACS applied materials & interfaces*, January 2013.

[90] A. K. Shalek, J. T. Gaublomme, L. Wang, N. Yosef, N. Chevrier, M. S. Andersen, J. T. Robinson, N. Pochet, D. Neuberg, R. S. Gertner, I. Amit, J. R. Brown, N. Hacohen, A. Regev, C. J. Wu, and H. Park. Nanowire-mediated delivery enables functional interrogation of primary immune cells: application to the analysis of chronic lymphocytic leukemia. *Nano letters*, 12(12):6498–504, December 2012.

[91] E. Peer, A. Artzy-Schnirman, L. Gepstein, and U. Sivan. Hollow nanoneedle array and its utilization for repeated administration of biomolecules to the same cells. *ACS nano*, 6(6):4940–6, June 2012.

[92] S. Park, Y.-S. Kim, W. B. Kim, and S. Jon. Carbon nanosyringe array as a platform for intracellular delivery. *Nano letters*, 9(4):1325–9, April 2009.

[93] C. Bachran, M. Sutherland, I. Heisler, P. Hebestreit, M. F. Melzig, and H. Fuchs. The saponin-mediated enhanced uptake of targeted saporin-based drugs is strongly dependent on the saponin structure. *Experimental biology and medicine (Maywood, N.J.)*, 231(4):412–20, April 2006.

[94] Y.-R. Na, S. Y. Kim, J. Gaublomme, A. Shalek, M. Jorgolli, H. Park, and E. G. Yang. Probing enzymatic activity inside living cells using a nanowire-cell "sandwich" assay. *Nano letters*, December 2012.

[95] F. Mumm, K. M. Beckwith, S. Bonde, K. L. Martinez, and P. Sikorski. A Transparent Nanowire-Based Cell Impalement Device Suitable for Detailed Cell-Nanowire Interaction Studies. *Small (Weinheim an der Bergstrasse, Germany)*, October 2012.

[96] ATCC. Product Information Sheet for CRL-1492, 2007.

[97] N. Groulx, F. Boudreault, S. N. Orlov, and R. Grygorczyk. Membrane reserves and hypotonic cell swelling. *The Journal of membrane biology*, 214(1):43–56, January 2006.

[98] M. Amarzguioui. Tolerance for mutations and chemical modifications in a siRNA. *Nucleic Acids Research*, 31(2):589–595, January 2003.

[99] M. Amarzguioui and H. Prydz. An algorithm for selection of functional siRNA sequences. *Biochemical and biophysical research communications*, 316(4):1050–8, April 2004.

[100] K. M. Beckwith. Surface-functionalized CuO nanowires in an SU-8 epoxy as a platform for biomolecule delivery into cells, 2010.

[101] J. Brozek, F. Grande, J. T. Anderson, and A. Keys. Densiometric analysis of body composition: Revision of some quantitative assumptions. *Annals of the New York Academy of Sciences*, 110:113–40, September 1963.

[102] F. Walther and P. Davydovskaya. Stability of the hydrophilic behavior of oxygen plasma activated SU-8. *Journal of . . .* , pages 1–11, 2007.

[103] V. Jokinen, P. Suvanto, and S. Franssila. Oxygen and nitrogen plasma hydrophilization and hydrophobic recovery of polymers. *Biomicrofluidics*, 6(1):16501–1650110, March 2012.

[104] D. Bodas and C. Khan-Malek. Hydrophilization and hydrophobic recovery of PDMS by oxygen plasma and chemical treatment—An SEM investigation. *Sensors and Actuators B: Chemical*, 123(1):368–373, April 2007.

[105] J. M. K. Ng, I. Gitlin, A. D. Stroock, and G. M. Whitesides. Components for integrated poly(dimethylsiloxane) microfluidic systems. *Electrophoresis*, 23(20):3461–73, October 2002.

[106] R. L. Williams, D. J. Wilson, and N. P. Rhodes. Stability of plasma-treated silicone rubber and its influence on the interfacial aspects of blood compatibility. *Biomaterials*, 25(19):4659–73, August 2004.

[107] M. Khorasani, H. Mirzadeh, and S. Irani. Plasma surface modification of poly (l-lactic acid) and poly (lactic-co-glycolic acid) films for improvement of nerve cells adhesion. *Radiation Physics and Chemistry*, 77(3):280–287, March 2008.

[108] C. Ozcan, P. Zorlutuna, V. Hasirci, and N. Hasirci. Influence of Oxygen Plasma Modification on Surface Free Energy of PMMA Films and Cell Attachment. *Macromolecular Symposia*, 269(1):128–137, August 2008.

[109] R. Marie, S. Schmid, A. Johansson, L. Ejsing, M. Nordström, D. Häfliger, C. B. Christensen, A. Boisen, and M. Dufva. Immobilisation of DNA to polymerised SU-8 photoresist. *Biosensors & bioelectronics*, 21(7):1327–32, January 2006.

[110] R. P. Kulkarni, K. Castelino, A. Majumdar, and S. E. Fraser. Intracellular transport dynamics of endosomes containing DNA polyplexes along the microtubule network. *Biophysical journal*, 90(5):L42–4, March 2006.

[111] J. Torstensen. Designing a live cell imaging system for studying nanowire-cell interactions, 2012.

[112] J. Barrow, a. S. Bernardo, C. W. Hay, M. Blaylock, L. Duncan, a. Mackenzie, K. McCreath, a. J. Kind, a. E. Schnieke, a. Colman, a. W. Hart, and K. Docherty. Purification and Characterization of a Population of EGFP-Expressing Cells from the Developing Pancreas of a Neurogenin3/EGFP Transgenic Mouse. *Organogenesis*, 2(1):22–7, January 2005.

[113] J. X. Bi, M. Wirth, C. Beer, E. J. Kim, M.-B. Gu, and A.-P. Zeng. Dynamic characterization of recombinant Chinese hamster ovary cells containing an inducible c-fos promoter GFP expression system as a biomarker. *Journal of biotechnology*, 93(3):231–42, February 2002.

[114] X. Li, X. Zhao, Y. Fang, X. Jiang, T. Duong, C. Fan, C. C. Huang, and S. R. Kain. Generation of destabilized green fluorescent protein as a transcription reporter. *The Journal of biological chemistry*, 273(52):34970–5, December 1998.

[115] H. Kagiwada, C. Nakamura, T. Kihara, H. Kamiishi, K. Kawano, N. Nakamura, and J. Miyake. The mechanical properties of a cell, as determined by its actin cytoskeleton, are important for nanoneedle insertion into a living cell. *Cytoskeleton (Hoboken, N.J.)*, 67(8):496–503, August 2010.

[116] Y. Shimizu, S. M. A. Haghparast, T. Kihara, and J. Miyake. Cortical rigidity of round cells in mitotic phase and suspended state. *Micron (Oxford, England : 1993)*, 43(12):1246–51, December 2012.

[117] I. Obataya, C. Nakamura, S. Han, N. Nakamura, and J. Miyake. Nanoscale operation of a living cell using an atomic force microscope with a nanoneedle. *Nano letters*, 5(1):27–30, January 2005.

[118] I. U. Vakarelski, S. C. Brown, K. Higashitani, and B. M. Moudgil. Penetration of living cell membranes with fortified carbon nanotube tips. *Langmuir : the ACS journal of surfaces and colloids*, 23(22):10893–6, October 2007.

[119] K. Yum, N. Wang, and M.-F. Yu. Nanoneedle: a multifunctional tool for biological studies in living cells. *Nanoscale*, 2(3):363–72, March 2010.

[120] Y. Amemiya, K. Kawano, M. Matsusaki, M. Akashi, N. Nakamura, and C. Nakamura. Formation of nanofilms on cell surfaces to improve the insertion efficiency of a nanoneedle into cells. *Biochemical and biophysical research communications*, 420(3):662–5, April 2012.

[121] E. J. Wallace and M. S. P. Sansom. Blocking of carbon nanotube based nanoinjectors by lipids: a simulation study. *Nano letters*, 8(9):2751–6, September 2008.

[122] T. Berthing, S. Bonde, K. R. Rostgaard, M. H. Madsen, C. B. Sø rensen, J. Nygå rd, and K. L. Martinez. Cell membrane conformation at vertical nanowire array interface revealed by fluorescence imaging. *Nanotechnology*, 23(41):415102, October 2012.

[123] L. Hanson, Z. C. Lin, C. Xie, Y. Cui, and B. Cui. Characterization of the Cell-Nanopillar Interface by Transmission Electron Microscopy. *Nano letters*, 12(11):5815–20, November 2012.

[124] S. W. Han, C. Nakamura, I. Obataya, N. Nakamura, and J. Miyake. A molecular delivery system by using AFM and nanoneedle. *Biosensors & bioelectronics*, 20(10):2120–5, April 2005.

[125] H. S. Shin, H. J. Kim, S. J. Sim, and N. L. Jeon. Shear stress effect on transfection of neurons cultured in microfluidic devices. *Journal of nanoscience and nanotechnology*, 9(12):7330–5, December 2009.

[126] S. S. Harris and T. D. Giorgio. Convective flow increases lipoplex delivery rate to in vitro cellular monolayers. *Gene therapy*, 12(6):512–20, March 2005.

[127] M. Fechheimer, J. F. Boylan, S. Parker, J. E. Sisken, G. L. Patel, and S. G. Zimmer. Transfection of mammalian cells with plasmid DNA by scrape loading and sonication loading. *Proceedings of the National Academy of Sciences of the United States of America*, 84(23):8463–7, December 1987.

[128] P. L. McNeil, R. F. Murphy, F. Lanni, and D. L. Taylor. A method for incorporating macromolecules into adherent cells. *The Journal of cell biology*, 98(4):1556–64, April 1984.

[129] X. Cui, D. Dean, Z. M. Ruggeri, and T. Boland. Cell damage evaluation of thermal inkjet printed Chinese hamster ovary cells. *Biotechnology and bioengineering*, 106(6):963–9, August 2010.

[130] J. Lee, A. Sharei, W. Y. Sim, A. Adamo, R. Langer, K. F. Jensen, and M. G. Bawendi. Nonendocytic delivery of functional engineered nanoparticles into the cytoplasm of live cells using a novel, high-throughput microfluidic device. *Nano letters*, 12(12):6322–7, December 2012.

[131] N. Ben-Dov and R. Korenstein. Enhancement of cell membrane invaginations, vesiculation and uptake of macromolecules by protonation of the cell surface. *PloS one*, 7(4):e35204, January 2012.

[132] J. Liu, Y. Sun, D. G. Drubin, and G. F. Oster. The mechanochemistry of endocytosis. *PLoS biology*, 7(9):e1000204, September 2009.

[133] C. N. Antonescu, F. Aguet, G. Danuser, and S. L. Schmid. Phosphatidylinositol-(4,5)-bisphosphate regulates clathrin-coated pit initiation, stabilization, and size. *Molecular biology of the cell*, 22(14):2588–600, July 2011.

[134] B.-Y. Ha. Stabilization and destabilization of cell membranes by multivalent ions. *Physical Review E*, 64(5):051902, October 2001.

[135] H. Potter. Transfection by electroporation. *Current protocols in molecular biology / edited by Frederick M. Ausubel ... [et al.]*, Chapter 9(813):Unit 9.3, May 2003.